Defining interactions between assembling HIV-1 virions and host cell plasma membrane proteins

By

Jonathan Richard Grover

**A dissertation submitted in partial fulfillment
of the requirements for the degree of
Doctor of Philosophy
(Microbiology and Immunology)
in the University of Michigan
2013**

Doctoral Committee:

**Associate Professor Akira Ono, Chair
Professor Kathleen L. Collins
Professor Alice Telesnitsky
Assistant Professor Sarah Veatch**

Dedication

For Ben, who fought valiantly on the battlefield and in the halls of academia.

Acknowledgements

I would like to graciously thank the many who have encouraged and guided me along the path to reach this point in my career. Specifically, I would like to thank K.R. Scott, Jeff Hengesbach, and Mr. Faust from Mountain Pointe High School; James Birk, Shelley Haydel, Yixin Shi, Valerie Stout, Hugh Mason, Barbara Gonzales, Jacquelyn Kilbourne, Deirdre Meldrum, Mark Holl, Roger Johnson, and Jeff Houkal from Arizona State University.

I would like to thank my thesis committee members Alice Telesnitsky and Kathy Collins for their many insightful suggestions and support at every stage of my graduate career. In particular, I would like to thank Akira Ono for his inexhaustible patience and optimism, he truly has been an outstanding friend, example, and mentor to me over the past 5 years. I would also like to acknowledge Sarah Veatch, who has served on my thesis committee, as well as collaborating with me on several projects. Sarah has been a friend, colleague and second mentor to me and I have greatly benefitted from her unwavering dedication to rigorous interpretation of experimental data. I would like to thank Christiane Wobus and Joel Swanson for allowing me to rotate in their labs. I would also like to thank the many faculty members who have provided advice, encouragement, suggestions, and reagents to me over the years, including Mike Imperiale, Phil Hanna (MIC405), Elliot Juni (MIC350), Vic DiRita (MMMP), Harry Mobley, Kathy Spindler (MIC415), Phil King, Steve King (BSL-3), Malini Raghavan, Cheong-Hee Chang, Beth Moore (MIC415), Tom Moore (MIC460), Jason Weinberg (Virology Journal Club), Bob Fuller (Intracellular Protein Trafficking Club), and Aaron Goldstrohm, as well as many others not listed here.

I would like to thank past and present members of the Ono Lab for their friendship, help, and guidance, including Ian Hogue, Vineela Chukkapalli, Nick Llewellyn, Kazuaki Monde, Jingga Inlora, Balaji Olety Amaranath, Gabrielle Todd, Jenni Chung, Madeline Nye, Jay Oh, Alex Myong, and Ed Trubin. I would like to thank the Veatch laboratory, especially Matt Stone, Elin Edwald, Jiang Zhao and Jing Wu for their help with my experiments and data analysis. I would like to thank the staff of the Department of Microbiology and Immunology, especially Heidi Thompson and Margaret Allen. I would also like to thank Sam Straight from the Center for Live-Cell Imaging and Chris Edwards from the Microscopy and Image Analysis Laboratory. I would like to thank Seth Thacker and Keith Bishop for helping to recruit me to the University of Michigan, and Rob Peters for being an outstanding graduate student mentor.

I would like to thank my parents Richard and Mary Grover for their love and for fostering my curiosity since childhood. They have always encouraged me to follow my passion for science wherever it takes me. I would like to thank my parents-in-law Heidi and Steve Robbins for their love and support. Finally, I would like to thank my loving, beautiful wife Natasha for her constant support and patience with me, even when I stay on the microscope all night, and my son Garrett for giving me a good excuse not to work every single night and weekend over the past two years.

I would like to acknowledge the organizations and institutions which have generously provided funding to support my graduate school career. I received one year of funding from the Program in Biomedical Sciences (PiBS) at the University of Michigan. I received two years of funding from the Molecular Mechanisms in Microbial Pathogenesis Training Program (MMMP, T32 AI007527-13), administered by Professor Victor DiRita.

I also received one year of funding from the Doctor Clayton Willison and Emma Elizabeth Willison Fund, administered by the Department of Microbiology and Immunology. The work presented in this thesis was further supported by the National Institutes of Health (R56 AI089282 and R21 AI095022).

The work presented in Chapter 2 of this thesis has been published previously:

Grover JR, Llewellyn GN, Soheilian F, Nagashima K, Veatch S, Ono A. (2013) Roles Played by Capsid-Dependent Induction of Membrane Curvature and Gag-ESCRT Interactions in Tetherin Recruitment to HIV-1 Assembly Sites. *Journal of Virology* 87(8):4650-4664.

Transmission electron microscopy analysis of Gag mutants, presented in Figure 2.3A, was performed by Ferri Soheilian and Kunio Nagashima at the Electron Microscopy Laboratory, SAIC-Frederick, Inc., National Cancer Institute, Frederick, MD. T cell infection and microscopy, presented in Figure 2.4 was performed with the assistance of G. Nicholas Llewellyn. Super-resolution localization microscopy experiments and data analyses, presented in Figures 2.5, 2.7, 3.1, 3.2, 3.3, 3.4, and 4.2, were performed in collaboration with Sarah Veatch in the Department of Biophysics at the University of Michigan. Matthew Stone also provided technical assistance with image processing.

Table of Contents

List of Figures

Abstract

Human immunodeficiency virus type 1 (HIV-1) is the causative agent of acquired immunodeficiency syndrome (AIDS) and is a significant burden on human health. As a successful pathogen, HIV-1 is able to overcome several components of the innate and adaptive immune systems. This is facilitated by the activities of the four accessory proteins Vif, Vpr, Vpu, and Nef.

The Vpu protein has been shown to target an antiviral protein, BST-2/tetherin, which inhibits the release of many enveloped viruses from infected cells. While much is known about the mechanism of tetherin antagonism by Vpu, the antiviral function of tetherin is poorly understood. It has been observed that tetherin is specifically recruited to sites of HIV-1 assembly, but the mechanism of this recruitment is unknown.

In my thesis work I have employed conventional and super-resolution microscopy techniques to determine the mechanism of tetherin recruitment to HIV-1 assembly sites. I have determined that both membrane curvature, mediated by the HIV-1 Gag protein, as well as interactions between Gag and the ESCRT machinery are the critical determinants of tetherin recruitment to HIV-1 assembly sites. I have also demonstrated that low levels of tetherin recruitment, induced by membrane curvature, are sufficient for inhibition of HIV-1 release.

Currently I am employing super-resolution microscopy to study interactions between HIV and other host proteins. Previously, we have shown that HIV interacts with and reorganizes plasma membrane microdomains in infected cells. In polarized T cells, which are a natural host of HIV-1 infection in vivo, we have shown that multimerization of Gag mediates polarization of HIV-1 particles to a rear-end protrusion termed the

uropod. Several proteins co-polarize with Gag to uropods, in a manner dependent upon the matrix domain of Gag.

My current work involves characterization of interactions between HIV-1 and PSGL-1, a protein which is specifically recruited to virus assembly sites in T cells. I have found that basic residues within the cytoplasmic tail of this protein are required for its recruitment to HIV-1 assembly sites. I am also employing conventional assays to examine the affects of various uropod-directed proteins, such as PSGL-1, on HIV-1 replication and dissemination.

CHAPTER I

Introduction

Overview of the HIV pandemic and HIV pathogenesis

Since its discovery in the early 1980s, HIV has spread world-wide, and remains a pandemic disease of great medical importance today [1-3]. There are currently approximately 34 million people living with HIV, with 2.5 million new infections and 1.7 million HIV-related deaths in 2011[4]. Despite considerable effort, an effective vaccine remains elusive. However, significant progress has been made in combating HIV infection, transmission, and disease progression by the development of highly active antiretroviral therapy (HAART). In combination, these antiviral drugs can significantly improve outcomes for those already infected with HIV [5]. Expanding and improving upon existing HAART therapy, as well as making these medications inexpensive and universally available to HIV infected people world-wide remains an ongoing effort. Both of these goals must likely be met in order to bring the HIV pandemic to an end, and potentially drive HIV to extinction, as has been done with other viruses in the past [6].

The establishment of a full-length, infectious molecular clone of HIV-1, soon after its discovery, has aided greatly in the study of HIV-1 molecular biology [7]. Understanding the molecular details of HIV replication, immune evasion, and virus-host interactions is a promising area for the identification of new drug targets, as well as the development of other strategies to combat HIV transmission and disease progression.

HIV-1 is the causative agent of acquired immunodeficiency syndrome (AIDS) [1, 2]. Following infection, viral titers rise and result in a temporary state of viremia. Once adaptive immune responses have been initiated, viral replication is significantly suppressed and viral titers decline to a low level, termed the set point. Importantly, however, the human immune system is unable to completely clear the infection and the patient enters a prolonged period of clinical latency. This period can last many years, especially when the patient is adherent to a regime of HAART therapy. Importantly, there is continued viral replication at low levels and adaptation of viral quasispecies which enhance viral fitness and provide the potential for the development of drug-resistance. The establishment of latent viral reservoirs within long-lived cell populations such as memory T cells and hematopoetic stem cells likely contribute to the inability of the immune system to completely clear HIV infection [8].

Eventually, viral titers rise accompanied by a decline in $CD4^+$ T cell counts, which are lysed by active HIV replication [1]. Once $CD4^+$ T cell numbers fall below 200 cells/ml of blood, the patient is considered to have clinical AIDS disease. At this point patients are particularly vulnerable to certain cancers, as well as a host of viral, bacterial, fungal, and parasitic infections, many of which are rarely seen in healthy individuals. Mortality of AIDS patients is always associated with one or more of these opportunistic infections rather than HIV itself [9]. Disease progression is also accelerated by the overall immune dysfunction, termed the bystander effect, which results from destruction of uninfected $CD4^+$ T helper cells, which coordinate and direct adaptive immune responses [10, 11]. Identification and characterization of latent viral reservoirs and their elimination

by either pharmacologic agents, or their reactivation and subsequent elimination by the immune system remains a promising area of investigation [12, 13].

The HIV Replication Cycle

HIV-1 is an enveloped virus belonging to the retrovirus family and lentivirus genus (Group VI in the Baltimore classification system). It contains a linear, positive sense, RNA genome which encodes 9 viral proteins (15 after proteolytic cleavage events) (Figure 1.1). HIV-1 infection of cells begins with the binding of infectious virions to their primary receptor CD4 [14], found on the surface of a subset of T lymphocytes as well as cells of the myeloid lineage, such as macrophages and dendritic cells. This binding is mediated by trimeric complexes of the viral envelope glycoprotein (Env), which is composed of two subunits, gp120 and gp41. Following this initial binding event, Env is able to interact with one of two chemokine receptors, either CXCR4 or CCR5, depending upon the tropism of the viral Env protein as well as the type of cell being infected [15]. Once primary and secondary receptors have been engaged by Env, there is a dramatic conformational change which exposes the fusion peptide of gp41, which mediates the fusion of the viral envelope and cellular membrane [16] (Figure 1.2).

Once the viral capsid has entered the cell, it undergoes uncoating to release the pre-integration complex (PIC) into the host cell cytoplasm. This complex is composed of a dimer of single-stranded, positive-sense genomic RNA of approximately 10 kb in length (bearing a 5’ cap and 3’ poly-A tail similar to cellular mRNA molecules) as well as the viral reverse-transcriptase enzyme (RT) and the viral integrase enzyme (IN). This complex also contains the viral capsid (CA) and nucleocapsid proteins (NC), as well as

other cellular and viral proteins. Through the process of reverse-transcription, mediated by the RT enzyme, the viral RNA genome is converted into negative-sense DNA, using a specific host tRNA ($tRNA^{Lys3}$) as a primer for DNA extension [17]. This is followed by synthesis of positive-sense DNA, also mediated by the RT enzyme, to yield a complementary double-stranded DNA molecule (cDNA) encoding the complete viral genome [18]. Upon interaction with the nuclear pore complex, the PIC is able to enter the nucleus, where viral cDNA is integrated into the host cell genome by the viral integrase enzyme [19, 20]. At this point the integrated provirus is able to function in a similar way to a host gene, which can be transcribed by the host RNA polymerase II, to give rise to both unspliced viral genomic RNA, as well as several spliced RNA species responsible for translation of all 9 viral proteins [21] (Figure 1.1).

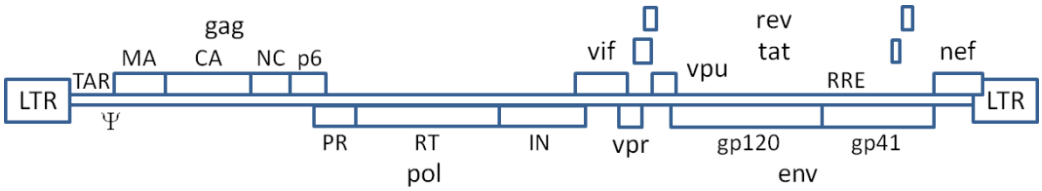

Figure 1.1. Schematic representation of the HIV-1 genome.
The HIV-1 genome is depicted as an integrated provirus composed of dsDNA which through LTR-mediated transcription and differential splicing results in translation of all 9 viral proteins. The locations of coding regions of individual domains are shown for Gag, Pol, and Env proteins. The locations of important structural elements formed on viral RNA molecules are also indicated (TAR, Ψ, and RRE). LTR long terminal repeat, TAR trans-activation response element, Ψ packaging signal, gag group specific antigen, MA matrix, CA capsid, NC nucleocapsid, p6 late domain, pol polymerase, PR protease, RT reverse transcriptase, IN integrase, vif viral infectivity factor, vpr viral protein R, vpu viral protein U, rev regulator of viral expression, tat trans-activator of transcription, env envelope, gp120 glycoprotein of 120 kDa, gp41 glycoprotein of 41 kDa, nef negative factor.

Once the integrated provirus is actively transcribed, viral proteins can be expressed in the cytosol. Production of the trans-activator of transcription protein (Tat) greatly enhances the processivity and rate of viral gene transcription through its

interaction with a structural feature near the 5' end of viral RNAs termed the trans-activation response element (TAR) and host transcription factors [22-28]. Because eukaryotic mRNAs are normally sequestered within the nucleus until they have undergone splicing, the full-length viral RNA, which also serves as mRNA for translation of the Gag and GagPol proteins, cannot be efficiently translocated to the cytoplasm without the aid of the regulator of viral expression protein (Rev). This activity of Rev to facilitate nuclear export of unspliced, viral RNA is dependent upon its interaction with another structural feature of viral RNA, termed the rev-response element (RRE) [29-32] (Figures 1.1 and 1.2).

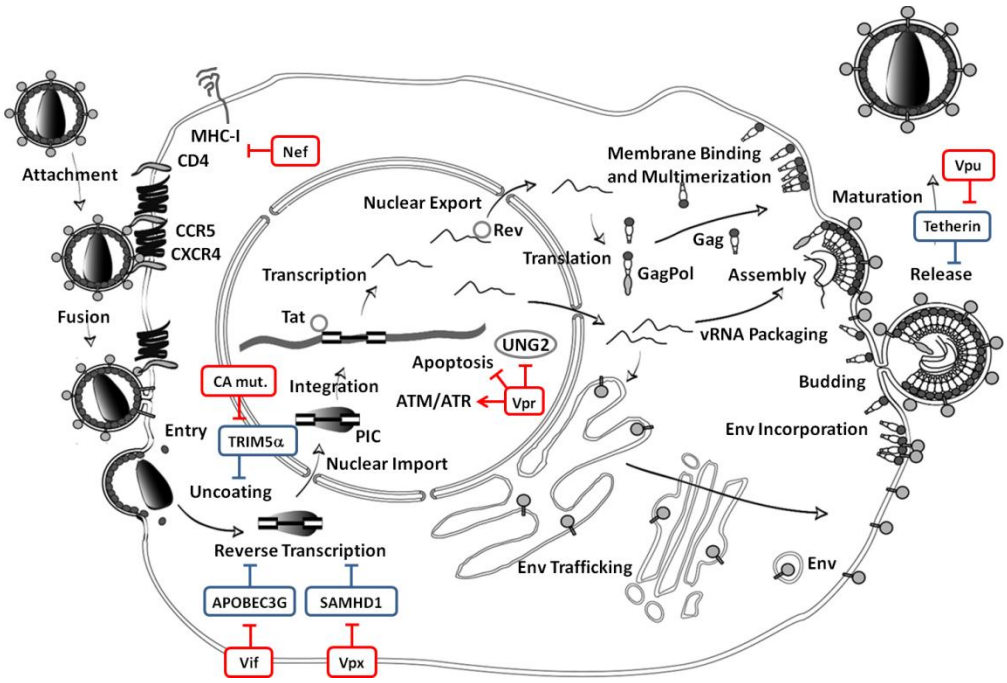

Figure 1.2. Overview of the HIV-1 life cycle.
Major events in the replication cycle of HIV-1 are depicted along with known antiviral restriction factors and viral countermeasures. Life cycle events are labeled in plain black text. Restriction factors are shown in blue boxes linked to steps in the life cycle with which they interfere or inhibit. Viral countermeasures and accessory proteins are shown in red boxes. All accessory proteins depicted are from HIV-1, with the exception of HIV-2/SIV Vpx protein. The viral proteins Tat, Rev, Gag, GagPol, and Env are shown at representative points during the HIV-1 replication cycle.

Upon translocation of full-length viral RNA into the cytoplasm, the viral precursor poly-proteins Gag and GagPol can be produced. The Gag protein is necessary and sufficient for the coordinated assembly of virus particles at the plasma membrane [33]. The GagPol fusion protein is synthesized through the aid of ribosomal frameshifting at a poly-purine tract located in the Sp2 region of the Gag coding sequence [34]. GagPol contains the viral enzymes protease (PR), reverse transcriptase (RT), and integrase (IN) fused, in tandem, to the C-terminus of the Gag precursor poly-protein [35] (Figures 1.1 and 1.2).

The Gag poly-protein is composed of 4 major structural domains, Matrix (MA), Capsid (CA), Nucleocapsid (NC), and the viral late domain (p6) (Figure 1.1). Removal of the initiator methionine residue of Gag, followed by N-terminal myristoylation of the exposed glycine residue by cellular enzymes allows Gag to stably interact with host cell membranes [36]. However, Gag also possesses the ability to interact specifically with phosphatidylinositol-(4,5)-bisphosphate [$PI(4,5)P_2$] through the highly-basic region (HBR) of the MA domain. This interaction is thought to facilitate both binding and targeting of Gag to the plasma membrane, in which $PI(4,5)P_2$ is predominantly found [37-41]. Once membrane binding has taken place, Gag has also been shown to interact with cholesterol-rich regions of the plasma membrane, termed lipid rafts [42]. Gag also interacts with other membrane microdomains such as tetraspanin-enriched microdomains (TEMs) [43-47] and uropod-directed microdomains (UDMs) in polarized T cells [48, 49] (Figure 1.3). In addition to interacting with membrane microdomains, Gag is also able to actively rearrange certain microdomains in ways not observed in uninfected cells [49-51].

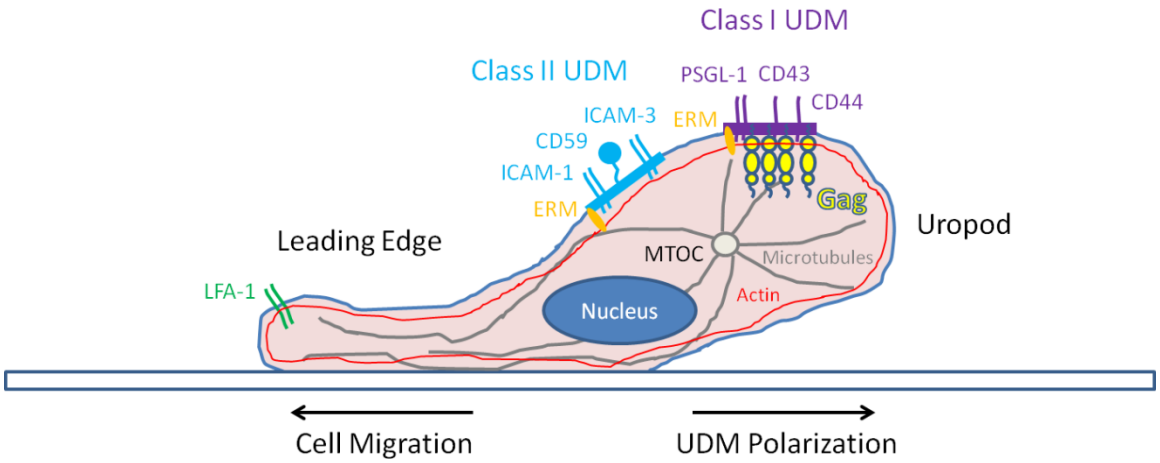

Figure 1.3. Schematic representation of a polarized T cell
A migrating, polarized T cell is depicted adhered to a substrate. Cells migrate toward the leading edge, which is enriched in LFA-1. Uropod directed microdomains polarize toward the uropod, which is opposite the leading edge, and is near the MTOC. Gag preferentially associates with class I UDMs composed of PSGL-1, CD43, and CD44. Both class I and class II UDMs likely polarize through the participation of ERM proteins, which link transmembrane proteins to the cortical Actin cytoskeleton when activated. LFA-1 lymphocyte adhesion glycoprotein 1, ERM Ezrin Radixin Moesin, ICAM-1 intracellular adhesion molecule 1, CD59 membrane attack complex inhibition factor, ICAM-3 intracellular adhesion molecule 3, PSGL-1 P-selectin glycoprotein ligand 1, CD43 Leukosialin, CD44 Extracellular matrix receptor III, MTOC Microtubule organizing center.

A previous study from our lab has demonstrated that assembling HIV-1 virions polarize to a rear end protrustion found in polarized T cells, termed the uropod. This polarization was found to be dependent upon membrane binding and higher-order multimerization of Gag, as well as a functional actin-myosin system. It was also shown that the presence of Gag in the uropod was correlated with increased cell-cell transmission of virus [48]. In unpolarized T cells, Gag has also been shown to interact with a subset of uropod-directed proteins (which normally polarize to uropods in the absence of Gag), termed class I uropod-directed microdomain (UDM) proteins, such as P-selectin glycoprotein ligand 1 (PSGL-1), Leukosialin (CD43), and Extracellular matrix receptor III (CD44). These interactions are dependent upon the overall charge, but not specific sequence of basic residues within the HBR of the MA domain. Interestingly, however, Gag does not associate with other UDM proteins such as Intracellular adhesion

molecules I and III (ICAM-1 and ICAM-3) or CD59, termed class II UDM proteins [49] (Figure 1.3).

Although polarization of Gag to uropods does not appear to require interaction with specific class I UDM proteins, they do associate specifically and tightly with assembling HIV-1 virions [49]. Although it is likely that Gag may associate with certain UDM proteins and not others for some purpose, relevant in the context of in-vivo virus infection, the role of these proteins in viral replication and dissemination remains unclear. In chapter 3 of this thesis I will address the fundamental underlying mechanism which facilitates Gag-UDM interactions, as well as the potential modulation of different aspects of HIV-1 infection by these proteins.

Formation of viral particles is accomplished by the coordinated process of membrane binding and multimerization of Gag. Multimerization is primarily dependent upon residues in the C-terminal domain of capsid (CA-CTD), as well as basic residues in the NC domain, which bind to RNA which is thought to serve as a scaffold for viral assembly [52, 53]. It should be noted that there are additional residues within the N-terminal domain of capsid (CA-NTD) which may also contribute to multimerization of Gag [54]. During the process of multimerization, Gag is able to produce positive membrane curvature in a processed termed virus budding [35]. This is likely mediated by residues in the CA-NTD, as well as a proposed structural change near the end of the CA-CTD [55]. Before being packaged into virions, HIV genomic RNA forms dimers through base-pairing interactions at the dimerization initiation site (DIS) [56]. Through a highly regulated process, dimeric viral genomic RNA is then incorporated into virus particles

by two zinc-finger motifs within the NC domain which interact with a structural motif of the viral RNA termed the packaging signal, or Ψ element [57-59] (Figures 1.1 and 1.2).

The viral envelope glycoprotein (Env) is synthesized as a precursor protein (gp160), which is extensively glycosylated by host machinery in the endoplasmic reticulum and golgi apparatus. Following these modifications, Env is trafficked by the secretory pathway to reach the plasma membrane. Once on the plasma membrane, Env is incorporated into assembling virus particles. Although poorly understood, the process of Env incorporation is known to depend upon specific interactions between the cytoplasmic tail of Env and certain residues in the MA domain of Gag in some cell-types [60, 61] (Figure 1.2).

Although Gag is necessary and sufficient for the production of spherical virus particles of approximately 100 nm in diameter, which contain viral genomic RNA, Env glycoprotein, and other host and viral proteins, it is unable to mediate scission of viral and cellular membranes without the participation of a family of cellular proteins which constitute the endosomal sorting complex required for transport (ESCRT) [62, 63].

This ESCRT complex is a large assembly of predominantly cytosolic proteins which, upon activation, can polymerize and assemble onto intracellular membranes and facilitate membrane scission. This process usually occurs when ESCRT proteins are recruited in sequential fashion to ubiquitinylated, transmembrane proteins on the cytoplasmic face of multivescicular body (MVB) membranes [64]. The ESCRT complex has also been shown to participate in membrane scission during cytokinesis, and is essential for cell division [65]. While assembly of retroviruses occurs at the plasma membrane in most cell types, it is topologically equivalent to the processes described

above, all of which involve budding in a direction away from the cytoplasm. For this reason, many viruses such as HIV-1 have evolved to co-opt the ESCRT machinery during viral budding.

Most ESCRT-dependent processes involve sequential recruitment of four complexes, termed ESCRT-0, ESCRT-I, ESCRT-II, and ESCRT-III. ESCRT-0 is primarily responsible for cargo recognition followed by recruitment of ESCRT-I. ESCRT-I, specifically the Tumor susceptibility gene 101 protein (Tsg101), interacts with a P(T/S)AP motif on the ESCRT-0 protein Hepatocyte growth factor-regulated tyrosine kinase substrate (HRS). This interaction allows the ESCRT-I complex to recruit ESCRT-II and ESCRT-III complexes sequentially. ESCRT-III proteins then assemble into hetero-oligomeric complexes which line the neck of the budding vesicle. Finally, a complex containing a catalytic AAA-type ATPase, Vacuolar protein sorting-associated protein 4 (Vps4A/Vps4B), is recruited to polymerized ESCRT-III assemblies and mediates the scission of membrane in an ATP-dependent manner [66].

HIV-1 Gag has been shown to recruit ESCRT-III complexes in a manner which is independent of ESCRT-0 and ESCRT-II [67]. The late domain of HIV-1, p6, contains a P(T/S)AP motif, which allows Gag to mimic the ESCRT-0 complex and interact directly with Tsg101 [68-70]. Recruitment of downstream ESCRT-III components by Tsg101 is dependent on its interaction with ESCRT-II [67]. Gag also been shown to interact with the ESCRT-associated protein Programmed cell death 6-interacting protein (Alix, PDCD6-IP, AIP1), which can recruit components of ESCRT-III directly, without a requirement for ESCRT-II [71]. Interaction with Alix is mediated by both residues in p6 [72], as well as the NC domain of Gag [73, 74].

In chapter 2 of this thesis, I explore the role of the ESCRT machinery in the targeting of an antiviral protein to assembling HIV-1 particles. As a conserved feature of many enveloped viruses, ESCRT-dependence is both an attractive possible means for the cell to recognize and target assembling viruses, as well as a potential target for therapeutic intervention of enveloped virus infections.

Finally, once virus particles have been successfully detached from the plasma membrane of infected cells, they undergo the process of maturation. During maturation, the Gag and GagPol precursor poly-proteins are cleaved by the viral protease enzyme (PR) into their individual domains, as well as the removal of two spacer peptides from Gag (Sp1 and Sp2 or p2 and p1). This processing results in generation of mature virus particles containing MA (p17), CA (p24), NC (p7), p6, PR (p10), RT (p51), and IN (p34) as individual proteins [75]. This process also results in the appearance of the conical capsid core characteristic of mature HIV-1 virions [62] (Figure 1.2). Concurrently, the Env glycoprotein (gp160) is cleaved by host proteases such as Furin into gp120 and gp41 subunits which associate through non-covalent interactions [76]. The gp120 subunit is responsible for receptor and co-receptor binding, while the transmembrane gp41 subunit is responsible for fusion with cell membranes [16].

Restriction Factors and Viral Countermeasures

As a retrovirus, HIV-1 encodes Gag, Pol, and Env which constitute the structural proteins and viral enzymes which mediate viral assembly and are essential for progression of the viral life cycle. In addition, HIV-1 encodes two small regulatory proteins Tat and Rev, which promote transcription of viral genes and nuclear export of

unspliced viral RNA respectively. As a lentivirus, HIV-1 also encodes 4 accessory proteins; Vif, Vpr, Vpu, and Nef [77] (Figure 1.1). While these proteins are not necessary for virus production in vitro in immortalized cell lines, they are necessary for efficient virus replication in primary cells such as T lymphocytes and monocyte-derived macrophages, and are believed to play important roles within the context of disease progression in vivo [78, 79]. One prominent example of this is the Nef protein, which was initially termed negative factor because of its dispensability in cell culture models [78, 80]. It has since been shown that Nef greatly enhances virus replication in vivo [81].

It is well known that retroviral tropism is highly species-specific. Nearly every primate species examined has been found to harbor distinct retroviruses [82]. This exquisite specificity is thought to arise from the presence of specific antiviral proteins, termed restriction factors, which limit viral replication in a highly species- and virus-specific manner. While these proteins may serve other functions, they are thought to be primarily antiviral in nature [83]. To be defined as a restriction factor, candidate proteins must meet several criteria. Their expression must be induced by interferon in non-immune cells, which is a classic hallmark of antiviral factors. They must be able to limit viral replication, and confer a restrictive phenotype when expressed in otherwise permissive cell types. They must undergo positive selection as host organisms adapt to the presence of viral infections. Finally, many restriction factors are also targeted for destruction or inhibition by viral proteins or countermeasures [84-86] (Figure 1.2).

In recent years, the functions of the 4 accessory proteins of HIV-1 have been increasingly linked with the ability of HIV-1 to evade host restriction factors and replicate efficiently [83]. The most well studied of these, Nef, has several important

activities which are all related to the ability of HIV-1 to avoid immune detection within infected cells. Upon infection Nef is able to extensively modify many cellular pathways, most importantly the down-modulation of CD4 and MHC class I from the cell surface through the cooperation of cellular cofactors including clathrin adapters [79]. In the case of CD4, this down-regulation is thought to both inhibit re-infection by additional viruses, as well as promote viral escape from the cell surface. By down-modulating MHC class I from the cell surface, Nef interferes with the ability of infected cells to present viral antigens and thereby escape killing by cytotoxic T lymphocytes [87, 88] (Figure 1.2).

The viral infectivity factor (Vif) protein of HIV-1 has been found to interact with and induce the degradation of certain members of the apolipoprotein B mRNA editing enzyme, catalytic polypeptide-like family of proteins [89]. Of these, APOBEC-3G, and -3F proteins are specifically incorporated into HIV-1 virions and induce hypermutations in the viral genome during the process of reverse transcription through their enzymatic activity as cytidine deaminases. By deaminating cytidine residues to uracil on the minus strand of viral cDNA, which corresponds to guanine to thymine changes on the positive, coding strand. The result of which is the introduction of stop codons or other deleterious amino acid substitutions which are detrimental to viral replication [90, 91]. It should also be noted that APOBEC proteins can also interfere with the process of reverse transcription through deamination-independent mechanisms [92] (Figure 1.2).

As with Nef and Vif, the viral protein R (Vpr) of HIV-1 has also been shown to perturb cellular processes and promote viral replication. Although the exact function of Vpr remains to be elucidated, it is known to be particularly important in macrophages [93]. As non-dividing, terminally differentiated cells, macrophages present a particularly

difficult environment for viral replication. This is due to limitation of certain resources in these cells, as well as the presence of many innate immune sensors which detect and inhibit viral replication. However, unlike other retroviruses, lentiviruses such as HIV-1 possess the unique ability to replicate within terminally differentiated cells. This ability is likely due in large part to the activities of Vpr, which is required for efficient viral replication in macrophages and dendritic cells [94]. Thusfar, Vpr has been observed to induce cell cycle arrest [95], modulate apoptosis [96, 97], activate the ATM and ATR DNA damage responses [98-100], induce expression of NK cell ligands [100, 101],and degrade the DNA uracil glycosylase UNG2 through interaction with DCAF1 [102]. Collectively, these activities or Vpr likely promote viral replication, particularly in terminally differentiated cells through creating an intracellular environment more conducive for reverse transcription to take place [94] (Figure 1.2).

Of great interest recently has been the discovery of a novel restriction factor, sterile alpha motif domain and HD domain-containing protein 1 (SAMHD1). This protein is present in most cells, but is thought to be active only in terminally differentiated cells such as macrophages and dendritic cells as well as in resting $CD4^+$ T cells. Its primary function in these cells is to deplete cellular dNTP pools through its enzymatic nucleotide phosphatase activity. With respect to retroviral replication, this activity is also detrimental to the synthesis of viral cDNA during reverse transcription. Although HIV-1 does not appear to be able to antagonize SAMHD1 activity, two closely related viruses, HIV-2 and SIV, both express an additional accessory protein Vpx (which appears to have been derived from Vpr) which is able to induce degradation of SAMHD1 [103-107]. Although the implications of this difference are not entirely clear, it is likely that HIV-1

has either not yet evolved the capability to antagonize SAMHD1 or that it has evolved to replicate primarily in activated T lymphocytes, in which SAMDH1 is not active, thereby making Vpx non-essential for its replication [108, 109] (Figure 1.2).

Another family of proteins, the tripartite motif-containing (TRIM) proteins, have been identified as antiviral restriction factors, some of which target retroviral capsids [110]. In particular TRIM5α from Rhesus macaques and TRIMCyp from Owl monkeys have both been shown to potently inhibit replication of HIV-1 [111, 112]. Soon after infection, these proteins are able to bind to retroviral capsids, inhibit reverse transcription, and accelerate uncoating [113-118]. Although humans also express TRIM5α, HIV-1 has escaped its restrictive activity though mutation of its capsid domain [110] (Figure 1.2).

The viral protein U (Vpu) of HIV-1 has also been of great interest recently. Although it was long known that Vpu decreases cell-surface expression of CD4 [119] and enhances production of virus from certain cell types [120-122], the mechanism of this enhancement has only recently become clear. Through the use of heterokaryons, formed from fusion of permissive and non-permissive cells, Vpu was shown to reverse the effect of some dominant negative factor which is present in non-permissive cells [123]. This negative factor was later identified to be BST-2/tetherin, which both inhibits HIV-1 release and is antagonized by Vpu [124, 125] (Figure 1.2).

Tetherin is present in all mammals, and exhibits a unique topology with respect to all known mammalian proteins. This small protein contains both an N-terminal transmembrane domain, as well as a predicted C-terminal glycosylphosphatidylinositol (GPI) anchor [126]. Tetherin has been shown to modulate the production of interferon by

plasmacytoid dendritic cells, through interaction with the ILT-7 receptor [127, 128], but growing evidence supports the hypothesis that its function is primarily antiviral in nature [129]. This model is supported by the finding that tetherin knockout mice display no obvious morphological abnormalities or immune dysfunction, other than lack of tetherin-mediated antiviral activity [130].

Much is known about the mechanisms by which several viruses counteract tetherin antiviral activity. The HIV-1 Vpu protein has been shown to bind directly to tetherin through interactions between their transmembrane domains [131]. Vpu has also been shown to induce degradation of tetherin through utilization of a cellular ubiquitin-ligase complex, β-TrCP [132, 133]. This interaction has also been shown to result in non-classical ubiquitination of tetherin [134, 135]. It has also been shown that Vpu is able to antagonize tetherin function through other mechanisms which do not involve ubiquitination and degradation [136-138].

Taken together, these findings have greatly expanded our understanding of how the innate immune system acts to limit the replication of viruses at the level of single cells. Restriction factors as defined above constitute a network of intrinsic cellular immunity which constitute a substantial barrier to viral infection, especially of retroviruses such as HIV-1. As successful and persistent pathogens, many viruses have evolved mechanisms to evade or inhibit these pathways, and thereby create a permissive cellular niche in which to replicate and avoid detection and destruction by the immune response [84-86].

Despite these detailed insights into tetherin antagonism by different viruses, the more fundamental question remains unanswered; how is tetherin recruited to virus

assembly sites in the absence of viral antagonism? While tetherin is known to associate intimately with assembling viruses, the mechanism behind this recruitment remains to be described [139]. It has been hypothesized by many that recruitment of tetherin to HIV-1 assembly sites is mediated by its presence in detergent-resistant membranes [126], which are also present at HIV-1 assembly sites [42]. In chapter 2 of this thesis, I address directly, for the first time, the question of how tetherin is recruited to HIV-1 assembly sites. This study has led to the identification of viral and cellular determinants which mediate and enhance tetherin recruitment to HIV-1 assembly sites. By understanding the fundamental mechanisms by which tetherin is able to sense and target HIV-1, we may gain greater insight into the ability of tetherin to broadly inhibit other enveloped viruses. We may also be able to design therapeutic strategies which enhance tetherin antiviral activity, or inhibit the viral countermeasures which antagonize its function.

Super-Resolution Microscopy Techniques and Applications

The interrogation of intact biological systems has been greatly aided by the development of fluorescence microscopy techniques. Although inherently limited by diffraction, light microscopy allows for the specific labeling of molecules of interest with chemical fluorophores or fluorescent proteins. This can be accomplished by a variety of different methods including direct fluorophore conjugation to molecules of interest or their cognate ligands, immunofluorescence by fluorescently-labeled antibodies, or genetic fusion of fluorescent proteins such as green fluorescent protein (GFP) to target proteins of interest. While more detailed spatial information can be acquired through the use of various electron microscopy techniques, these are severely limited in their ability to label

specific molecules, as well as the laborious process of sample preparation [140]. Since the discovery of GFP [141] and other related fluorescent proteins from various marine organisms [142], these proteins have emerged as powerful tools for fluorescence microscopy.

Recently, advancements in optics, imaging techniques, and image processing algorithms have allowed for the development of various forms of super-resolution microscopy. Using these techniques, detailed spatial information about the location of single molecules can be obtained well below the diffraction limit of light (~200 nm).

There are several obstacles to the localization of single molecules or fluorophores with high precision beyond the limits imposed by diffraction. These include the sensitivity of detectors to capture sufficient signal from individual fluorophores, the separation of true signal from other noise and background fluorescence which may be present in the sample, as well as the ability to discriminate individual molecules from each other when they are present in high abundance. A variety of strategies can be used to circumvent or avoid these problems [143].

There are several types of super-resolution microscopy, including structured illumination microscopy (SIM) [144, 145], stimulated emission depletion microscopy (STED) [146-148] , photoactivated localization microscopy (PALM) [149], and stochastic optical reconstruction microscopy (STORM/dSTORM) [150, 151].

In general terms, localization of individual molecules can be accomplished by assuming that the diffraction-limited images created by single fluorophores on a detector can be described by an Airy function. Given that these functions closely resemble Gaussian functions, they can be fit mathematically, which allows for localization of

single fluorophores with extremely high precision (10-20 nm) [143]. More sensitive detection of individual fluorophores has been achieved through the development of the electron multiplying charge coupled devide (EMCCD). These devices have superior sensitivity and speed when compared with conventional charge coupled devices (CCDs) [152].

In order to eliminate excessive background signal and out-of-focus light frequently present in biological samples, total internal reflection fluorescence (TIRF) illumination is typically used. In TIRF microscopy, a coherent laser excitation source is positioned so that it strikes the coverslip at an angle at or below the critical angle (θ_c). When introduced in this way, excitation light is internally reflected within the coverslip, rather than being refracted into the sample. Through interaction with the surface of the coverslip immediately opposed to the sample, an evanescent wave is generated which penetrates only 50-200 nm into the sample, depending on the wavelength used and the angle of incidence [153] (Figure 1.4). This technique is particularly well suited for the study of processes which take place at the plasma membrane, and is frequently used for super-resolution microscopy methods because of the minimal contribution of background and out-of-focus fluorescence [143].

In order to distinguish single fluorophores when present at a high density, a subset of total fluorophores in the sample must be emitting fluorescence at any given time. This can be accomplished through the use of periodic illumination patters (SIM) [144, 145] or through stimulated emission of fluorophores (STED) [146-148]. Alternatively, certain organic fluorophores and fluorescent proteins are capable of either photoconversion

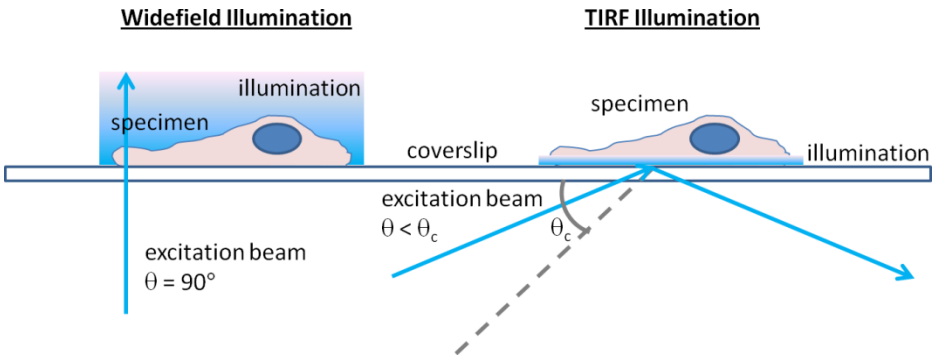

Figure 1.4. Explanation of total internal reflection microscopy (TIRF).
In conventional, or widefield illumination microscopy, excitation light is directed perpendicular to the coverslip. This results in illumination of a large section of the sample, which also results in out-of-focus fluorescence and background signals. In TIRF illumination, the excitation beam strikes the coverslip at an angle which is less than the critical angle or θ_c. The critical angle is defined as the angle at which incident light is completely reflected within the coverslip, rather than being refracted into the sample. When total internal reflection has been achieved, an evanescent wave is generated at the glass–sample interface with the same wavelength as the excitation source. This allows for selective illumination of fluorophores which are very near the interface. This penetration depth is usually 50–200 nm, depending on the incident angle and wavelength used.

or reversible photo-blinking. In the case of organic cyanine and rhodamine based fluorophores, reversible conversion between bright and dark states can be accomplished by placing samples in a reducing buffer (Figure 1.5).

Conventional STORM utilizes fluorophore pairs conjugated to molecules of interest, which are activated and deactivated by different wavelengths of light to accomplish reversible photoconversion [150]. Recently, an improved technique referred to as direct-STORM (dSTORM) has been developed, which utilizes single fluorophores, such as Alexa Fluor 647, which can be both activated and deactivated by a single wavelength of light (Figure 1.5). This technique is much easier to accomplish because of the ease of single fluorophore-conjugation, as well as the use of less-complicated optical systems [151, 154].

Photoactivatable fluorescent proteins such as photoactivatable GFP (PA-GFP) and photoactivatable mCherry (PA-mCherry) can be converted from dark to fluorescent states

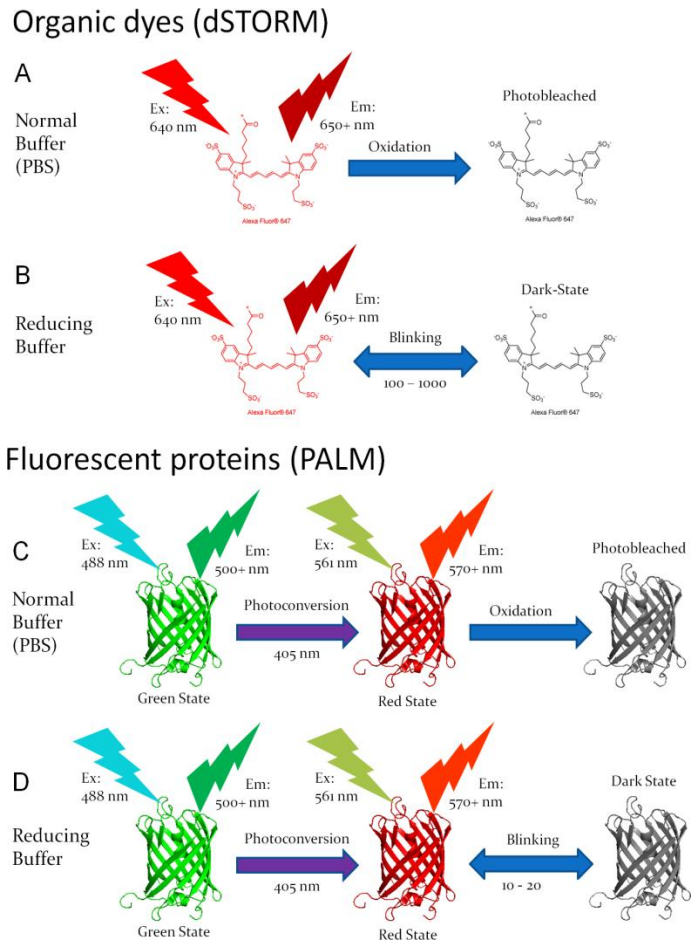

Figure 1.5. Schematic overview of dSTORM and PALM techniques used in this thesis.
(A) Under normal, oxidizing conditions excitation by high intensity laser light results in irreversible photobleaching of fluorophores such as Alexa Fluor 647, due to oxidation of the fluorophore. (B) Under reducing conditions, fluorophores can transition many times between their bright, fluorescent state and a dark state, because oxygen is not available for oxidation of the fluorophore. (C,D) Similarly, fluorescent proteins such as mEos3.2 (mEos2 is depicted here, PDB: 3S05) can be photoconverted from a green-emitting state to a red-emitting state by low levels of UV (405 nm) laser stimulation. (C) Under normal conditions, excitation of the red state by high intensity laser light results in irreversible photobleaching of the chromophore. (D) Under reducing conditions, however, mEos3.2 behaves in a similar way to Alexa Fluor 647, undergoing reversible photo-blinking between its bright, fluorescent state and a dark state.

by ultraviolet (UV) light (PALM). Other fluorescent proteins such as EosFP derivatives, Dendra, Dronpa, Kaede, and others are capable of being converted from one fluorescent state to another [155]. When combined with rapid photobleaching by high intensity excitation, a subset of fluorophores can be selectively imaged over time to generate a reconstructed image representing the ensemble of all fluorphores, each localized with

high precision [143]. Recently it has been reported that EosFP-derived proteins, in particular, exhibit superior spectral properties which make them ideally suited to super-resolution microscopy methods [149, 156, 157]. It has also been shown that these proteins are able to undergo reversible photoblinking under reducing conditions [158] (Figure 1.5).

For the studies presented in chapters 2 and 3 of this thesis, we chose to utilize a system which combines the advantages of PALM and dSTORM. In particular, we utilized Alexa Fluor 647 and the monomeric, photoconvertible fluorescent protein mEos3.2 for these experiments because of their superior spectral properties and compatibility with reducing buffers [154, 157, 158].

Given that many viruses such as HIV-1 are smaller than the diffraction limit of conventional light microscopy (~100 nm diameter), super-resolution localization microscopy offers a powerful method to study viral assembly and virus-host interactions at the level of single virus particles with unprecedented detail. Thus far, various super-resolution microscopy techniques have been employed to study interactions between tetherin and HIV-1 assembly sites [159, 160], HIV-1 virion morphology [149, 161, 162], HIV-1 protein distribution during virus entry [163, 164], and Env incorporation to virus particles [61]. Super-resolution microscopy has also been applied to study influenza HA protein [165], vaccinia virus [166, 167], and RNA virus replication complexes in plants [168].

In work presented in this thesis, I have applied super-resolution localization microscopy techniques to identify and characterize different mechanisms by which host proteins can be incorporated into HIV-1 assembly sites.

REFERENCES

1. Barre-Sinoussi, F., et al., *Isolation of a T-lymphotropic retrovirus from a patient at risk for acquired immune deficiency syndrome (AIDS).* Science, 1983. **220**(4599): p. 868-71.

2. Gallo, R.C., et al., *Isolation of human T-cell leukemia virus in acquired immune deficiency syndrome (AIDS).* Science, 1983. **220**(4599): p. 865-7.

3. Montagnier, L., *25 years after HIV discovery: prospects for cure and vaccine.* Virology, 2010. **397**(2): p. 248-54.

4. WHO. *Global summary of the AIDS epidemic*. 2011.

5. Pantaleo, G. and Y. Levy, *Vaccine and immunotherapeutic interventions.* Curr Opin HIV AIDS, 2013. **8**(3): p. 236-42.

6. Vella, S., et al., *The history of antiretroviral therapy and of its implementation in resource-limited areas of the world.* AIDS, 2012. **26**(10): p. 1231-41.

7. Adachi, A., et al., *Production of acquired immunodeficiency syndrome-associated retrovirus in human and nonhuman cells transfected with an infectious molecular clone.* J Virol, 1986. **59**(2): p. 284-91.

8. Lassen, K., et al., *The multifactorial nature of HIV-1 latency.* Trends Mol Med, 2004. **10**(11): p. 525-31.

9. Pasman, L., *The complication of coinfection.* Yale J Biol Med, 2012. **85**(1): p. 127-32.

10. Cloyd, M.W., J.J. Chen, and I. Wang, *How does HIV cause AIDS? The homing theory.* Mol Med Today, 2000. **6**(3): p. 108-11.

11. Gougeon, M.L. and L. Montagnier, *Apoptosis in AIDS.* Science, 1993. **260**(5112): p. 1269-70.

12. Onafuwa-Nuga, A., L.A. McNamara, and K.L. Collins, *Towards a cure for HIV: the identification and characterization of HIV reservoirs in optimally treated people.* Cell Res, 2010. **20**(11): p. 1185-7.

13. Xing, S. and R.F. Siliciano, *Targeting HIV latency: pharmacologic strategies toward eradication.* Drug Discov Today, 2012.

14. Levy, J.A., et al., *Isolation of lymphocytopathic retroviruses from San Francisco patients with AIDS.* Science, 1984. **225**(4664): p. 840-2.

15. Zhang, C.W., et al., *Expression, purification, and characterization of recombinant HIV gp140. The gp41 ectodomain of HIV or simian immunodeficiency virus is*

sufficient to maintain the retroviral envelope glycoprotein as a trimer. J Biol Chem, 2001. **276**(43): p. 39577-85.

16. Blumenthal, R., S. Durell, and M. Viard, *HIV entry and envelope glycoprotein-mediated fusion.* J Biol Chem, 2012. **287**(49): p. 40841-9.

17. Barat, C., et al., *HIV-1 reverse transcriptase specifically interacts with the anticodon domain of its cognate primer tRNA.* EMBO J, 1989. **8**(11): p. 3279-85.

18. Hu, W.S. and S.H. Hughes, *HIV-1 reverse transcription.* Cold Spring Harb Perspect Med, 2012. **2**(10).

19. Krishnan, L. and A. Engelman, *Retroviral integrase proteins and HIV-1 DNA integration.* J Biol Chem, 2012. **287**(49): p. 40858-66.

20. Vink, C. and R.H. Plasterk, *The human immunodeficiency virus integrase protein.* Trends Genet, 1993. **9**(12): p. 433-8.

21. Stoltzfus, C.M., *Chapter 1. Regulation of HIV-1 alternative RNA splicing and its role in virus replication.* Adv Virus Res, 2009. **74**: p. 1-40.

22. Debaisieux, S., et al., *The ins and outs of HIV-1 Tat.* Traffic, 2012. **13**(3): p. 355-63.

23. Garcia, J.A., et al., *Functional domains required for tat-induced transcriptional activation of the HIV-1 long terminal repeat.* EMBO J, 1988. **7**(10): p. 3143-7.

24. Kao, S.Y., et al., *Anti-termination of transcription within the long terminal repeat of HIV-1 by tat gene product.* Nature, 1987. **330**(6147): p. 489-93.

25. Feng, S. and E.C. Holland, *HIV-1 tat trans-activation requires the loop sequence within tar.* Nature, 1988. **334**(6178): p. 165-7.

26. Laspia, M.F., A.P. Rice, and M.B. Mathews, *HIV-1 Tat protein increases transcriptional initiation and stabilizes elongation.* Cell, 1989. **59**(2): p. 283-92.

27. Selby, M.J., et al., *Structure, sequence, and position of the stem-loop in tar determine transcriptional elongation by tat through the HIV-1 long terminal repeat.* Genes Dev, 1989. **3**(4): p. 547-58.

28. Long, K.S. and D.M. Crothers, *Characterization of the solution conformations of unbound and Tat peptide-bound forms of HIV-1 TAR RNA.* Biochemistry, 1999. **38**(31): p. 10059-69.

29. Suhasini, M. and T.R. Reddy, *Cellular proteins and HIV-1 Rev function.* Curr HIV Res, 2009. **7**(1): p. 91-100.

30. Malim, M.H., et al., *The HIV-1 rev trans-activator acts through a structured target sequence to activate nuclear export of unspliced viral mRNA.* Nature, 1989. **338**(6212): p. 254-7.

31. Heaphy, S., et al., *HIV-1 regulator of virion expression (Rev) protein binds to an RNA stem-loop structure located within the Rev response element region.* Cell, 1990. **60**(4): p. 685-93.

32. Kjems, J., et al., *Structural analysis of the interaction between the human immunodeficiency virus Rev protein and the Rev response element.* Proc Natl Acad Sci U S A, 1991. **88**(3): p. 683-7.

33. Shioda, T. and H. Shibuta, *Production of human immunodeficiency virus (HIV)-like particles from cells infected with recombinant vaccinia viruses carrying the gag gene of HIV.* Virology, 1990. **175**(1): p. 139-48.

34. Wilson, W., et al., *HIV expression strategies: ribosomal frameshifting is directed by a short sequence in both mammalian and yeast systems.* Cell, 1988. **55**(6): p. 1159-69.

35. Ganser-Pornillos, B.K., M. Yeager, and O. Pornillos, *Assembly and architecture of HIV.* Adv Exp Med Biol, 2012. **726**: p. 441-65.

36. Gottlinger, H.G., J.G. Sodroski, and W.A. Haseltine, *Role of capsid precursor processing and myristoylation in morphogenesis and infectivity of human immunodeficiency virus type 1.* Proc Natl Acad Sci U S A, 1989. **86**(15): p. 5781-5.

37. Ono, A., et al., *Phosphatidylinositol (4,5) bisphosphate regulates HIV-1 Gag targeting to the plasma membrane.* Proc Natl Acad Sci U S A, 2004. **101**(41): p. 14889-94.

38. Saad, J.S., et al., *Structural basis for targeting HIV-1 Gag proteins to the plasma membrane for virus assembly.* Proc Natl Acad Sci U S A, 2006. **103**(30): p. 11364-9.

39. Chukkapalli, V., et al., *Interaction between the human immunodeficiency virus type 1 Gag matrix domain and phosphatidylinositol-(4,5)-bisphosphate is essential for efficient gag membrane binding.* J Virol, 2008. **82**(5): p. 2405-17.

40. Ono, A., *HIV-1 Assembly at the Plasma Membrane: Gag Trafficking and Localization.* Future Virol, 2009. **4**(3): p. 241-257.

41. Chukkapalli, V. and A. Ono, *Molecular determinants that regulate plasma membrane association of HIV-1 Gag.* J Mol Biol, 2011. **410**(4): p. 512-24.

42. Ono, A. and E.O. Freed, *Plasma membrane rafts play a critical role in HIV-1 assembly and release.* Proc Natl Acad Sci U S A, 2001. **98**(24): p. 13925-30.

43. Nydegger, S., et al., *Mapping of tetraspanin-enriched microdomains that can function as gateways for HIV-1.* J Cell Biol, 2006. **173**(5): p. 795-807.

44. Jolly, C. and Q.J. Sattentau, *Human immunodeficiency virus type 1 assembly, budding, and cell-cell spread in T cells take place in tetraspanin-enriched plasma membrane domains.* J Virol, 2007. **81**(15): p. 7873-84.

45. Garcia, E., D.S. Nikolic, and V. Piguet, *HIV-1 replication in dendritic cells occurs through a tetraspanin-containing compartment enriched in AP-3.* Traffic, 2008. **9**(2): p. 200-14.

46. Grigorov, B., et al., *A role for CD81 on the late steps of HIV-1 replication in a chronically infected T cell line.* Retrovirology, 2009. **6**: p. 28.

47. Thali, M., *Tetraspanin functions during HIV-1 and influenza virus replication.* Biochem Soc Trans, 2011. **39**(2): p. 529-31.

48. Llewellyn, G.N., et al., *Nucleocapsid promotes localization of HIV-1 gag to uropods that participate in virological synapses between T cells.* PLoS Pathog, 2010. **6**(10): p. e1001167.

49. Llewellyn, G.N., et al., *HIV-1 Gag Associates with Specific Uropod-Directed Microdomains in a Manner Dependent on its MA Highly Basic Region.* J Virol, 2013.

50. Krementsov, D.N., et al., *HIV-1 assembly differentially alters dynamics and partitioning of tetraspanins and raft components.* Traffic, 2010. **11**(11): p. 1401-14.

51. Hogue, I.B., et al., *Gag induces the coalescence of clustered lipid rafts and tetraspanin-enriched microdomains at HIV-1 assembly sites on the plasma membrane.* J Virol, 2011. **85**(19): p. 9749-66.

52. Burniston, M.T., et al., *Human immunodeficiency virus type 1 Gag polyprotein multimerization requires the nucleocapsid domain and RNA and is promoted by the capsid-dimer interface and the basic region of matrix protein.* J Virol, 1999. **73**(10): p. 8527-40.

53. Hogue, I.B., A. Hoppe, and A. Ono, *Quantitative fluorescence resonance energy transfer microscopy analysis of the human immunodeficiency virus type 1 Gag-Gag interaction: relative contributions of the CA and NC domains and membrane binding.* J Virol, 2009. **83**(14): p. 7322-36.

54. Bharat, T.A., et al., *Structure of the immature retroviral capsid at 8 A resolution by cryo-electron microscopy.* Nature, 2012. **487**(7407): p. 385-9.

55. Datta, S.A., et al., *On the role of the SP1 domain in HIV-1 particle assembly: a molecular switch?* J Virol, 2011. **85**(9): p. 4111-21.

56. Skripkin, E., et al., *Identification of the primary site of the human immunodeficiency virus type 1 RNA dimerization in vitro.* Proc Natl Acad Sci U S A, 1994. **91**(11): p. 4945-9.

57. Lu, K., X. Heng, and M.F. Summers, *Structural determinants and mechanism of HIV-1 genome packaging.* J Mol Biol, 2011. **410**(4): p. 609-33.

58. Lu, K., et al., *NMR detection of structures in the HIV-1 5'-leader RNA that regulate genome packaging.* Science, 2011. **334**(6053): p. 242-5.

59. South, T.L. and M.F. Summers, *Zinc- and sequence-dependent binding to nucleic acids by the N-terminal zinc finger of the HIV-1 nucleocapsid protein: NMR structure of the complex with the Psi-site analog, dACGCC.* Protein Sci, 1993. **2**(1): p. 3-19.

60. Postler, T.S. and R.C. Desrosiers, *The tale of the long tail: the cytoplasmic domain of HIV-1 gp41.* J Virol, 2013. **87**(1): p. 2-15.

61. Muranyi, W., et al., *Super-resolution microscopy reveals specific recruitment of HIV-1 envelope proteins to viral assembly sites dependent on the envelope C-terminal tail.* PLoS Pathog, 2013. **9**(2): p. e1003198.

62. Sundquist, W.I. and H.G. Krausslich, *HIV-1 assembly, budding, and maturation.* Cold Spring Harb Perspect Med, 2012. **2**(7): p. a006924.

63. Garrus, J.E., et al., *Tsg101 and the vacuolar protein sorting pathway are essential for HIV-1 budding.* Cell, 2001. **107**(1): p. 55-65.

64. McCullough, J., L.A. Colf, and W.I. Sundquist, *Membrane Fission Reactions of the Mammalian ESCRT Pathway.* Annu Rev Biochem, 2013.

65. Morita, E., et al., *Human ESCRT and ALIX proteins interact with proteins of the midbody and function in cytokinesis.* EMBO J, 2007. **26**(19): p. 4215-27.

66. Hurley, J.H. and P.I. Hanson, *Membrane budding and scission by the ESCRT machinery: it's all in the neck.* Nat Rev Mol Cell Biol, 2010. **11**(8): p. 556-66.

67. von Schwedler, U.K., et al., *The protein network of HIV budding.* Cell, 2003. **114**(6): p. 701-13.

68. Pornillos, O., et al., *HIV Gag mimics the Tsg101-recruiting activity of the human Hrs protein.* J Cell Biol, 2003. **162**(3): p. 425-34.

69. VerPlank, L., et al., *Tsg101, a homologue of ubiquitin-conjugating (E2) enzymes, binds the L domain in HIV type 1 Pr55(Gag).* Proc Natl Acad Sci U S A, 2001. **98**(14): p. 7724-9.

70. Pornillos, O., et al., *Structure of the Tsg101 UEV domain in complex with the PTAP motif of the HIV-1 p6 protein.* Nat Struct Biol, 2002. **9**(11): p. 812-7.

71. Dowlatshahi, D.P., et al., *ALIX is a Lys63-specific polyubiquitin binding protein that functions in retrovirus budding.* Dev Cell, 2012. **23**(6): p. 1247-54.

72. Strack, B., et al., *AIP1/ALIX is a binding partner for HIV-1 p6 and EIAV p9 functioning in virus budding.* Cell, 2003. **114**(6): p. 689-99.

73. Popov, S., et al., *Human immunodeficiency virus type 1 Gag engages the Bro1 domain of ALIX/AIP1 through the nucleocapsid.* J Virol, 2008. **82**(3): p. 1389-98.

74. Dussupt, V., et al., *Basic residues in the nucleocapsid domain of Gag are critical for late events of HIV-1 budding.* J Virol, 2011. **85**(5): p. 2304-15.

75. Konvalinka, J., et al., *Proteolytic processing of particle-associated retroviral polyproteins by homologous and heterologous viral proteinases.* Eur J Biochem, 1995. **228**(1): p. 191-8.

76. Nakayama, K., *Furin: a mammalian subtilisin/Kex2p-like endoprotease involved in processing of a wide variety of precursor proteins.* Biochem J, 1997. **327 (Pt 3)**: p. 625-35.

77. Malim, M.H. and M. Emerman, *HIV-1 accessory proteins--ensuring viral survival in a hostile environment.* Cell Host Microbe, 2008. **3**(6): p. 388-98.

78. Nomaguchi, M., et al., *Species tropism of HIV-1 modulated by viral accessory proteins.* Front Microbiol, 2012. **3**: p. 267.

79. Nishino, Y., et al., *Human immunodeficiency virus type 1 vif, vpr, and vpu mutants can produce persistently infected cells.* Arch Virol, 1991. **120**(3-4): p. 181-92.

80. Niederman, T.M., W. Hu, and L. Ratner, *Simian immunodeficiency virus negative factor suppresses the level of viral mRNA in COS cells.* J Virol, 1991. **65**(7): p. 3538-46.

81. Zou, W., et al., *Nef functions in BLT mice to enhance HIV-1 replication and deplete CD4+CD8+ thymocytes.* Retrovirology, 2012. **9**: p. 44.

82. Fauci, A.S. and R.C. Desrosiers, *Pathogenesis of HIV and SIV.* 1997.

83. Hatziioannou, T. and P.D. Bieniasz, *Antiretroviral restriction factors.* Curr Opin Virol, 2011. **1**(6): p. 526-32.

84. Harris, R.S., J.F. Hultquist, and D.T. Evans, *The restriction factors of human immunodeficiency virus.* J Biol Chem, 2012. **287**(49): p. 40875-83.

85. Duggal, N.K. and M. Emerman, *Evolutionary conflicts between viruses and restriction factors shape immunity.* Nat Rev Immunol, 2012. **12**(10): p. 687-95.

86. Malim, M.H. and P.D. Bieniasz, *HIV Restriction Factors and Mechanisms of Evasion.* Cold Spring Harb Perspect Med, 2012. **2**(5): p. a006940.

87. Wonderlich, E.R., J.A. Leonard, and K.L. Collins, *HIV immune evasion disruption of antigen presentation by the HIV Nef protein.* Adv Virus Res, 2011. **80**: p. 103-27.

88. Collins, K.L., et al., *HIV-1 Nef protein protects infected primary cells against killing by cytotoxic T lymphocytes.* Nature, 1998. **391**(6665): p. 397-401.

89. Sheehy, A.M., et al., *Isolation of a human gene that inhibits HIV-1 infection and is suppressed by the viral Vif protein.* Nature, 2002. **418**(6898): p. 646-50.

90. Romani, B., S. Engelbrecht, and R.H. Glashoff, *Antiviral roles of APOBEC proteins against HIV-1 and suppression by Vif.* Arch Virol, 2009. **154**(10): p. 1579-88.

91. Mangeat, B., et al., *Broad antiretroviral defence by human APOBEC3G through lethal editing of nascent reverse transcripts.* Nature, 2003. **424**(6944): p. 99-103.

92. Shindo, K., et al., *The enzymatic activity of CEM15/Apobec-3G is essential for the regulation of the infectivity of HIV-1 virion but not a sole determinant of its antiviral activity.* J Biol Chem, 2003. **278**(45): p. 44412-6.

93. Subbramanian, R.A., et al., *Human immunodeficiency virus type 1 Vpr is a positive regulator of viral transcription and infectivity in primary human macrophages.* J Exp Med, 1998. **187**(7): p. 1103-11.

94. Mashiba, M. and K.L. Collins, *Molecular mechanisms of HIV immune evasion of the innate immune response in myeloid cells.* Viruses, 2013. **5**(1): p. 1-14.

95. Jowett, J.B., et al., *The human immunodeficiency virus type 1 vpr gene arrests infected T cells in the G2 + M phase of the cell cycle.* J Virol, 1995. **69**(10): p. 6304-13.

96. Stewart, S.A., et al., *Human immunodeficiency virus type 1 Vpr induces apoptosis following cell cycle arrest.* J Virol, 1997. **71**(7): p. 5579-92.

97. Conti, L., et al., *The HIV-1 vpr protein acts as a negative regulator of apoptosis in a human lymphoblastoid T cell line: possible implications for the pathogenesis of AIDS.* J Exp Med, 1998. **187**(3): p. 403-13.

98. Poon, B., et al., *Human immunodeficiency virus type 1 vpr gene induces phenotypic effects similar to those of the DNA alkylating agent, nitrogen mustard.* J Virol, 1997. **71**(5): p. 3961-71.

99. Ward, J., et al., *HIV-1 Vpr triggers natural killer cell-mediated lysis of infected cells through activation of the ATR-mediated DNA damage response.* PLoS Pathog, 2009. **5**(10): p. e1000613.

100. Norman, J.M., et al., *The antiviral factor APOBEC3G enhances the recognition of HIV-infected primary T cells by natural killer cells.* Nat Immunol, 2011. **12**(10): p. 975-83.

101. Richard, J., et al., *HIV-1 Vpr up-regulates expression of ligands for the activating NKG2D receptor and promotes NK cell-mediated killing.* Blood, 2010. **115**(7): p. 1354-63.

102. Ahn, J., et al., *HIV-1 Vpr loads uracil DNA glycosylase-2 onto DCAF1, a substrate recognition subunit of a cullin 4A-ring E3 ubiquitin ligase for proteasome-dependent degradation.* J Biol Chem, 2010. **285**(48): p. 37333-41.

103. Laguette, N., et al., *SAMHD1 is the dendritic- and myeloid-cell-specific HIV-1 restriction factor counteracted by Vpx.* Nature, 2011. **474**(7353): p. 654-7.

104. Hrecka, K., et al., *Vpx relieves inhibition of HIV-1 infection of macrophages mediated by the SAMHD1 protein.* Nature, 2011. **474**(7353): p. 658-61.

105. Goldstone, D.C., et al., *HIV-1 restriction factor SAMHD1 is a deoxynucleoside triphosphate triphosphohydrolase.* Nature, 2011. **480**(7377): p. 379-82.

106. Powell, R.D., et al., *Aicardi-Goutieres syndrome gene and HIV-1 restriction factor SAMHD1 is a dGTP-regulated deoxynucleotide triphosphohydrolase.* J Biol Chem, 2011. **286**(51): p. 43596-600.

107. Berger, A., et al., *SAMHD1-deficient CD14+ cells from individuals with Aicardi-Goutieres syndrome are highly susceptible to HIV-1 infection.* PLoS Pathog, 2011. **7**(12): p. e1002425.

108. Baldauf, H.M., et al., *SAMHD1 restricts HIV-1 infection in resting CD4(+) T cells.* Nat Med, 2012. **18**(11): p. 1682-7.

109. Laguette, N. and M. Benkirane, *How SAMHD1 changes our view of viral restriction.* Trends Immunol, 2012. **33**(1): p. 26-33.

110. Grutter, M.G. and J. Luban, *TRIM5 structure, HIV-1 capsid recognition, and innate immune signaling.* Curr Opin Virol, 2012. **2**(2): p. 142-50.

111. Stremlau, M., et al., *The cytoplasmic body component TRIM5alpha restricts HIV-1 infection in Old World monkeys.* Nature, 2004. **427**(6977): p. 848-53.

112. Sayah, D.M., et al., *Cyclophilin A retrotransposition into TRIM5 explains owl monkey resistance to HIV-1.* Nature, 2004. **430**(6999): p. 569-73.

113. Diaz-Griffero, F., et al., *Requirements for capsid-binding and an effector function in TRIMCyp-mediated restriction of HIV-1.* Virology, 2006. **351**(2): p. 404-19.

114. Ganser-Pornillos, B.K., et al., *Hexagonal assembly of a restricting TRIM5alpha protein.* Proc Natl Acad Sci U S A, 2011. **108**(2): p. 534-9.

115. Biris, N., et al., *Structure of the rhesus monkey TRIM5alpha PRYSPRY domain, the HIV capsid recognition module.* Proc Natl Acad Sci U S A, 2012. **109**(33): p. 13278-83.

116. Roa, A., et al., *RING domain mutations uncouple TRIM5alpha restriction of HIV-1 from inhibition of reverse transcription and acceleration of uncoating.* J Virol, 2012. **86**(3): p. 1717-27.

117. Kim, J., C. Tipper, and J. Sodroski, *Role of TRIM5alpha RING domain E3 ubiquitin ligase activity in capsid disassembly, reverse transcription blockade, and restriction of simian immunodeficiency virus.* J Virol, 2011. **85**(16): p. 8116-32.

118. Tareen, S.U. and M. Emerman, *Human Trim5alpha has additional activities that are uncoupled from retroviral capsid recognition.* Virology, 2011. **409**(1): p. 113-20.

119. Geleziunas, R., S. Bour, and M.A. Wainberg, *Cell surface down-modulation of CD4 after infection by HIV-1.* FASEB J, 1994. **8**(9): p. 593-600.

120. Gottlinger, H.G., et al., *Vpu protein of human immunodeficiency virus type 1 enhances the release of capsids produced by gag gene constructs of widely divergent retroviruses.* Proc Natl Acad Sci U S A, 1993. **90**(15): p. 7381-5.

121. Geraghty, R.J., et al., *Cell type-dependence for Vpu function.* J Med Primatol, 1994. **23**(2-3): p. 146-50.

122. Schubert, U., K.A. Clouse, and K. Strebel, *Augmentation of virus secretion by the human immunodeficiency virus type 1 Vpu protein is cell type independent and occurs in cultured human primary macrophages and lymphocytes.* J Virol, 1995. **69**(12): p. 7699-711.

123. Varthakavi, V., et al., *Viral protein U counteracts a human host cell restriction that inhibits HIV-1 particle production.* Proc Natl Acad Sci U S A, 2003. **100**(25): p. 15154-9.

124. Neil, S.J., T. Zang, and P.D. Bieniasz, *Tetherin inhibits retrovirus release and is antagonized by HIV-1 Vpu.* Nature, 2008. **451**(7177): p. 425-30.

125. Van Damme, N., et al., *The interferon-induced protein BST-2 restricts HIV-1 release and is downregulated from the cell surface by the viral Vpu protein.* Cell Host Microbe, 2008. **3**(4): p. 245-52.

126. Kupzig, S., et al., *Bst-2/HM1.24 is a raft-associated apical membrane protein with an unusual topology.* Traffic, 2003. **4**(10): p. 694-709.

127. Cao, W., et al., *Regulation of TLR7/9 responses in plasmacytoid dendritic cells by BST2 and ILT7 receptor interaction.* J Exp Med, 2009. **206**(7): p. 1603-14.

128. Cao, W. and L. Bover, *Signaling and ligand interaction of ILT7: receptor-mediated regulatory mechanisms for plasmacytoid dendritic cells.* Immunol Rev, 2010. **234**(1): p. 163-76.

129. Swiecki, M., N.S. Omattage, and T.J. Brett, *BST-2/tetherin: structural biology, viral antagonism, and immunobiology of a potent host antiviral factor.* Mol Immunol, 2013. **54**(2): p. 132-9.

130. Liberatore, R.A. and P.D. Bieniasz, *Tetherin is a key effector of the antiretroviral activity of type I interferon in vitro and in vivo.* Proc Natl Acad Sci U S A, 2011. **108**(44): p. 18097-101.

131. Vigan, R. and S.J. Neil, *Determinants of tetherin antagonism in the transmembrane domain of the human immunodeficiency virus type 1 Vpu protein.* J Virol, 2010. **84**(24): p. 12958-70.

132. Mitchell, R.S., et al., *Vpu antagonizes BST-2-mediated restriction of HIV-1 release via beta-TrCP and endo-lysosomal trafficking.* PLoS Pathog, 2009. **5**(5): p. e1000450.

133. Mangeat, B., et al., *HIV-1 Vpu neutralizes the antiviral factor Tetherin/BST-2 by binding it and directing its beta-TrCP2-dependent degradation.* PLoS Pathog, 2009. **5**(9): p. e1000574.

134. Gustin, J.K., et al., *Ubiquitination of BST-2 protein by HIV-1 Vpu protein does not require lysine, serine, or threonine residues within the BST-2 cytoplasmic domain.* J Biol Chem, 2012. **287**(18): p. 14837-50.

135. Tokarev, A.A., J. Munguia, and J.C. Guatelli, *Serine-threonine ubiquitination mediates downregulation of BST-2/tetherin and relief of restricted virion release by HIV-1 Vpu.* J Virol, 2011. **85**(1): p. 51-63.

136. Dube, M., et al., *Antagonism of tetherin restriction of HIV-1 release by Vpu involves binding and sequestration of the restriction factor in a perinuclear compartment.* PLoS Pathog, 2010. **6**(4): p. e1000856.

137. Tervo, H.M., et al., *beta-TrCP is dispensable for Vpu's ability to overcome the CD317/Tetherin-imposed restriction to HIV-1 release.* Retrovirology, 2011. **8**: p. 9.

138. Schmidt, S., et al., *HIV-1 Vpu blocks recycling and biosynthetic transport of the intrinsic immunity factor CD317/tetherin to overcome the virion release restriction.* MBio, 2011. **2**(3): p. e00036-11.

139. Fitzpatrick, K., et al., *Direct restriction of virus release and incorporation of the interferon-induced protein BST-2 into HIV-1 particles.* PLoS Pathog, 2010. **6**(3): p. e1000701.

140. Moerner, W.E., *Microscopy beyond the diffraction limit using actively controlled single molecules.* J Microsc, 2012. **246**(3): p. 213-20.

141. Shimomura, O., F.H. Johnson, and Y. Saiga, *Extraction, purification and properties of aequorin, a bioluminescent protein from the luminous hydromedusan, Aequorea.* J Cell Comp Physiol, 1962. **59**: p. 223-39.

142. Bourgeois, D. and V. Adam, *Reversible photoswitching in fluorescent proteins: a mechanistic view.* IUBMB Life, 2012. **64**(6): p. 482-91.

143. Schermelleh, L., R. Heintzmann, and H. Leonhardt, *A guide to super-resolution fluorescence microscopy.* J Cell Biol, 2010. **190**(2): p. 165-75.

144. Gustafsson, M.G., *Surpassing the lateral resolution limit by a factor of two using structured illumination microscopy.* J Microsc, 2000. **198**(Pt 2): p. 82-7.

145. Heintzmann, R. and C. Cremer, *Laterally modulated excitation microscopy: Improvement of resolution by using a diffraction grating.* Optical Biopsies and Microscopic Techniques Iii, Proceedings Of, 1999. **3568**: p. 185-196.

146. Hell, S.W. and J. Wichmann, *Breaking the diffraction resolution limit by stimulated emission: stimulated-emission-depletion fluorescence microscopy.* Opt Lett, 1994. **19**(11): p. 780-2.

147. Klar, T.A., E. Engel, and S.W. Hell, *Breaking Abbe's diffraction resolution limit in fluorescence microscopy with stimulated emission depletion beams of various shapes.* Phys Rev E Stat Nonlin Soft Matter Phys, 2001. **64**(6 Pt 2): p. 066613.

148. Dyba, M., S. Jakobs, and S.W. Hell, *Immunofluorescence stimulated emission depletion microscopy.* Nat Biotechnol, 2003. **21**(11): p. 1303-4.

149. Betzig, E., et al., *Imaging intracellular fluorescent proteins at nanometer resolution.* Science, 2006. **313**(5793): p. 1642-5.

150. Rust, M.J., M. Bates, and X. Zhuang, *Sub-diffraction-limit imaging by stochastic optical reconstruction microscopy (STORM).* Nat Methods, 2006. **3**(10): p. 793-5.

151. van de Linde, S., et al., *Direct stochastic optical reconstruction microscopy with standard fluorescent probes.* Nat Protoc, 2011. **6**(7): p. 991-1009.

152. Coates, C.G., et al., *Optimizing low-light microscopy with back-illuminated electron multiplying charge-coupled device: enhanced sensitivity, speed, and resolution.* J Biomed Opt, 2004. **9**(6): p. 1244-52.

153. Axelrod, D., N.L. Thompson, and T.P. Burghardt, *Total internal inflection fluorescent microscopy.* J Microsc, 1983. **129**(Pt 1): p. 19-28.

154. Lampe, A., et al., *Multi-colour direct STORM with red emitting carbocyanines.* Biol Cell, 2012. **104**(4): p. 229-37.

155. Baker, S.M., R.W. Buckheit, 3rd, and M.M. Falk, *Green-to-red photoconvertible fluorescent proteins: tracking cell and protein dynamics on standard wide-field mercury arc-based microscopes.* BMC Cell Biol, 2010. **11**: p. 15.

156. McKinney, S.A., et al., *A bright and photostable photoconvertible fluorescent protein.* Nat Methods, 2009. **6**(2): p. 131-3.

157. Zhang, M., et al., *Rational design of true monomeric and bright photoactivatable fluorescent proteins.* Nat Methods, 2012. **9**(7): p. 727-9.

158. Endesfelder, U., et al., *Chemically induced photoswitching of fluorescent probes--a general concept for super-resolution microscopy.* Molecules, 2011. **16**(4): p. 3106-18.

159. Hammonds, J., et al., *The tetherin/BST-2 coiled-coil ectodomain mediates plasma membrane microdomain localization and restriction of particle release.* J Virol, 2012. **86**(4): p. 2259-72.

160. Lehmann, M., et al., *Quantitative multicolor super-resolution microscopy reveals tetherin HIV-1 interaction.* PLoS Pathog, 2011. **7**(12): p. e1002456.

161. Gunzenhauser, J., et al., *Quantitative super-resolution imaging reveals protein stoichiometry and nanoscale morphology of assembling HIV-Gag virions.* Nano Lett, 2012. **12**(9): p. 4705-10.

162. Malkusch, S., et al., *Single-molecule coordinate-based analysis of the morphology of HIV-1 assembly sites with near-molecular spatial resolution.* Histochem Cell Biol, 2013. **139**(1): p. 173-9.

163. Lelek, M., et al., *Superresolution imaging of HIV in infected cells with FlAsH-PALM.* Proc Natl Acad Sci U S A, 2012. **109**(22): p. 8564-9.

164. Pereira, C.F., et al., *HIV taken by STORM: Super-resolution fluorescence microscopy of a viral infection.* Virology Journal, 2012. **9**.

165. Itano, M.S., et al., *Super-resolution imaging of C-type lectin and influenza hemagglutinin nanodomains on plasma membranes using blink microscopy.* Biophys J, 2012. **102**(7): p. 1534-42.

166. Horsington, J., et al., *Sub-viral imaging of vaccinia virus using super-resolution microscopy.* J Virol Methods, 2012. **186**(1-2): p. 132-6.

167. Horsington, J., et al., *A36-dependent Actin Filament Nucleation Promotes Release of Vaccinia Virus.* PLoS Pathog, 2013. **9**(3): p. e1003239.

168. Linnik, O., et al., *Unraveling the structure of viral replication complexes at super-resolution.* Front Plant Sci, 2013. **4**: p. 6.

CHAPTER II

Roles played by capsid-dependent induction of membrane curvature and Gag-ESCRT interactions in tetherin recruitment to HIV-1 assembly sites

Abstract

Tetherin/BST-2 (hereafter tetherin) is an antiviral protein that restricts release of diverse enveloped viruses from infected cells through physically tethering virus envelope and host plasma membrane. For HIV-1, specific recruitment of tetherin to assembly sites has been observed as its colocalization with viral structural protein Gag or its accumulation to virus particles. Because of its broad range of targets, we hypothesized that tetherin is recruited through conserved features shared among various enveloped viruses, such as lipid raft association, membrane curvature, or ESCRT dependence. We observed that reduction of cellular cholesterol does not block tetherin anti-HIV-1 function, excluding an essential role for lipid rafts. In contrast, mutations in the capsid domain of Gag, which inhibit induction of membrane curvature, prevented tetherin-Gag colocalization detectable by confocal microscopy. Disruption of Gag-ESCRT interactions also inhibited tetherin-Gag colocalization, when disruption was accomplished via amino acid substitutions in late domain motifs, expression of a dominant negative Tsg101

derivative, or siRNA-mediated depletion of Tsg101 or Alix. However, further analyses of these conditions by quantitative super-resolution localization microscopy revealed that Gag-tetherin coclustering is significantly reduced, but persists at intermediate levels. Notably, this residual tetherin recruitment was still sufficient for the full restriction of HIV-1 release. Unlike the late domain mutants, the capsid mutants defective in inducing membrane curvature showed little or no coclustering with tetherin in super-resolution analyses. These results support a model in which both Gag-induced membrane curvature and Gag-ESCRT interactions promote tetherin recruitment, but the recruitment level achieved by the former is sufficient for full restriction.

Introduction

Tetherin (BST-2/CD317/HM1.24/PDCA-1) is an interferon-inducible protein, which restricts the release of HIV-1 virions and causes their accumulation at the cell surface [1, 2]. Evidence obtained by fluorescence and transmission electron microscopy studies show that tetherin accumulates at sites of virus assembly [3-10]. This is consistent with a model where tetherin inhibits virus release by directly linking cell and viral membranes [3, 5, 6, 9]. This restrictive function is most likely a result of the unique topology of tetherin, which contains both an N-terminal transmembrane domain and a predicted C-terminal GPI-anchor. The ability of tetherin to form dimers or possibly higher-order multimers has also been shown to contribute to its antiviral function [11-15]. As with other GPI-anchored proteins, tetherin is thought to reside in lipid rafts, based on its resistance to detergent solubilization and cholesterol dependence of this detergent resistance [16-18]. Tetherin is able to inhibit a broad range of unrelated enveloped

viruses, ruling out a direct interaction with any particular viral protein as a requirement for restriction of virus release [19, 20].

HIV-1 is able to overcome tetherin-mediated restriction through the action of its accessory protein Vpu [1, 2]. Recent studies have determined the nature of the interaction between Vpu and tetherin and revealed that Vpu promotes degradation of tetherin and sequestration of tetherin away from assembly sites (for reviews, see [19-21]). In contrast, the mechanism by which tetherin interacts with assembling viruses remains unknown.

The assembly process of HIV-1 likely proceeds in a stepwise fashion [22, 23]. Early steps include binding of Gag to the plasma membrane, mediated by the matrix (MA) domain [24]. Dimerization of Gag is mediated by the capsid (CA) domain, and higher order multimerization is mediated by interactions between the nucleocapsid (NC) domain and RNA [23]. Finally, as multimerization progresses, Gag is able to induce membrane curvature and, via the late domain (in p6) and NC regions, recruit cellular ESCRT machinery to ultimately facilitate scission of host and viral membranes [25]. During these steps, assembling Gag also associates with cholesterol-rich lipid rafts as well as other membrane microdomains, such as tetraspanin-enriched microdomains [26, 27]. Similar to dependence on cellular ESCRT machinery for efficient virus release [28, 29], association with lipid rafts is a common aspect shared among the assembly of many enveloped viruses [30]. Because of the association between Gag and lipid rafts, many have hypothesized that lipid rafts play an important role in the recruitment of tetherin to virus assembly sites [7, 31].

To better understand the mechanisms by which tetherin restricts a broad spectrum of enveloped viruses, we sought to determine how tetherin is recruited to sites of HIV-1

assembly in the absence of Vpu. In this study, we examined the contributions of lipid rafts, membrane curvature, and interactions with cellular ESCRT machinery to the process of tetherin recruitment to viral assembly sites.

Materials and Methods

Plasmids and siRNA

pNL4-3 [32], pNL4-3/Udel (a kind gift from Dr. Klaus Strebel) [33], pNL4-3/Gag-Venus, pNL4-3/Fyn(10)ΔMA/Gag, and pNL4-3/Fyn(10)fullMA/Gag [34], pNL4-3/$PH_{PLC\delta1}$ΔMA/Gag [26], pCMV/Tsg-5' (a kind gift from Dr. Stanley Cohen) [35], and pCDNA3.1/HIV-Tat101 (a kind gift from Dr. David Markovitz) [36], were described previously. pCMV/Rev, a kind gift from Dr. Eric Freed, was originally obtained from Dr. S. Venkatesan [37]. Udel versions of previously described pNL4-3-based plasmids were created by replacing the SalI/BamHI fragment of pNL4-3 with the corresponding region of pNL4-3/Udel, which does not express Vpu [33]. A plasmid encoding the full length cDNA of human BST-2/Tetherin under the control of a CMV promoter, pCMV6XL-5 hBST-2, was obtained from Origene (Rockville, MD). Plasmids used to make pseudotyped virus stocks, pCMVNLGagPolRRE [38] and pHCMV-G (a kind gift from Dr. Jane Burns) [39], were described previously. Capsid mutations previously shown to disrupt membrane curvature and efficient particle formation, P99A [40] and EE75,76AA [41], were introduced into pNL4-3/Gag-Venus/Udel by PCR mutagenesis to give pNL4-3/P99A/Gag-Venus/Udel, pNL4-3/EE75,76AA/Gag-Venus/Udel. pNL4-3/$PTAP^{-}$/Gag-Venus/Udel (p6 residues 7-10 were changed from PTAP to LIRL [42]), pNL4-3/CCY^{-}/Gag-Venus/Udel (bearing NC C28S, NC C49S, and p6 Y36S mutations [43]), and

pNL4-3/Y36S/Gag-Venus/Udel (p6 Y36S mutation [44]) were generated by standard PCR mutagenesis techniques. The gene encoding the photo-switchable fluorescent protein mEos2 was obtained from the pRSETa mEos2 plasmid from Addgene (Cambridge, MA). The bright, monomeric version of the Eos fluorescent protein, mEos3.2, was generated by PCR mutagenesis of the parental mEos2 protein (bearing I102N, H158E, and Y189A mutations) as described [45]. pNL4-3/Gag-mEos3.2/Udel and its derivatives were constructed by replacing the Venus coding sequence with mEos3.2. The CA/NC mutant used in this study, pNL4-3/20LK/WM/14A1G/Gag-mEos3.2/Udel, bears the MA mutation 20LK [46] to facilitate efficient membrane binding in the absence of normal multimerization, which are disrupted by capsid C-terminal mutations W184A and M185A (WM) and mutations of the 15 basic amino acids of the NC domain to alanine or glycine (14A1G) [47]. siRNA sequences directed against Tsg101 (CCUCCAGUCUUCUCUCGUC) and Alix (GAAGGAUGCUUUCGAUAAA) were described previously [48, 49]. A control siRNA, which does not target any known human mRNA sequences (UUCUCCGAACGUGUCACGU), was also used [50]. Double-stranded RNA oligonucleotides were synthesized by Integrated DNA Technologies (Coralville, IA).

Antibodies

Anti-BST-2/tetherin polyclonal rabbit serum, generated by Dr. Klaus Strebel [51], and anti-HIV-Ig polyclonal human serum were obtained from the NIH AIDS Research & Reference Reagent Program (Germantown, MD). Monoclonal mouse antibodies against CD46, CD55, CD59, and Tsg101 were obtained from BD Biosciences (San Diego, CA).

Polyclonal rabbit anti-GFP was obtained from Clontech (Mountain View, CA). Mouse polyclonal anti-PDC6I (Alix) was obtained from Abcam (Cambridge, MA). Monoclonal mouse anti-α-tubulin was obtained from Sigma (St. Louis, MO). Species- and/or isotype-specific Alexa Fluor 488-, 594-, and 647-conjugated secondary antibodies were obtained from Invitrogen (Carlsbad, CA). Alexa Fluor 647-conjugated monoclonal anti-human CD317 (tetherin) was obtained from BioLegend (San Diego, CA).

Cells

HeLa cells were maintained in DMEM supplemented with 5% FBS. HT-1080 cells (ATCC #CCL-121) were maintained in EMEM supplemented with 10% FBS. For virus release assays, cells were plated at a density of $5.6x10^5$ per well in 6-well culture plates and incubated overnight. Cells were then transfected with 2 μg of pNL4-3-based plasmids using Lipofectamine 2000 (Invitrogen, Carlsbad, CA) according to the manufacturer's instructions. In HT-1080 cells, 2 μg pNL4-3-based plasmids were used with or without 50 ng pCMV6XL-5 hBST2. Transfection for microscopy was performed as previously described [26]. For T cell experiments, A3.01 and a derivative cell line, P2 [52], were maintained in RPMI-1640 with 10% FBS.

Cholesterol Depletion and Virus Release Assays

Cholesterol depletion [38] and virus release assays [34] were performed as previously described. VLP release assays of PR^- Gag, Gag-Venus, and Gag-mEos3.2 were performed in a similar manner with the exception that cell lysates were subjected to boiling with a low concentration of SDS prior to immunoprecipitation and VLP lysates

were loaded directly, without immunoprecipitation, to minimize epitope masking resulting from the lack of functional protease in these molecular clones [53].

Antibody Copatching Assay, Confocal Microscopy, and Image Analysis

HeLa cells were plated and transfected as described above followed by 16-hour incubation at 37°C. For antibody copatching assay, cells were stained by primary antibodies at 1:100 in DMEM-5% FBS for 10 minutes at room temperature, washed 3 times with PBS, and stained by secondary antibodies at 1:200 in DMEM-5% FBS for 10 minutes at room temperature. Cells were then washed 3 times and fixed with 4% PFA in PBS for 30 minutes at room temperature. For standard immunofluoresence microscopy, cells were fixed with 4% PFA in PBS for 30 minutes at room temperature and stained by primary and secondary antibodies for 1 hour each. Samples were mounted in Fluoromount-G (Southern Biotech, Birmingham, AL) and imaged on a Leica SP5X microscope (Leica, Wetzlar, Germany). Images were acquired with a 100X PL APO objective (NA=1.40) with 5X scanning zoom at a resolution of 1024x1024 (30 nm per pixel). Excitation was done with 488 nm, 514 nm, and 590 nm laser lines. Acquisition bandwidths were 500-550 nm, 525-575 nm, and 600-650 nm, respectively.

To calculate the degree of colocalization between markers, at least 10 regions of interest, each from different fields, were analyzed per condition. Regions of interest were randomly selected from cells where two proteins of interest were present. For Gag-tetherin colocalization measurements, we excluded cells that do not show distinct Gag puncta from analyses. Pearson's correlation coefficient was calculated using ImageJ 1.43u (NIH, http://rsb.info.nih.gov/ij/) with the JACoP plugin [54]. For confocal images

of tetherin, a smoothing filter was applied in ImageJ after images were analyzed to remove excess background signal. This filter sets the intensity value at each pixel equal to the average of its nearest neighbors in at 3x3 pixel square area.

T Cell Infection and Microscopy

Generation of pseudotyped virus stocks, infection of A3.01 and P2 T cells, and immunofluorescence microscopy were performed as described previously [52]. Images were analyzed as described above for HeLa cells, with the exception that a median filter was applied in ImageJ prior to analysis to remove out of focus signals from epifluorecence images. For virus release assay, $4x10^5$ P2 T cells were spinoculated with VSV-G-pseudotyped virus in the presence of 0.8 μg polybrene and incubated for 2 days prior to metabolic labeling.

Transmission Electron Microscopy Analysis of Gag-Venus Mutants

HeLa cells were plated and transfected as described above. Cells were fixed 16 hours post-transfection with 2% glutaraldehyde in PBS. Cells were analyzed on a Hitachi H7600 transmission electron microscope as previously described [55].

Super-Resolution Localization Microscopy and Cross-Correlation Analysis

HeLa cells were plated and transfected as described above. Cells were fixed at 16 hours post-transfection in 4% PFA with 0.1% glutaraldehyde for 10 minutes at room temperature. Cells were then stained by Alexa Fluor 647-conjugated monoclonal anti-tetherin antibody for 2 hours at room temperature. Cells were washed extensively with

PBS and placed in imaging buffer composed of 50mM Tris-HCl pH 9.0, 10mM NaCl, 1% β-ME, 10% glucose, and an enzymatic oxygen scavenging system as described previously [56]. Samples were imaged in total internal reflection using an inverted IX81-ZDC microscope with a cellTIRF module (Olympus America, Center Valley, PA) and 100X UAPO TIRF objective (NA=1.49). Images were acquired on an EMCCD camera (iXon-897, Andor, Belfast, Ireland). Red and far red emissions were separated onto two halves of the EMCCD camera using a DV2 dualview imaging system equipped with a 650nm long pass dichroic and emission filters (Photometrics, Tucson, AZ). Alexa-647 fluorophores were activated and imaged with 640nm laser excitation (CUBE 640-75FP, Coherent, Santa Clara, CA), while Gag-mEos3.2 fluorophores were activated at 405nm (CUBE 405-50FP, Coherent, Santa Clara, CA) and imaged using laser excitation at 561nm (Sapphire 561-150 CW, Coherent, Santa Clara, CA). In both cases, laser intensities were adjusted such that single fluorophores could be distinguished in individual images. Super-resolution images were reconstructed from 7500 individual diffraction limited images according to previously described methods [56] implemented in custom software written in Matlab (Mathworks, Natick, MA). Briefly, single molecule peaks were identified and fit to a two dimensional Gaussian shape. The ensemble of peaks was then culled to remove outliers in brightness, size, aspect ratio, and localization error. The culling algorithm is designed to remove likely contributions from signals that do not originate from single activated fluorophores so that they do not contribute to the final image. Therefore, in the final images, the smallest/dimmest puncta, which do not contain more-than-one single activation events, are likely to represent single molecules. Culled events are not correlated in space. Fiduciary markers were used to transform

Alexa647 and mEos3.2 images following previously published methods [57], and stage drift was corrected by aligning single color super-resolution images generated from signals acquired every 100-500 frames by localizing the maxima of cross-correlation functions. Super-resolution images were reconstructed by incrementing the intensity of pixels at positions corresponding to localized single molecules after correcting for stage drift. Image resolution is estimated by comparing the auto-correlation of images reconstructed from all identified single molecule centers to those of images reconstructed from data grouped to account for localized single molecules that remain activated in sequential frames as described previously [58]. Cross-correlation functions, $c(r)$, as a function of radius, r, for cells were evaluated from ungrouped reconstructed images, were computed using fast Fourier transforms as described previously [59], and were normalized to 1 at large radius.

To facilitate the comparison of the levels of cross-correlations between conditions, we report the integrated intensity under cross-correlation curves, out to a radius of 1μm. To accomplish this, curves tabulated from individual cells were first fit to the sum of Gaussian and exponential functions in order to average noise at large radii. Best fit curves were then integrated according to $I = 2\pi \sum_{r=0}^{1\mu m} r(c(r) - 1)\Delta r$, where Δr is the distance between adjacent points in the tabulated correlation functions (25nm). The number of Gag (tetherin) proteins correlated with the average tetherin (Gag) protein out to a radius of 1μm is given by $N = \rho I$, where ρ is the average surface density of Gag (tetherin). The values presented in Figures 2.5F and 2.7D (integrated cross-correlation) are integrated intensity (I) divided by integrated area ($2\pi \sum_{r=0}^{1\mu m} r\Delta r$). The resulting value is equal to the increased surface density of Gag (tetherin) coclustered with tetherin (Gag).

The Pearson's correlation coefficient used to quantify colocalization in confocal microscopy images and the integrated cross-correlation analysis method used for super-resolution localization microscopy images are not directly comparable. The Pearson's coefficient is the covariance (cross-correlation at r=0) between the two images divided by the variance (square root of the autocorrelation function at r=0) of each individual image [59], whereas the integrated cross-correlation values are for r=0-1 μm and not affected by the auto-correlation functions. Unfortunately, it is not possible to evaluate reliable Pearson's coefficients from super-resolution images due to over-counting artifacts in auto-correlation functions (details described in [58]).

siRNA Knockdowns

HeLa cells were plated at a density of 10^5 cells per well in 24-well culture plates (Corning, Fairport, NY) and incubated overnight. Cells were then transfected with 20 pM siRNA using Lipofectamine 2000 (Invitrogen, Carlsbad, CA) according to the manufacturer's instructions. After 24 hours, cells were trypsinized, transferred into Lab-Tek 8-well chamber slides (Thermo Fisher, Waltham, MA; for confocal microscopy), Lab-Tek 4-well chamber coverslips (for super-resolution microscopy), or 6-well culture plates (Corning, Fairport, NY; for western blot analysis and virus release assays), and further incubated for 24 hours. For microscopy, cells were then transfected with 0.6 μg pNL4-3-based plasmids and incubated for an additional 16 hours prior to fixation and staining as described above for confocal or super-resolution localization microscopy (a total of 64 hours after siRNA transfection). For western blot analysis, cells were lysed at 64 hours after siRNA transfection and lysates were subjected to SDS-PAGE and

immunoblotting. For virus release assays, cells were transfected with siRNA as described above, transfected with pNL4-3-based plasmids at 48 hours after siRNA transfection and incubated for an additional 16 hours (a total of 64 hours after siRNA transfection) prior to metabolic labeling.

Results

Tetherin does not copatch significantly with lipid raft markers in HeLa cells

Given the known involvement of lipid rafts in the assembly of many tetherin-susceptible enveloped viruses, it is possible that lipid rafts may direct tetherin to sites of HIV-1 assembly. To determine whether tetherin is associated with lipid rafts, we used an antibody copatching assay to examine the distribution of endogenous tetherin and lipid raft markers on the surface of HeLa cells. By the same assay, Gag has been previously shown to strongly associate with lipid raft markers in HeLa cells [26]. In the present study, we observed substantial copatching of tetherin with Gag-YFP but not with a non-raft marker CD46 (Figure 2.1). We also observed a moderate level of copatching between two lipid raft markers NFP-GPI (a GPI-anchored non-fluorescent GFP variant) and CD59 and between NFP-HATM (a fusion between the transmembrane domain of influenza HA and NFP) and CD55 in the absence of Gag (Figure 2.1). However, no significant copatching was observed between tetherin and four different lipid raft markers CD55, CD59, NFP-GPI, and NFP-HATM in the absence of Gag (Figure 2.1). These results suggest that, although tetherin can be recovered from detergent resistant membrane fractions, it does not appear to have a strong affinity for lipid rafts detected in this experiment at the plasma membrane of HeLa cells.

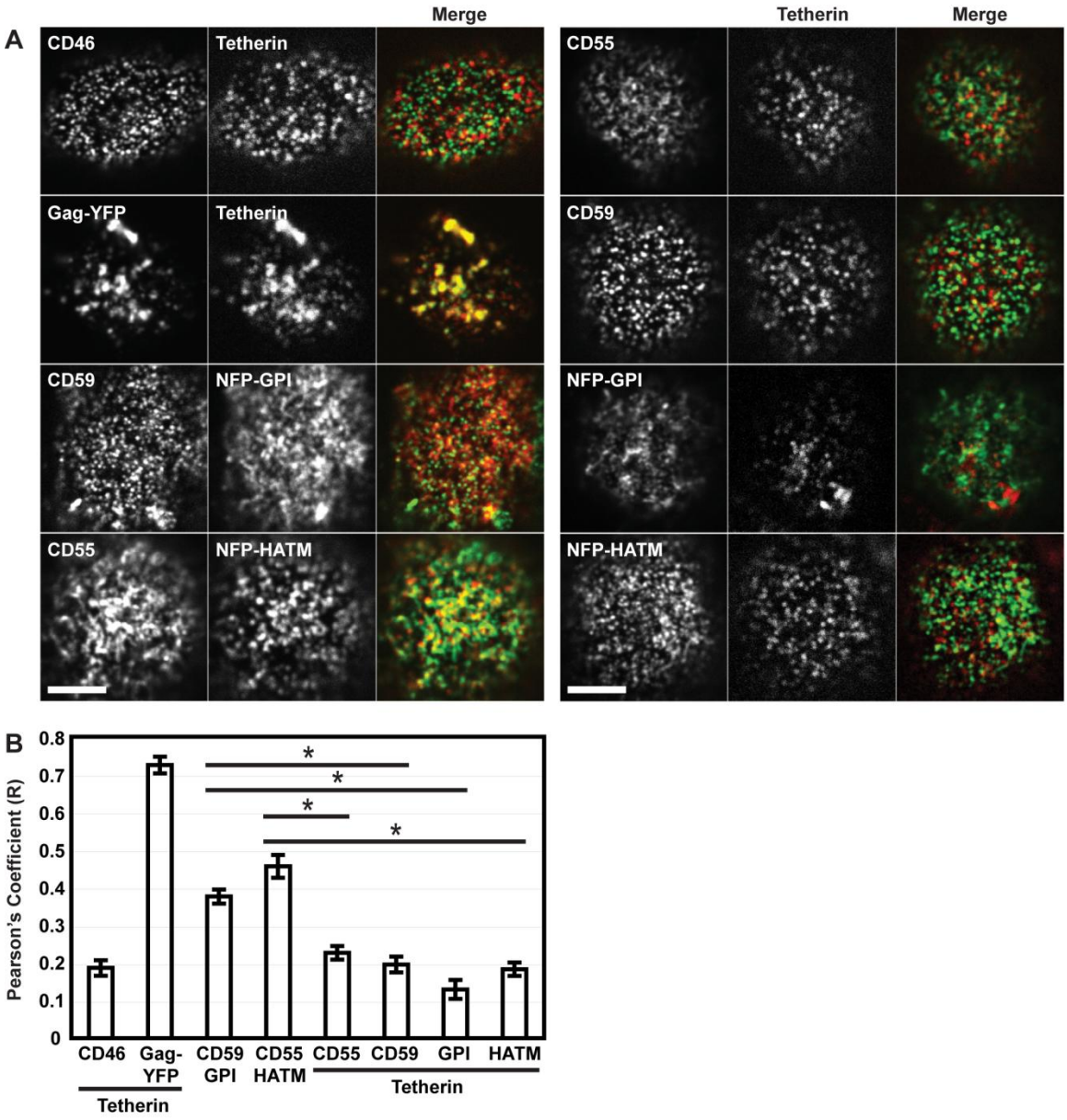

Figure 2.1. Tetherin copatches with Gag-YFP but not with CD46 or lipid raft markers.
HeLa cells were treated with primary antibodies against indicated proteins expressed on the cell surface for 10 minutes, followed by treatment with species- and/or isotype-specific fluorescent secondary antibodies for 10 minutes, and fixation with 4% PFA for 30 minutes. Cells expressing Gag-YFP were treated with antibodies to patch tetherin alone prior to fixation. (A) Representative images of the dorsal surface of cells are shown. (B) Pearson's correlation coefficients were calculated for fluorescence intensities of green and red signals at each pixel. Data shown are from 10 regions of interest, each from different cells, from one representative experiment out of two performed, displayed as mean Pearson's correlation (R) values ± SEM. P values were determined using Student's t test. *, $p < 0.05$. Scale bar = 5.0 μm.

Tetherin antiviral function is insensitive to cholesterol depletion

While a recent report showed that treatment of cells by anti-tetherin antibody does not apparently alter cell-surface distribution of tetherin [60], we cannot rule out the possibility that antibody treatment may alter the native microdomain partitioning of tetherin. To assess tetherin-raft association and its significance by an alternative approach, we sought to determine whether lipid rafts play a role in tetherin antiviral function. To this end, we depleted cellular cholesterol that is essential for lipid-raft integrity by methyl-β-cyclodextrin (MβCD) and examined the effect of this treatment on tetherin-mediated inhibition of virus release. We found that under both mild (30 minutes with 5 mM MβCD) and more stringent (30 minutes with 10 mM MβCD) cholesterol-depleting conditions, tetherin remains a potent inhibitor of WT Gag release in HeLa cells as assessed by Vpu dependence of virus release (Figure 2.2 A-C). While association of Vpu with lipid rafts is debated [17, 61, 62], such association could be a confounding factor in the experiments using HeLa cells. To directly examine the effect of tetherin, we used HT-1080 cells that do not express endogenous tetherin. We observed that in these cells, exogenously expressed tetherin inhibits virus release regardless of cholesterol depletion treatments (Figure 2.2 D-F). However, cholesterol depletion is also known to significantly inhibit membrane binding and release of WT Gag [38, 63]. To separate the effects of cholesterol depletion on virus particle production and tetherin function, we conducted similar experiments using Fyn(10)fullMA Gag, which contains the first 10 amino acids of Fyn kinase at the N-terminus of Gag. Virus particle production of this Gag derivative is less sensitive to cholesterol depletion than WT Gag [63]. We found that tetherin also potently inhibits release of Fyn(10)fullMA Gag under cholesterol depleting

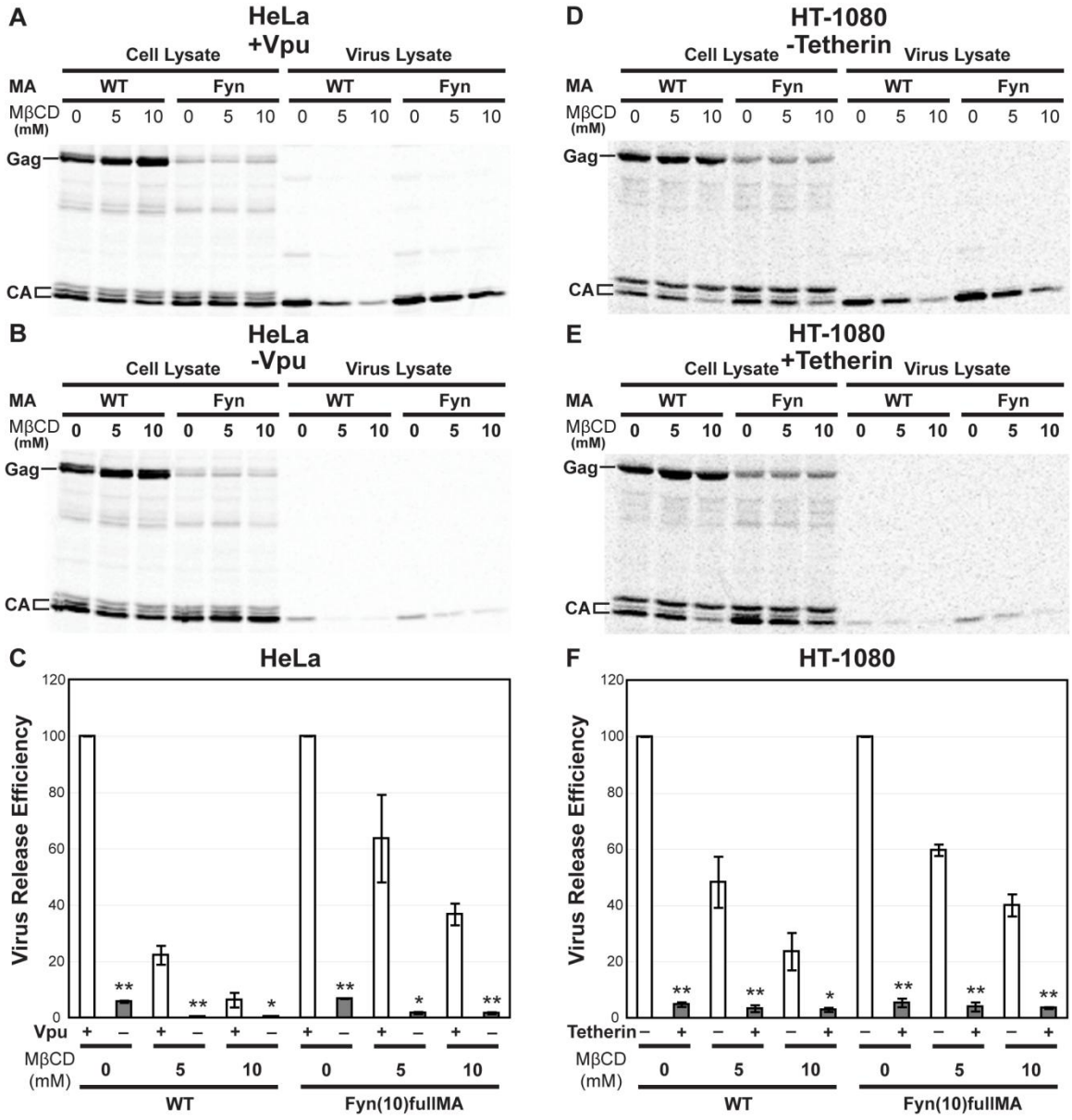

Figure 2.2. Tetherin antiviral function is insensitive to cholesterol depletion.
Virus release assays were performed in HeLa cells transfected with HIV-1 molecular clones that express Vpu or not (A, B, and C) and in HT-1080 cells transfected with Vpu-deficient molecular clones with or without exogenously expressed tetherin (D, E, and F). These molecular clones encode either WT Gag or Fyn(10)fullMA Gag. Cells were cultured in Met/Cys-deficient media containing FBS or cholesterol-depleted serum (CDS) and 5 mM or 10 mM MβCD prior to metabolic labeling with [^{35}S] Met/Cys for two hours. Virus release efficiency was determined as (virus-associated Gag)/(total Gag) and normalized to virus release efficiency in cells cultured in the medium containing FBS under Vpu (+) or tetherin (-) conditions. Data shown are from three independent experiments displayed as mean ±1 standard deviation. *, $p < 0.05$; **, $p < 0.01$.

conditions in HeLa and HT-1080 cells (Figure 2.2). These results indicate that tetherin antiviral function is insensitive to cholesterol depletion. Altogether, cholesterol depletion and microscopy data suggest that lipid rafts do not play an essential role in tetherin association with assembling Gag and tetherin-mediated inhibition of HIV-1 release.

CA mutations that impair induction of membrane curvature block tetherin recruitment

Next, we focused on whether membrane curvature and recruitment of cellular ESCRT machinery, which are common events among assembly of many unrelated enveloped viruses, are required for tetherin recruitment to assembly sites. To test the role of membrane curvature in tetherin recruitment, we utilized two different Gag mutants that are able to bind the plasma membrane and multimerize but are unable to induce the typical membrane curvature seen with WT Gag [26]. These two mutations, CA P99A [40] and CA EE75,76AA [41], were introduced into an HIV-1 molecular clone encoding a Gag-YFP fusion. To validate whether these Gag mutations have the expected impacts on membrane curvature in the context of Gag-YFP fusions, we first performed transmission electron microscopy analyses and VLP release assays using HeLa cells transfected with Vpu^+ molecular clones expressing WT, P99A, and EE75,76AA Gag-YFP (Figure 2.3A and B). We found that consistent with the membrane curvature defect observed for non-YFP tagged versions (unpublished data) [26, 41], both P99A and EE75,76AA produced electron-dense patches beneath the plasma membrane and were reduced in VLP production, although the defect was much more severe with the EE75,76AA mutant. Residual release of Gag by the P99A mutant is likely due to

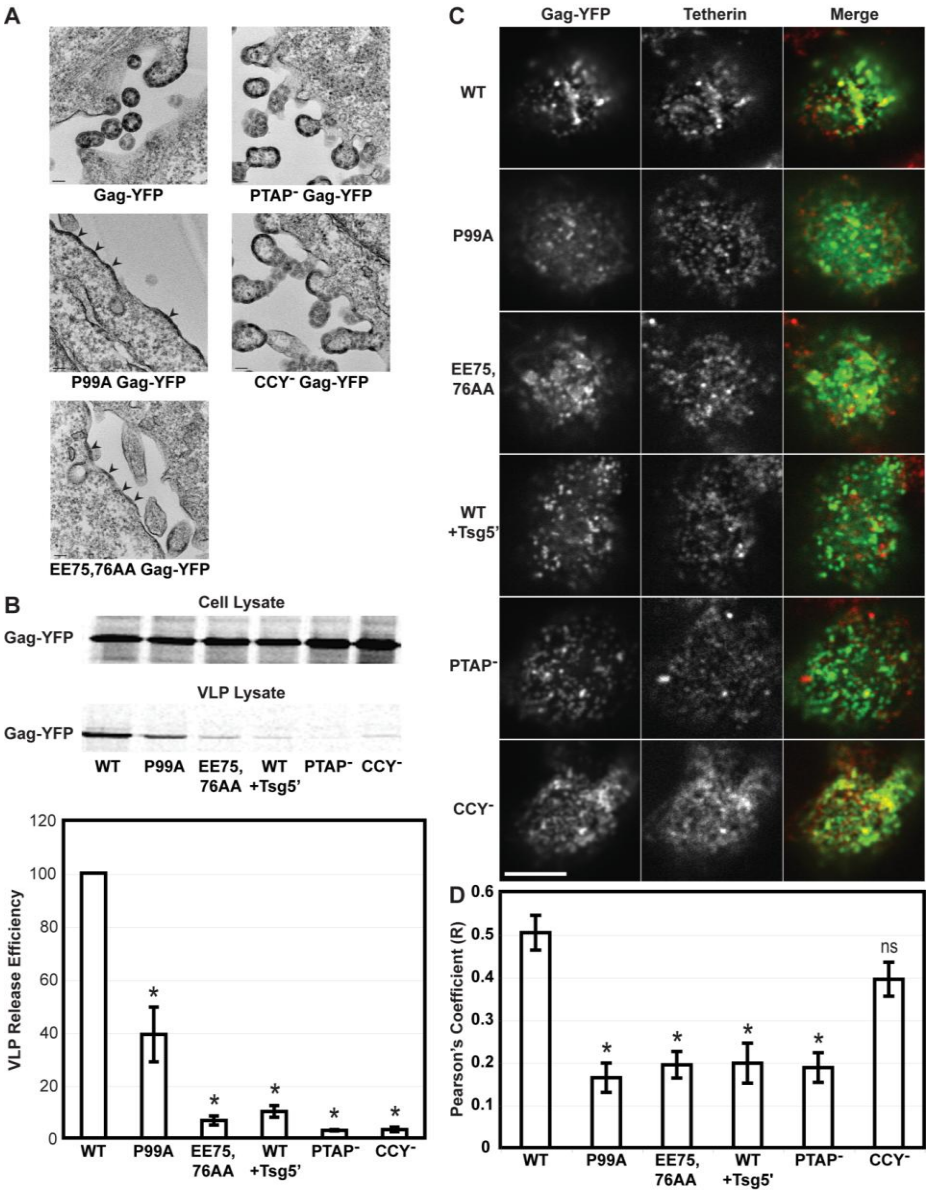

Figure 2.3. Membrane curvature and Tsg101 binding correlate with tetherin recruitment in HeLa cells.

(A) HeLa cells expressing Vpu^+ molecular clones encoding indicated mutants of Gag-YFP were analyzed by transmission electron microscopy. Arrows indicate electron-dense patches that are likely to represent membrane-associated Gag-YFP multimers. Scale bar = 100 nm. (B) VLP release assay of Vpu^+ Gag-YFP constructs was performed for indicated Gag-YFP constructs in HeLa cells as in Figure 2.2. Representative autoradiogram is shown along with quantitation of VLP release efficiency. Data shown are from 2 independent experiments displayed as mean VLP release efficiency. (C and D) HeLa cells expressing molecular clones encoding indicated Gag-YFP constructs and lacking the *vpu* gene were fixed at 16 hours post-transfection with 4% PFA for 30 minutes and immunostained for endogenous tetherin expressed on the cell surface. (C) Representative images of the dorsal surface of cells are shown. Scale bar = 5.0 μm. (D) Degree of colocalization between Gag-YFP and tetherin was calculated in the same manner as in Figure 2.1. Results are shown for one of two independent experiments and displayed as mean R ± SEM. *, $p < 0.01$; ns, not significant. TEM analysis, shown in panel A, was performed by Ferri Soheilian and Kunio Nagashima.

assembly, budding, and release of the spherical VLPs that are still observed to occur in an apparently WT-like manner albeit at the low levels (unpublished data) [26]. We next introduced the same CA mutations into a molecular clone lacking Vpu expression (pNL4-3/Gag-YFP/Udel) and examined the distributions of tetherin and Gag in the absence of Vpu-mediated down-modulation of tetherin by immunostaining. Cells were fixed prior to immunostaining to prevent antibody-driven copatching. Both CA mutants show significantly lower colocalization with tetherin than WT Gag-YFP (Figure 2.3C and D). These results identify the CA amino acid residues substituted in these mutants as molecular determinants in tetherin recruitment to HIV-1 assembly sites and suggest a possible role for membrane curvature in tetherin recruitment. Alternatively, these mutants may be defective at a stage of assembly prior to when tetherin recruitment occurs.

The Interaction between Gag and Tsg101 enhances tetherin recruitment in HeLa cells

Following the induction of membrane curvature and the formation of viral buds, ESCRT-mediated scission of viral and host membranes occurs. An ESCRT-I protein Tsg101, as well as an ESCRT-related protein Alix (AIP1/PDCD6IP), serve as an interface of the ESCRT machinery with Gag and facilitate efficient virus release [64-68]. To determine whether the ESCRT complex contributes to tetherin recruitment, we examined the impact of a dominant negative form of Tsg101, called Tsg-5', on tetherin-Gag colocalization. Tsg-5' corresponds to the N-terminal half of Tsg101 that binds HIV-1 p6 [64, 69] and lacks the C-terminal half of the protein responsible for recruiting other ESCRT proteins [68, 70]. Expression of this protein has been shown to inhibit virus

release of HIV-1 [66]. We observed a significant reduction in tetherin-Gag colocalization when Tsg-5' was expressed (Figure 2.3C and D), suggesting that the interaction between ESCRT and Gag is responsible for specific recruitment of tetherin.

Tsg101 binds to Pro-(Thr/Ser)-Ala-Pro (PT/SAP) motifs, including the PTAP motif in Gag p6 domain [64, 69, 71]. To abrogate this binding, we exchanged the PTAP motif sequence of the p6 domain for Leu-Ile-Arg-Leu, referred to as $PTAP^-$ Gag-YFP. This change is known to inhibit virus release [42, 72]. Binding of Alix occurs through two different regions of Gag. The first known motif, $LYPx_nL$, is within p6, and its binding to Alix can be disrupted by the p6 Y36S mutation [43, 44]. The second binding site lies within the NC domain [43, 73], and its interaction with Alix can be disrupted by the double mutant NC C28S/C49S [43]. To remove both Alix binding sites from Gag, we constructed a triple mutant (NC C28S/C49S and p6 Y36S), referred to as CCY^- Gag-YFP. In the *vpu*-positive context, both $PTAP^-$ and CCY^- mutants exhibited a budding-arrested phenotype characteristic of late domain/ESCRT disruption and failed to release VLPs (Figure 2.3A and B). In the case of CCY^- mutant, the failure of VLP release may also be partially due to an additional defect in Gag assembly caused by mutations in the zinc fingers of the NC domain [74, 75]. When expressed in HeLa cells, in the *vpu*-negative context, $PTAP^-$ Gag-YFP showed significantly less colocalization with tetherin, while CCY^- Gag-YFP showed levels of colocalization which were not significantly less than WT Gag-YFP (Figure 2.3C and D). We also observed similar levels of colocalization with the single mutant p6 Y36S (data not shown). These results suggest that in HeLa cells, the interaction between Tsg101 and the PTAP motif of Gag p6 domain promotes recruitment of tetherin.

The interaction between Gag and ESCRT enhances tetherin recruitment in T cells

To test whether members of the ESCRT complex participate in tetherin recruitment in T cells, which are a natural host cell type for HIV-1 *in vivo*, we infected A3.01 T cells with stocks of VSV-G-pseudotyped HIV-1 encoding WT Gag-YFP, $PTAP^-$ Gag-YFP and Y36S Gag-YFP and lacking *vpu*. After 48 hours, cells were fixed and immunostained for surface tetherin. In contrast to the observation that only the Tsg101 binding site of Gag is required for tetherin recruitment in HeLa cells, both $PTAP^-$ and Y36S mutations decreased colocalization of Gag-YFP with tetherin in A3.01 T cells (Figure 2.4). However, we noted that the impact of the Y36S change was modest (Figure 2.4). Similar results were also observed in primary human $CD4^+$ T cells (data not shown). These data show that both Tsg101 and Alix binding sites within Gag p6 domain enhance tetherin recruitment to Gag assembly sites in T cells. In A3.01 cells, the CCY^- triple mutant failed to form distinct puncta at the plasma membrane unlike in HeLa cells and, therefore, was not assessed for tetherin recruitment (data not shown).

siRNA knockdown of Tsg101 or Alix decreases tetherin recruitment in HeLa cells

To further assess the importance of Tsg101 and Alix in tetherin recruitment, we analyzed the effect of siRNA-mediated depletion of endogenous Tsg101 and Alix proteins in HeLa cells (Figure 2.5). Using previously reported siRNA duplex sequences [48, 49], substantial depletion was achieved for both proteins (Figure 2.5A). We found that depletion of either Tsg101 or Alix caused a marked decrease in tetherin colocalization with Gag-YFP. In contrast, significant colocalization was observed in cells transfected with non-target control siRNA (Figure 2.5B and C).

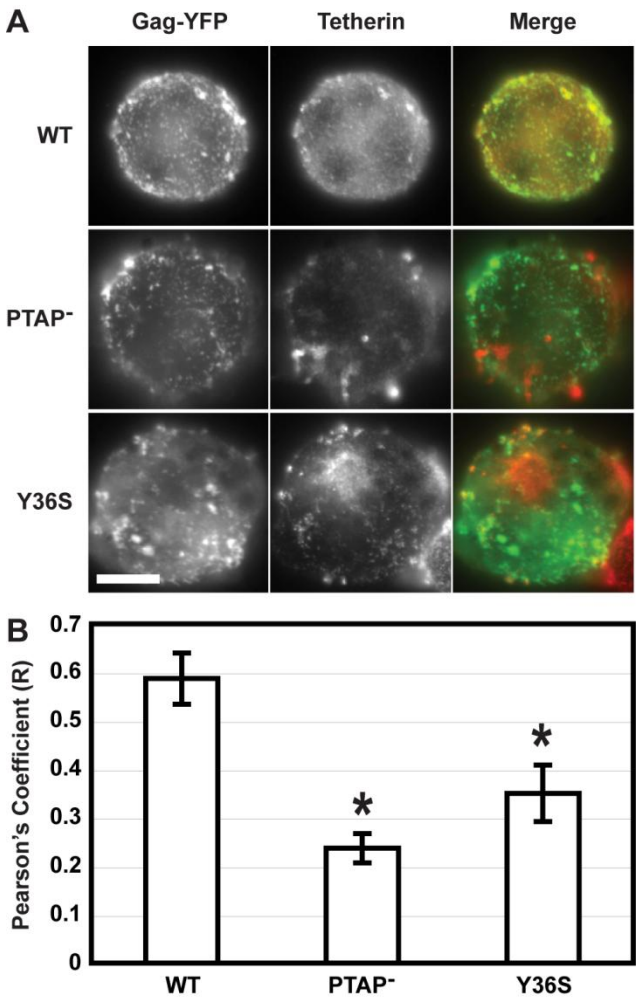

Figure 2.4. Both Tsg101- and Alix-binding sites in Gag are required for maximal tetherin recruitment in T cells.
A3.01 T Cells were infected with VSV-G-pseudotyped viruses expressing indicated Gag-YFP derivatives and lacking the *vpu* gene. After 48 hours cells were fixed with 4% PFA for 30 minutes and immunostained for endogenous tetherin expressed on the cell surface. (A) Representative images of the dorsal surface of cells are shown. Scale bar = 5.0 μm. (B) Quantitation of colocalization was performed as in Figure 2.1 after application of median filter. Results are shown for one of two independent experiments and displayed as mean R ± SEM. *, $p < 0.01$. This experiment was performed with the assistance of G. Nicholas Llewellyn.

These data indicate that both Tsg101 and Alix enhance tetherin recruitment to assembling Gag-YFP in HeLa cells. In addition to the observed loss of colocalization between tetherin and Gag after Tsg101 or Alix depletion, it is of note that both conditions also appear to show a more diffuse staining pattern for tetherin (Figure 2.5B). This could either indicate that recruitment of tetherin to assembly sites results in a more punctate

staining pattern of tetherin, as seen with WT Gag-YFP, or potentially that depletion of these proteins may alter the native distribution of tetherin at the plasma membrane, or both.

To analyze the contribution of ESCRT-Gag interactions to tetherin recruitment at the level of single virus particles, we utilized super-resolution localization microscopy. To achieve high-resolution information by this technique, proteins of interest are either tagged with photo-switchable or photo-activatable fluorescent proteins or immunolabeled by certain organic fluorophores, which are capable of reversible photo-switching in a reducing buffer [56, 76]. For our experiments, we fused Gag to the recently developed, green-to-red photo-switchable fluorescent protein mEos3.2 [45]. Unlike its parent protein mEos2 [77], which is able to form dimers and tetramers, mEos3.2 is truly monomeric and presumably does not affect the multimerization state of fusion proteins. mEos3.2 has also been shown to exhibit superior spectral qualities and is capable of reversible photo-switching in reducing buffer, making it an ideal fusion protein for super-resolution localization microscopy [45]. For our experiments, we depleted Tsg101 and Alix in HeLa cell by siRNA as in previous experiments. Cells were then transfected with a molecular clone expressing a Gag-mEos3.2 fusion protein and lacking *vpu*. Cells were then fixed, labeled with an AlexaFluor-647-conjugated monoclonal antibody directed to tetherin, and placed in a reducing buffer [78] before imaging by TIRF microscopy [56]. Given the high resolution that was achieved by this technique (25 nm for Gag-mEos3.2 and 15 nm for tetherin), we chose to quantify images using cross-correlation analysis, which reflects the degree of coclustering of two proteins as a function of distance, rather than Pearson's correlation, which reflects whether or not two proteins are located within the same image

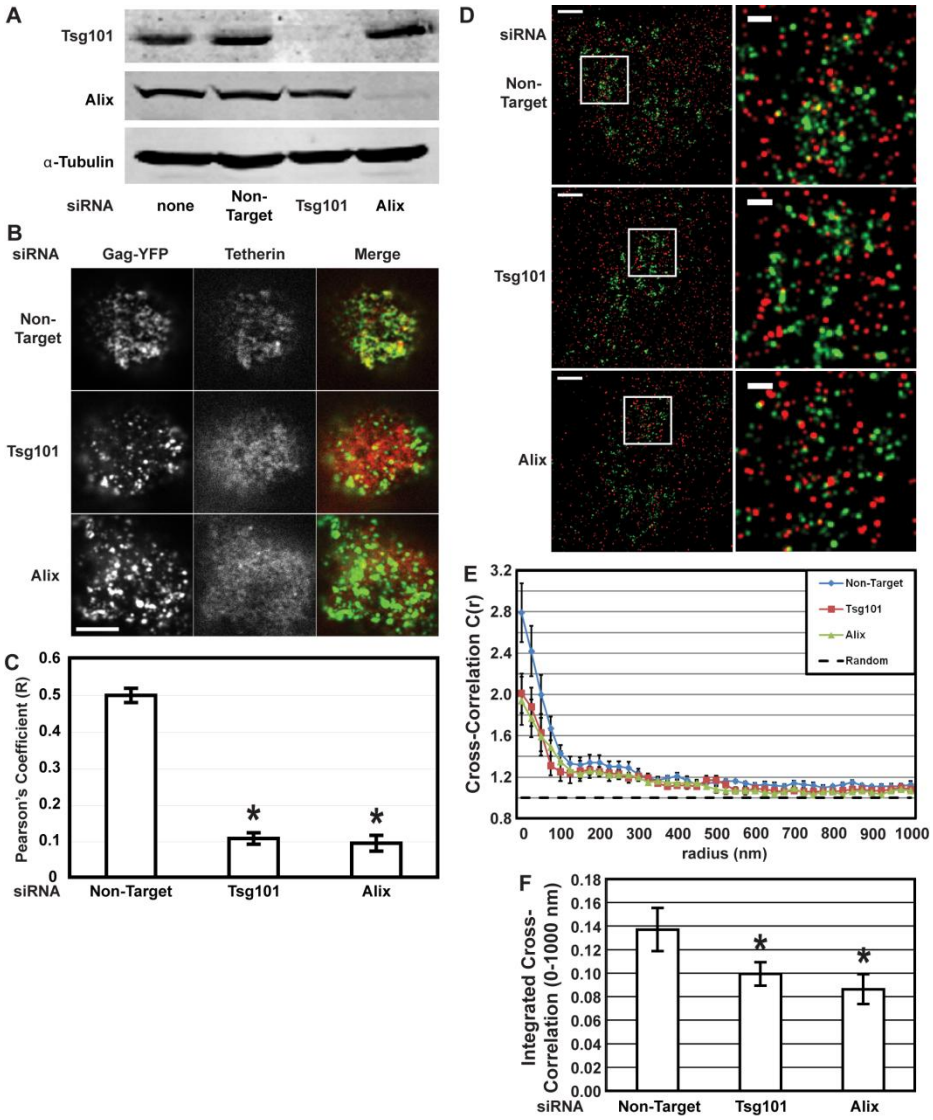

Figure 2.5. siRNA-mediated depletion of Tsg101 or Alix decreases tetherin recruitment in HeLa cells. (A) Western blotting analysis of Tsg101 and Alix in cells transfected with indicated siRNA and lysed at 64 hours post-transfection. Alpha-tubulin is shown as a loading control. (B and C) HeLa cells were transfected sequentially with the indicated siRNA and a molecular clone encoding Gag-YFP without Vpu. At 64 hours post-transfection with siRNA (16 hours post-transfection with Gag-YFP expression plasmids), cells were fixed by 4% PFA for 30 minutes and immunostained for endogenous tetherin. (B) Representative images of the dorsal surface of cells are shown. Scale bar = 5.0 μm. (C) Degree of colocalization was calculated in the same manner as in Figure 2.1. The result is shown for one of two independent experiments and displayed as mean R ± SEM. *, $p < 0.01$. (D) HeLa cells were transfected with indicated siRNA, followed by transfection with a Vpu-deficient molecular clone expressing Gag-mEos3.2. Cells were then fixed, stained with AlexaFluor-647 anti-tetherin antibody, and imaged by TIRF. Super-resolution images were reconstructed as described in Materials and Methods. Representative images are shown. Magnified images for boxed areas in the left panels are shown on the right. Scale bars are 2 μm for the left panels and 500 nm for the right panels. (E) Images of five cells per condition were acquired in each of two independent experiments (total 10 cells) and used for measurement of Gag-tetherin cross-correlation. Cross-correlation values are shown as mean ± SEM. Dashed line indicates random distribution (cross correlation =1). (F) Integrated cross-correlation was calculated as described in Materials and Methods and is shown as mean integrated cross-correlation ± SEM. *, $p < 0.05$.

pixel. To determine the degree of coclustering between tetherin and Gag-mEos3.2, we employed a statistical cross-correlation analysis, which measures the increased probability of finding a detected tetherin protein at a given distance from a detected Gag protein, or vice versa [58]. A normalized cross-correlation of 1 is observed when the distribution of detected molecules in one color channel is independent of the distribution of detected molecules in the other color channel. In contrast, a correlation greater than 1 is observed when signals from the two channels are not independent and show coclustering. When we quantified images of WT Gag-mEos3.2 and tetherin for cross correlation up to radii of 1 μm, we observed a high degree of cross correlation particularly within 100 nm when cells were treated with a non-target siRNA (Figure 2.5D–E). In contrast, when Tsg101 or Alix were depleted by siRNA, we observed intermediate levels of tetherin-Gag coclustering at the same range of radii (Figure 2.5D–E). To facilitate the comparison between conditions, we used the integrated cross-correlation between r=0 and r=1000 nm (see Materials and Methods) (Figure 2.5F). By this method, both Tsg101- and Alix-depleted cells showed significantly less coclustering between tetherin and Gag-mEos3.2 than cells treated with control siRNA. The reduction in Gag-tetherin colocalization caused by the same siRNA treatment (Figure 2.5C) appears more severe than that in coclustering (Figure 2.5F). This is likely due to differences between the methods used to quantify colocalization and coclustering in the two experiments. In particular, diffuse tetherin signals observed in Tsg101- or Alix-depleted cells, which reduce the contrast in tetherin localization inside versus outside Gag patches, are likely to contribute to reduction of Pearson's correlation coefficients, whereas they would not necessarily affect cross-correlations. Regardless, both confocal and super-

resolution microscopy data indicate that both Tsg101 and Alix promote tetherin recruitment to HIV-1 assembly sites and yet that intermediate levels of recruitment still occur in Tsg101- or Alix-depleted HeLa cells.

Intermediate levels of tetherin recruitment are sufficient for virus-release inhibition

To determine whether the maximal colocalization/coclustering between tetherin and Gag, which was observed to be ESCRT-dependent (Figure 2.5), is required for tetherin function, we sought to assess the ability of tetherin to inhibit release of WT HIV-1 upon depletion of Alix. Previous studies showed that unlike depletion of other ESCRT proteins such as Tsg101, depletion of Alix has little effect on ESCRT-mediated release of HIV-1[79, 80]. Therefore, the effect of Alix depletion on tetherin function can be examined specifically without confounding effect on particle scission. We treated HeLa cells with siRNAs in the same transfection procedure as in Figure 2.5 and measured tetherin activity by comparing Vpu^+ and Vpu^- molecular clones in these HeLa cells. We found that virus release of Vpu^- HIV-1 was inhibited compared with that of Vpu^+ HIV-1 in Alix-depleted HeLa cells as potently as, or even slightly more potently than, in HeLa cells treated with control siRNA (~25 fold versus ~21 fold; Figure 2.6A-C). These results suggest that while Alix is required for a maximal colocalization and coclustering between tetherin and Gag, this high level of clustering is not necessary for the full antiviral activity of tetherin.

Virus release enhancement by Vpu is well documented for a T cell line A3.01 [33], which has been shown to express a detectable level of tetherin on the cell surface [6, 51] (Figure 2.4). In contrast to HeLa cells, late domain motifs and hence ESCRT

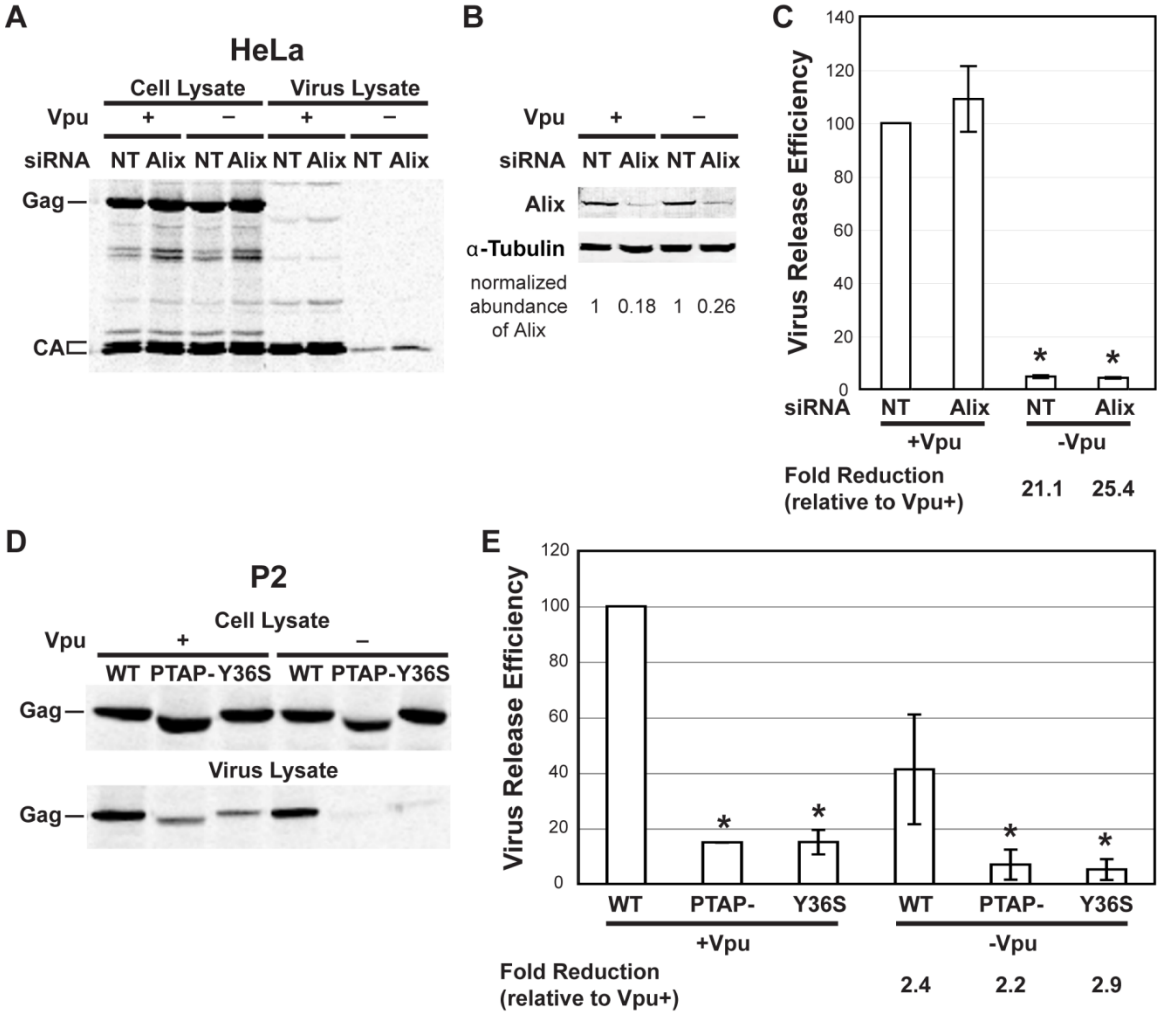

Figure 2.6. Disruption of Gag-ESCRT interactions does not affect tetherin function.
(A-C) HeLa cells were transfected with either non-target or Alix-directed siRNA. At 48 hours after transfection, cells were further transfected with either Vpu^+ or Vpu^- HIV-1 molecular clones. Cells were incubated for 16 hours (64 hours post-transfection with siRNA), followed by metabolic labeling and immunoprecipitation with HIV-Ig as in Figure 2.1. Representative autoradiograms of cell- and virus-associated proteins are shown for experiments using HeLa cells (A). (B) The cellular amounts of Alix and α-tubulin in cells treated as in panel A were examined by immunoblotting. Note that the same transfection procedure was used to deplete Tsg101 and Alix in Figure 2.5. (C) Quantitation of virus release efficiency from 3 independent experiments is shown as mean ±1 standard deviation. (D and E) P2 T cells were spinoculated with the indicated viruses with or without Vpu and incubated for 48 hours, followed by metabolic labeling and immunoprecipitation. One of three autoradiograms is shown (D). (E) Quantitation of 3 independent experiments is shown. *, $p < 0.05$.

recruitment appear to play a less critical role in virus release in T cells including an A3.01 cell clone [72]. Taking advantage of this difference, we sought to assess the contribution of both Tsg101 and Alix interactions in tetherin function in an A3.01-derived cell clone, P2. For these experiments P2 cells were spinoculated with VSV-G-pseudotyped viruses expressing either WT, PTAP^{-}, or Y36S Gag proteins either with or without *vpu*. In these experiments, the p6 mutants produced virus particles at a markedly impaired but still detectable level in the presence of Vpu (Figure 2.6D and E). Notably, deletion of Vpu reduced virus release to the similar extent for WT and p6 mutant Gag proteins. In other words, we did not observe any reversal of virus release restriction when either the Tsg101- or primary Alix-binding sites were mutated in Gag. These results corroborate the results obtained with siRNA experiments performed using HeLa cells (Figure 2.6A-C) and suggest that Gag-ESCRT interactions are not required for the antiviral activity of tetherin.

Altogether, these results indicate that although Gag-ESCRT interactions cause a detectable and significant increase in tetherin recruitment, the intermediate levels of tetherin recruitment observed when Tsg101 or Alix are depleted are sufficient for full inhibition of virus particle release.

Intermediate levels of tetherin recruitment, which are sufficient for virus release inhibition, are dependent on intact CA sequences required for Gag-induced membrane curvature

To identify molecular determinants for the intermediate levels of tetherin recruitment observed in previous experiments, which is sufficient for full inhibition of

virus release, we analyzed coclustering between endogenous tetherin and several Gag mutants in HeLa cells by super-resolution localization microscopy. As in Figure 2.3, we utilized two CA mutants that form electron-dense Gag patches at the plasma membrane but fail to induce membrane curvature efficiently (P99A Gag-mEos3.2 and EE75,76AA Gag-mEos3.2). We also examined the effect of Tsg5' expression and mutations of Tsg101- and Alix-binding motifs in Gag ($PTAP^-$ Gag-mEos3.2 and CCY^- Gag-mEos3.2) on tetherin-Gag coclustering. Virus release assays showed that replacement of YFP with mEos3.2 does not grossly affect efficiencies of VLP release by Gag mutants except that the virus release defect of P99A Gag was more severe in the mEos3.2 context than in the YFP context (data not shown). To establish a baseline for analysis, we also used a Gag-derivative that contains mutations at both CA dimer interface and NC basic residues (20LK/WM/14A1G/Gag-mEos3.2; hereafter CA/NC Gag-mEos3.2). Due to these mutations, this Gag derivative was expected to be highly defective in multimerization and therefore was expected to not cocluster with tetherin. As expected, by standard TIRF microscopy, which is inherently diffraction-limited, CA/NC Gag displays a largely uniform, diffuse membrane-lining phenotype with some patches (Figure 2.7A) that may represent membrane topology [81]. Reconstructed super-resolution images show various sizes of small puncta of CA/NC Gag-mEos3.2 at the plasma membrane, which likely represent single molecules and perhaps small clusters of Gag molecules (Figure 2.7B). WT and other mutants appeared to show more of larger puncta (Figure 2.7B; data not sown). After analyzing the Gag mutants described above in the same manner as in Figure 2.5, we found that there are three distinct categories of tetherin-Gag coclustering (Figure 2.7B and C). First, WT Gag-mEos3.2 showed a high level of tetherin-Gag coclustering.

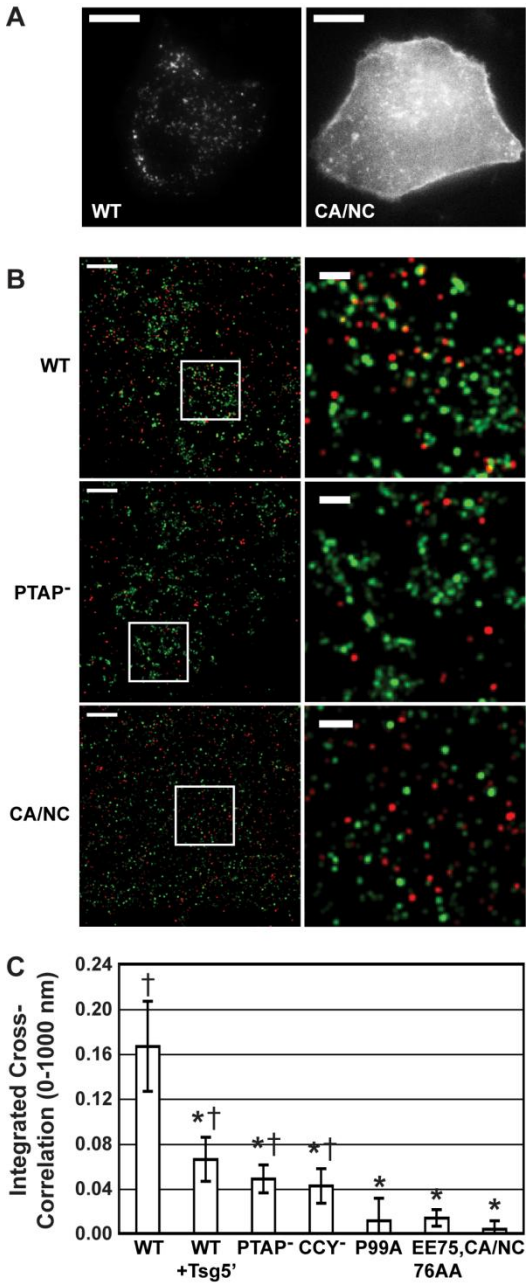

Figure 2.7. Both membrane curvature and Gag-ESCRT interactions enhance tetherin recruitment in HeLa cells.

(A) Cells expressing molecular clones encoding either WT Gag-mEos3.2 or CA/NC mutant Gag-mEos3.2 and lacking the *vpu* gene were fixed and imaged by conventional TIRF microscopy. (B) Cells expressing the indicated Gag-mEos3.2 constructs in the absence of Vpu were stained for tetherin and imaged by TIRF as in Figure 2.5, and super-resolution microscopy images were reconstructed as described in Materials and Methods. Representative images are shown for WT, PTAP$^-$, and CA/NC Gag-mEos3.2. Magnified images for boxed areas in the left panels are shown on the right. Scale bars are 2 μm for the left panels and 500 nm for the right panels. (C) Images of five cells per condition were acquired in each of two independent experiments (total 10 cells) and used for measurement of Gag-tetherin cross-correlation. Integrated cross-correlation was calculated as described in Materials and Methods and is shown as mean ± SEM. *, significantly less than WT ($p < 0.05$); †, significantly greater than CA/NC ($p < 0.05$).

Second, when Gag-ESCRT interactions are disrupted (WT+Tsg5', PTAP$^-$, and CCY$^-$), significantly less tetherin coclustered with Gag (Figure 2.7B and C). Notably, as was observed in the siRNA experiments (Figure 2.5F), intermediate levels of tetherin-Gag coclustering were detected under these conditions in which Gag interactions with Tsg101 or Alix were blocked genetically rather than by reducing the expression levels of these host factors. Third, we observed negligible levels of tetherin-Gag coclustering with P99A and EE75,76AA Gag-mEos3.2, which are not significantly more than that seen with CA/NC Gag-mEos3.2. The intermediate levels of tetherin recruitment observed upon disruption of Gag-ESCRT interactions (second category) were significantly greater than that seen for CA mutants that fail to induce membrane curvature (P99A and EE75,76AA Gag-mEos3.2) and CA/NC Gag-mEos3.2 (third category) (Figure 2.7C).

These results indicate that intermediate levels of tetherin recruitment, which are sufficient for virus release inhibition (Figure 2.6), are observed when Tsg101 or Alix are depleted (Figure 2.5) or when ESCRT-interacting motifs of Gag are disrupted (Figure 2.7). In addition, these intermediate levels of tetherin recruitment are abolished by mutations that disrupt either Gag multimerization or virus-induced membrane curvature (Figure 2.7). Given that the two CA N-terminal domain mutants used in this study (P99A and EE75,76AA) still contain the intact major Gag-multimerization domains (the CA C-terminal domain and the NC domain) and show dense patches of multimerized Gag at the plasma membrane by electron microscopy (Figure 2.3), it is likely that membrane curvature, but not Gag multimerization per se, is required for tetherin recruitment to assembly sites.

Discussion

HIV-1 encodes four accessory genes that have been implicated in combating host defense responses (Vif, Vpr, Vpu, and Nef) [82], exemplifying the necessity for immune evasion by successful viral pathogens. Such evolutionary interplay between virus and host is epitomized by the relationship between HIV-1 Vpu and human tetherin. Tetherin appears to have arisen early in mammalian evolution and remains a potent inhibitor of many enveloped viruses [20]. Considering the broad range of susceptible viruses, it is unlikely that tetherin recruitment is mediated by a direct interaction between tetherin and the Gag polyprotein. In support of this notion, we and others have observed that tetherin potently inhibited release of Gag derivatives lacking the juxta-membrane MA domain that could potentially interact with the short cytoplasmic tail of tetherin [83] (unpublished data). Instead of the MA sequence, this study identified amino acid residues in the CA N-terminal domain and late domain motifs as molecular determinants for recruitment of tetherin to HIV-1 assembly sites at the plasma membrane. Importantly, mutations in the former impair Gag-induced membrane curvature, whereas those in the latter disrupt Gag-ESCRT interactions. Therefore, these results support a model in which both membrane curvature and the presence of ESCRT promote tetherin accumulation to the assembly sites of HIV-1.

We and others have hypothesized that tetherin recruitment may be mediated by lipid rafts on the plasma membrane. This seemed an attractive model because lipid rafts are incorporated into the membranes of many enveloped viruses. Another line of evidence in support of this hypothesis is the presence of tetherin in Triton X-insoluble membrane fractions [16, 18]. Even though a study on tetherin chimeras in which the GPI

anchor is replaced with a heterologous transmembrane domain showed that lipid raft association measured by detergent resistance is not sufficient [84], it was possible that association of tetherin with lipid rafts may play an important role. In the present study, however, by an antibody copatching assay we found that tetherin itself does not appear to associate strongly with multiple lipid raft markers (CD55, CD59, NFP-GPI, and NFP-HATM) at the plasma membrane, all of which were previously shown to copatch strongly with WT Gag [26]. Another recent study also failed to detect significant colocalization between tetherin and a lipid raft marker GM1 by super-resolution microscopy techniques [10]. It is a valid concern that tetherin localization in the copatching assay may not reflect its native partitioning to microdomains unlike other raft proteins, since antibody treatment could alter tetherin function [60]. However, we also found that cholesterol depletion that disrupts integrity of lipid rafts has little effect on tetherin function. These results indicate that, although tetherin may still have an affinity for a specific subset of lipid rafts before its recruitment to virus assembly sites, such prior association with cholesterol-dependent lipid rafts is not required for tetherin antiviral function.

Conventional and super resolution microscopy of Gag late domain mutants did, however, reveal a potential role for Gag-ESCRT interaction in enhancing tetherin recruitment to virus assembly sites in HeLa and T cells. Moreover, siRNA knockdown experiments confirmed that expression of both Tsg101 and Alix is required for the high levels of tetherin recruitment seen with WT Gag in HeLa cells. A previous study that analyzed nascent particles formed by PTAP$^-$ Gag using immuno-SEM showed that WT tetherin does not appear to specifically accumulate at HIV-1 assembly sites [9]. Although WT Gag particles were not examined in that study, this observation is consistent with our

findings supporting a role for ESCRT in enhancing tetherin recruitment. Notably, and somewhat unexpectedly, the high levels of tetherin recruitment, which is manifested as tetherin-Gag colocalization detected by confocal microscopy, was dispensable for the full activity of virus release restriction.

Conventional and super resolution microscopy showed largely consistent results for most conditions. However, a triple Gag mutant defective in Alix interaction (CCY^-) did not show a significant decrease in tetherin recruitment as quantified by Pearson's coefficients of confocal images in HeLa cells, but did show significantly less coclustering with tetherin in HeLa cells by super-resolution microscopy analysis. While the origin of this difference remains unclear, it is possible that tetherin accumulates at or near the relatively large protrusive tubular membrane structures containing CCY^- Gag patches (Figure 2.3A) and thereby leads to the WT-level Pearson's correlation coefficient values without actually associating with Gag clusters. It is also possible that these structures may form more frequently on the top surface of cells than on the bottom surface. Indeed, we noticed that the Gag-positive tubular structures were detected on the bottom surface of cells imaged by super-resolution microscopy but only in the minority of cells (unpublished observation). Super-resolution analyses also revealed the difference in the levels of tetherin association with Gag mutants defective in ESCRT interactions versus those defective in inducing membrane curvature (Figure 2.7), which were indistinguishable in confocal microscopy analyses (Figure 2.3). Analysis of a multimerization-defective Gag (CA/NC Gag) mutant by super-resolution techniques also suggests the presence of Gag clusters on the cell surface (Figure 2.7). These observations, together with recent studies [10, 85, 86], highlight the utility of using super-resolution

microscopy to analyze virus-host interactions at the level of single virus assembly sites and to study early as well as late events in virus assembly.

While the exact mechanism by which Tsg101 and Alix enhance tetherin recruitment to HIV-1 assembly sites remains to be elucidated, this activity likely occurs later in the assembly process, since tetherin is not recruited to the same extent by Gag mutants defective in inducing membrane curvature (Figure 2.4) despite the presence of an intact late domain in these mutants. Although HIV-1 Gag may associate with Alix early during assembly as seen with EIAV Gag, recruitment of downstream ESCRT components occurs later during the process [87, 88]. It is possible that ESCRT proteins may form a barrier, which limits diffusion away from budding viruses. Notably, while recruitment of Tsg101 and Alix and hence the ESCRT machinery to assembly sites appears to be important for enhanced tetherin recruitment, formation of the pinching off machinery composed of ESCRT-III is not sufficient. In Alix-depleted cells, the ESCRT-III machinery is still functional [79, 80] (Figure 2.6), but the high levels of tetherin recruitment were not observed (Figure 2.5), indicating that this recruitment relies not only on the presence of ESCRT, but the presence of Alix or Alix-dependent process.

Although the additional level of tetherin recruitment promoted by Gag-ESCRT interactions appears unnecessary for tetherin-mediated inhibition of HIV-1, which forms relatively small, spherical virus particles, it is possible that larger enveloped viruses, such as filamentous orthomyxoviruses or filoviruses, may require greater amounts of tetherin to prevent their escape from infected cells. It would be interesting to examine the effects of ESCRT disruption on tetherin-mediated inhibition of these viruses.

Our findings did, however, provide evidence that Gag-induced membrane curvature results in intermediate levels of tetherin recruitment, which are sufficient to inhibit virus release. This result suggests that tetherin itself may be attracted to membrane curvature. Unfortunately, the contribution of membrane curvature to the antiviral effect of tetherin cannot be examined using virus release assays. This is because in contrast to Gag-ESCRT interactions, membrane curvature is inseparable from virus particle release. Most membrane-curvature-defective Gag constructs fail to release VLPs regardless of Vpu expression (e.g., EE75,76AA Gag-YFP). Some curvature mutants (e.g., P99A Gag-YFP) release a low level of VLPs, but this is through assembly, budding, and release that proceed in an apparently WT-like manner albeit less frequently (unpublished data) [26]. As such, the low but detectable VLP release of P99A Gag-YFP was dependent on Vpu (unpublished data). Thus, in either case, it is not feasible to examine using Gag mutants to what extent membrane curvature promotes tetherin-mediated inhibition of virus release. However, it may be possible to address this point using tetherin mutants. There are several examples of cellular proteins that are able to both sense and manipulate membrane curvature via protein domains that form curved structures [89, 90]. Intriguingly, based on crystallography analyses, it was hypothesized that a tetherin tetramer can form curved assemblies that may sense membrane curvature [14]. In this regard, it will be interesting to examine requirements for recruitment of tetherin mutants that can dimerize but are predicted to fail to oligomerize [13, 15, 86]. All enveloped viruses that assemble at the plasma membrane, whether dependent upon ESCRT machinery or not, must deform this membrane during budding, and therefore the membrane-curvature-dependent tetherin recruitment can explain the broad range of

tetherin-susceptible viruses. It remains to be seen whether tetherin distinguishes virus-induced and non-virus-induced membrane curvature and whether higher levels of tetherin recruitment, which are dependent on ESCRT engagement, are relevant in the context of other enveloped viruses.

Acknowledgments

We would like to thank Drs. Kathleen Collins, Eric Freed, Alice Telesnitsky, and members of our laboratory for helpful discussions and critical review of the manuscript. We also thank Matthew Stone for help with image analysis and Jingga Inlora and Madeline Nye for technical assistance. We thank Drs. Jane Burns, Stanley Cohen, Eric Freed, Heinrich Göttlinger, and Klaus Strebel for reagents. The following reagents were obtained through the AIDS Research and Reference Reagent Program, Division of AIDS, NIAID, NIH: HIV-Ig from NABI and NHLBI and anti-BST-2 from Dr. Klaus Strebel. This work was supported by NIH grants, R00 GM087810 (to SLV), R56 AI089282 (to AO), and R21 AI095022 (to AO). JRG is supported by an NIH training grant T32 AI007527-13.

References

1. Neil, S.J., T. Zang, and P.D. Bieniasz, *Tetherin inhibits retrovirus release and is antagonized by HIV-1 Vpu.* Nature, 2008. **451**(7177): p. 425-30.

2. Van Damme, N., et al., *The interferon-induced protein BST-2 restricts HIV-1 release and is downregulated from the cell surface by the viral Vpu protein.* Cell Host Microbe, 2008. **3**(4): p. 245-52.

3. Fitzpatrick, K., et al., *Direct restriction of virus release and incorporation of the interferon-induced protein BST-2 into HIV-1 particles.* PLoS Pathog, 2010. **6**(3): p. e1000701.

4. Goffinet, C., et al., *HIV-1 antagonism of CD317 is species specific and involves Vpu-mediated proteasomal degradation of the restriction factor.* Cell Host Microbe, 2009. **5**(3): p. 285-97.

5. Habermann, A., et al., *CD317/tetherin is enriched in the HIV-1 envelope and downregulated from the plasma membrane upon virus infection.* J Virol, 2010. **84**(9): p. 4646-58.

6. Hammonds, J., et al., *Immunoelectron microscopic evidence for Tetherin/BST2 as the physical bridge between HIV-1 virions and the plasma membrane.* PLoS Pathog, 2010. **6**(2): p. e1000749.

7. Jouvenet, N., et al., *Broad-spectrum inhibition of retroviral and filoviral particle release by tetherin.* J Virol, 2009. **83**(4): p. 1837-44.

8. Mitchell, R.S., et al., *Vpu antagonizes BST-2-mediated restriction of HIV-1 release via beta-TrCP and endo-lysosomal trafficking.* PLoS Pathog, 2009. **5**(5): p. e1000450.

9. Perez-Caballero, D., et al., *Tetherin inhibits HIV-1 release by directly tethering virions to cells.* Cell, 2009. **139**(3): p. 499-511.

10. Lehmann, M., et al., *Quantitative multicolor super-resolution microscopy reveals tetherin HIV-1 interaction.* PLoS Pathog, 2011. **7**(12): p. e1002456.

11. Andrew, A.J., et al., *The formation of cysteine-linked dimers of BST-2/tetherin is important for inhibition of HIV-1 virus release but not for sensitivity to Vpu.* Retrovirology, 2009. **6**: p. 80.

12. Hinz, A., et al., *Structural basis of HIV-1 tethering to membranes by the BST-2/tetherin ectodomain.* Cell Host Microbe, 2010. **7**(4): p. 314-23.

13. Yang, H., et al., *Structural insight into the mechanisms of enveloped virus tethering by tetherin.* Proc Natl Acad Sci U S A, 2010. **107**(43): p. 18428-32.

14. Swiecki, M., et al., *Structural and biophysical analysis of BST-2/tetherin ectodomains reveals an evolutionary conserved design to inhibit virus release.* J Biol Chem, 2011. **286**(4): p. 2987-97.

15. Schubert, H.L., et al., *Structural and functional studies on the extracellular domain of BST2/tetherin in reduced and oxidized conformations.* Proc Natl Acad Sci U S A, 2010. **107**(42): p. 17951-6.

16. Kupzig, S., et al., *Bst-2/HM1.24 is a raft-associated apical membrane protein with an unusual topology.* Traffic, 2003. **4**(10): p. 694-709.

17. Lopez, L.A., et al., *Anti-tetherin activities of HIV-1 Vpu and Ebola virus glycoprotein do not involve tetherin removal from lipid rafts.* J Virol, 2012.

18. Masuyama, N., et al., *HM1.24 is internalized from lipid rafts by clathrin-mediated endocytosis through interaction with alpha-adaptin.* J Biol Chem, 2009. **284**(23): p. 15927-41.

19. Douglas, J.L., et al., *The great escape: viral strategies to counter BST-2/tetherin.* PLoS Pathog, 2010. **6**(5): p. e1000913.

20. Evans, D.T., et al., *BST-2/tetherin: a new component of the innate immune response to enveloped viruses.* Trends Microbiol, 2010. **18**(9): p. 388-96.

21. Dube, M., et al., *Modulation of HIV-1-host interaction: role of the Vpu accessory protein.* Retrovirology, 2010. **7**: p. 114.

22. Balasubramaniam, M. and E.O. Freed, *New Insights into HIV Assembly and Trafficking.* Physiology (Bethesda), 2011. **26**(4): p. 236-51.

23. Bieniasz, P.D., *The cell biology of HIV-1 virion genesis.* Cell Host Microbe, 2009. **5**(6): p. 550-8.

24. Chukkapalli, V. and A. Ono, *Molecular determinants that regulate plasma membrane association of HIV-1 Gag.* J Mol Biol, 2011. **410**(4): p. 512-24.

25. Weiss, E.R. and H. Gottlinger, *The role of cellular factors in promoting HIV budding.* J Mol Biol, 2011. **410**(4): p. 525-33.

26. Hogue, I.B., et al., *Gag Induces the Coalescence of Clustered Lipid Rafts and Tetraspanin-Enriched Microdomains at HIV-1 Assembly Sites on the Plasma Membrane.* J Virol, 2011. **85**(19): p. 9749-66.

27. Krementsov, D.N., et al., *HIV-1 assembly differentially alters dynamics and partitioning of tetraspanins and raft components.* Traffic, 2010. **11**(11): p. 1401-14.

28. Chen, B.J. and R.A. Lamb, *Mechanisms for enveloped virus budding: can some viruses do without an ESCRT?* Virology, 2008. **372**(2): p. 221-32.

29. Hurley, J.H. and P.I. Hanson, *Membrane budding and scission by the ESCRT machinery: it's all in the neck.* Nat Rev Mol Cell Biol, 2010. **11**(8): p. 556-66.

30. Ono, A., *Relationships between plasma membrane microdomains and HIV-1 assembly.* Biol Cell, 2010. **102**(6): p. 335-50.

31. Hammonds, J. and P. Spearman, *An imperfect rule for the particle roost.* Cell Host Microbe, 2010. **7**(4): p. 261-3.

32. Adachi, A., et al., *Production of acquired immunodeficiency syndrome-associated retrovirus in human and nonhuman cells transfected with an infectious molecular clone.* J Virol, 1986. **59**(2): p. 284-91.

33. Klimkait, T., et al., *The human immunodeficiency virus type 1-specific protein vpu is required for efficient virus maturation and release.* J Virol, 1990. **64**(2): p. 621-9.

34. Chukkapalli, V., et al., *Interaction between the human immunodeficiency virus type 1 Gag matrix domain and phosphatidylinositol-(4,5)-bisphosphate is essential for efficient gag membrane binding.* J Virol, 2008. **82**(5): p. 2405-17.

35. Sun, Z., et al., *Tumor susceptibility gene 101 protein represses androgen receptor transactivation and interacts with p300.* Cancer, 1999. **86**(4): p. 689-96.

36. Ott, M., et al., *Acetylation of the HIV-1 Tat protein by p300 is important for its transcriptional activity.* Curr Biol, 1999. **9**(24): p. 1489-92.

37. Ahmad, N., R.K. Maitra, and S. Venkatesan, *Rev-induced modulation of Nef protein underlies temporal regulation of human immunodeficiency virus replication.* Proc Natl Acad Sci U S A, 1989. **86**(16): p. 6111-5.

38. Ono, A. and E.O. Freed, *Plasma membrane rafts play a critical role in HIV-1 assembly and release.* Proc Natl Acad Sci U S A, 2001. **98**(24): p. 13925-30.

39. Yee, J.K., T. Friedmann, and J.C. Burns, *Generation of high-titer pseudotyped retroviral vectors with very broad host range.* Methods Cell Biol, 1994. **43 Pt A**: p. 99-112.

40. Kong, L.B., et al., *Cryoelectron microscopic examination of human immunodeficiency virus type 1 virions with mutations in the cyclophilin A binding loop.* J Virol, 1998. **72**(5): p. 4403-7.

41. von Schwedler, U.K., et al., *Functional surfaces of the human immunodeficiency virus type 1 capsid protein.* J Virol, 2003. **77**(9): p. 5439-50.

42. Huang, M., et al., *p6Gag is required for particle production from full-length human immunodeficiency virus type 1 molecular clones expressing protease.* J Virol, 1995. **69**(11): p. 6810-8.

43. Popov, S., et al., *Human immunodeficiency virus type 1 Gag engages the Bro1 domain of ALIX/AIP1 through the nucleocapsid.* J Virol, 2008. **82**(3): p. 1389-98.

44. Gottlinger, H.G., et al., *Effect of mutations affecting the p6 gag protein on human immunodeficiency virus particle release.* Proc Natl Acad Sci U S A, 1991. **88**(8): p. 3195-9.

45. Zhang, M., et al., *Rational design of true monomeric and bright photoactivatable fluorescent proteins.* Nat Methods, 2012. **9**(7): p. 727-9.

46. Kiernan, R.E., A. Ono, and E.O. Freed, *Reversion of a human immunodeficiency virus type 1 matrix mutation affecting Gag membrane binding, endogenous reverse transcriptase activity, and virus infectivity.* J Virol, 1999. **73**(6): p. 4728-37.

47. Hogue, I.B., A. Hoppe, and A. Ono, *Quantitative fluorescence resonance energy transfer microscopy analysis of the human immunodeficiency virus type 1 Gag-Gag interaction: relative contributions of the CA and NC domains and membrane binding.* J Virol, 2009. **83**(14): p. 7322-36.

48. Janvier, K., et al., *The ESCRT-0 component HRS is required for HIV-1 Vpu-mediated BST-2/tetherin down-regulation.* PLoS Pathog, 2011. **7**(2): p. e1001265.

49. Pan, S., et al., *Involvement of the conserved adaptor protein Alix in actin cytoskeleton assembly.* J Biol Chem, 2006. **281**(45): p. 34640-50.

50. Morita, E., et al., *Human ESCRT-III and VPS4 proteins are required for centrosome and spindle maintenance.* Proc Natl Acad Sci U S A, 2010. **107**(29): p. 12889-94.

51. Miyagi, E., et al., *Vpu enhances HIV-1 virus release in the absence of Bst-2 cell surface down-modulation and intracellular depletion.* Proc Natl Acad Sci U S A, 2009. **106**(8): p. 2868-73.

52. Llewellyn, G.N., et al., *Nucleocapsid promotes localization of HIV-1 gag to uropods that participate in virological synapses between T cells.* PLoS Pathog, 2010. **6**(10): p. e1001167.

53. Ono, A., et al., *Association of human immunodeficiency virus type 1 gag with membrane does not require highly basic sequences in the nucleocapsid: use of a novel Gag multimerization assay.* J Virol, 2005. **79**(22): p. 14131-40.

54. Bolte, S. and F.P. Cordelieres, *A guided tour into subcellular colocalization analysis in light microscopy.* J Microsc, 2006. **224**(Pt 3): p. 213-32.

55. Gonda, M.A., et al., *Ultrastructural studies of surface features of human normal and tumor cells in tissue culture by scanning and transmission electron microscopy.* J Natl Cancer Inst, 1976. **56**(2): p. 245-63.

56. Rust, M.J., M. Bates, and X. Zhuang, *Sub-diffraction-limit imaging by stochastic optical reconstruction microscopy (STORM).* Nat Methods, 2006. **3**(10): p. 793-5.

57. Churchman, L.S., et al., *Single molecule high-resolution colocalization of Cy3 and Cy5 attached to macromolecules measures intramolecular distances through time.* Proc Natl Acad Sci U S A, 2005. **102**(5): p. 1419-23.

58. Veatch, S.L., et al., *Correlation functions quantify super-resolution images and estimate apparent clustering due to over-counting.* PLoS One, 2012. **7**(2): p. e31457.

59. Hammond, S., et al., *Roles for SH2 and SH3 domains in Lyn kinase association with activated FcepsilonRI in RBL mast cells revealed by patterned surface analysis.* J Struct Biol, 2009. **168**(1): p. 161-7.

60. Miyagi, E., et al., *Antibody-mediated enhancement of HIV-1 and HIV-2 production from BST-2/tetherin-positive cells.* J Virol, 2011. **85**(22): p. 11981-94.

61. Fritz, J.V., et al., *HIV-1 Vpu's lipid raft association is dispensable for counteraction of the particle release restriction imposed by CD317/Tetherin.* Virology, 2012. **424**(1): p. 33-44.

62. Ruiz, A., et al., *Membrane raft association of the Vpu protein of human immunodeficiency virus type 1 correlates with enhanced virus release.* Virology, 2010. **408**(1): p. 89-102.

63. Ono, A., A.A. Waheed, and E.O. Freed, *Depletion of cellular cholesterol inhibits membrane binding and higher-order multimerization of human immunodeficiency virus type 1 Gag.* Virology, 2007. **360**(1): p. 27-35.

64. Garrus, J.E., et al., *Tsg101 and the vacuolar protein sorting pathway are essential for HIV-1 budding.* Cell, 2001. **107**(1): p. 55-65.

65. Martin-Serrano, J., T. Zang, and P.D. Bieniasz, *HIV-1 and Ebola virus encode small peptide motifs that recruit Tsg101 to sites of particle assembly to facilitate egress.* Nat Med, 2001. **7**(12): p. 1313-9.

66. Demirov, D.G., et al., *Overexpression of the N-terminal domain of TSG101 inhibits HIV-1 budding by blocking late domain function.* Proc Natl Acad Sci U S A, 2002. **99**(2): p. 955-60.

67. Strack, B., et al., *AIP1/ALIX is a binding partner for HIV-1 p6 and EIAV p9 functioning in virus budding.* Cell, 2003. **114**(6): p. 689-99.

68. von Schwedler, U.K., et al., *The protein network of HIV budding.* Cell, 2003. **114**(6): p. 701-13.

69. Pornillos, O., et al., *Structure of the Tsg101 UEV domain in complex with the PTAP motif of the HIV-1 p6 protein.* Nat Struct Biol, 2002. **9**(11): p. 812-7.

70. Stuchell, M.D., et al., *The human endosomal sorting complex required for transport (ESCRT-I) and its role in HIV-1 budding.* J Biol Chem, 2004. **279**(34): p. 36059-71.

71. VerPlank, L., et al., *Tsg101, a homologue of ubiquitin-conjugating (E2) enzymes, binds the L domain in HIV type 1 Pr55(Gag).* Proc Natl Acad Sci U S A, 2001. **98**(14): p. 7724-9.

72. Demirov, D.G., J.M. Orenstein, and E.O. Freed, *The late domain of human immunodeficiency virus type 1 p6 promotes virus release in a cell type-dependent manner.* J Virol, 2002. **76**(1): p. 105-17.

73. Bouamr, F., et al., *Basic Residues in the Nucleocapsid Domain of Gag Are Critical for Late Events of HIV-1 Budding.* Journal of Virology, 2011. **85**(5): p. 2304-2315.

74. Kafaie, J., et al., *Mapping of nucleocapsid residues important for HIV-1 genomic RNA dimerization and packaging.* Virology, 2008. **375**(2): p. 592-610.

75. Grigorov, B., et al., *Intracellular HIV-1 Gag localization is impaired by mutations in the nucleocapsid zinc fingers.* Retrovirology, 2007. **4**: p. 54.

76. Betzig, E., et al., *Imaging intracellular fluorescent proteins at nanometer resolution.* Science, 2006. **313**(5793): p. 1642-5.

77. McKinney, S.A., et al., *A bright and photostable photoconvertible fluorescent protein.* Nat Methods, 2009. **6**(2): p. 131-3.

78. Endesfelder, U., et al., *Chemically induced photoswitching of fluorescent probes--a general concept for super-resolution microscopy.* Molecules, 2011. **16**(4): p. 3106-18.

79. Martin-Serrano, J., et al., *Divergent retroviral late-budding domains recruit vacuolar protein sorting factors by using alternative adaptor proteins.* Proc Natl Acad Sci U S A, 2003. **100**(21): p. 12414-9.

80. Morita, E., et al., *ESCRT-III protein requirements for HIV-1 budding.* Cell Host Microbe, 2011. **9**(3): p. 235-42.

81. van Rheenen, J. and K. Jalink, *Agonist-induced PIP(2) hydrolysis inhibits cortical actin dynamics: regulation at a global but not at a micrometer scale.* Mol Biol Cell, 2002. **13**(9): p. 3257-67.

82. Malim, M.H. and M. Emerman, *HIV-1 accessory proteins--ensuring viral survival in a hostile environment.* Cell Host Microbe, 2008. **3**(6): p. 388-98.

83. Reil, H., et al., *Efficient HIV-1 replication can occur in the absence of the viral matrix protein.* EMBO J, 1998. **17**(9): p. 2699-708.

84. Andrew, A.J., S. Kao, and K. Strebel, *C-terminal hydrophobic region in human bone marrow stromal cell antigen 2 (BST-2)/tetherin protein functions as second transmembrane motif.* J Biol Chem, 2011. **286**(46): p. 39967-81.

85. Chojnacki, J., et al., *Maturation-dependent HIV-1 surface protein redistribution revealed by fluorescence nanoscopy.* Science, 2012. **338**(6106): p. 524-8.

86. Hammonds, J., et al., *The tetherin/BST-2 coiled-coil ectodomain mediates plasma membrane microdomain localization and restriction of particle release.* J Virol, 2012. **86**(4): p. 2259-72.

87. Baumgartel, V., et al., *Live-cell visualization of dynamics of HIV budding site interactions with an ESCRT component.* Nat Cell Biol, 2011. **13**(4): p. 469-74.

88. Jouvenet, N., et al., *Dynamics of ESCRT protein recruitment during retroviral assembly.* Nat Cell Biol, 2011. **13**(4): p. 394-401.

89. Bhatia, V.K., N.S. Hatzakis, and D. Stamou, *A unifying mechanism accounts for sensing of membrane curvature by BAR domains, amphipathic helices and membrane-anchored proteins.* Semin Cell Dev Biol, 2010. **21**(4): p. 381-90.

90. Antonny, B., *Mechanisms of membrane curvature sensing.* Annu Rev Biochem, 2011. **80**: p. 101-23.

CHAPTER III

Characterization of HIV-1 interactions with uropod-directed microdomains by quantitative super-resolution localization microscopy

Abstract

The process of HIV-1 assembly begins with binding and targeting of the major viral structural protein, Gag, to the plasma membrane of the host cell in most cell types. This complex and highly-regulated interaction involves the participation of various membrane components. After membrane binding has taken place, Gag is able to recruit the viral envelope protein, Env, as well as interact with several cell-surface proteins, some of which constitute distinct microdomains on the plasma membrane. Gag is also capable of reorganizing some of these domains through an undefined mechanism. In polarized T cells, which are a natural host of HIV-1 infection in vivo, Gag has been shown to interact with a subset of microdomains which polarize to a rear-end protrusion termed the uropod. In the current study, we employ quantitative super-resolution localization microscopy to investigate and define the underlying mechanism by which Gag interacts with uropod-directed microdomain proteins. We also use more conventional assays to determine the consequences of these interactions to HIV-1 viral replication.

By super-resolution localization microscopy and cross-correlation analysis, we have determined that basic residues in the matrix domain of Gag as well as basic residues in the cytoplasmic tail of PSGL-1 are required for efficient co-clustering of these proteins. We have also determined that Ezrin, Radixin, and Moesin proteins do not play a role in this interaction and are slightly inhibitory. Finally, we have determined that expression of uropod-directed proteins PSGL-1, CD43, CD44, and ICAM-3 moderately reduces infectivity and cell-to-cell transfer of HIV-1.

Introduction

As an enveloped virus, HIV-1 interacts with and assembles at the plasma membrane in most cell types. The process of membrane binding is driven exclusively by the matrix (MA) domain of the Gag precursor polyprotein (Pr55), which initiates and coordinates viral assembly at the plasma membrane. Initial membrane binding and targeting of Gag are mediated by co-translational, N-terminal myristoylation of Gag as well as specific interactions between the highly-basic region (HBR) of the MA domain and the plasma-membrane specific phospholipid, phosphatidylinositol-(4,5)-bisphosphate $PI(4,5)P_2$ [1-5].

RNA is able to inhibit non-specific membrane binding of Gag; however, this inhibition can be overcome by $PI(4,5)P_2$ interaction [6, 7]. Additional evidence has suggested that other acidic lipids present in the plasma membrane, such as phosphatidylserine (PS), as well as uncharged, zwitterionic lipids, such as phosphatidylcholine (PC) and phosphatidylethanolamine (PE), may also contribute to and stabilize membrane binding of Gag [8, 9]. It has also been proposed that cholesterol and

acyl chain composition may influence the ability of Gag to bind to these lipids in cells [8]. Given that most of these studies were carried out using simple, defined lipid mixtures and Gag synthesized in vitro, it remains to be seen which of these interactions are critical for HIV-1 assembly at intact cellular membranes.

Once membrane binding has taken place, Gag associates with cholesterol-rich areas of the membrane which are resistant to detergent solubilization, termed lipid rafts [10]. This association has been shown to enhance multimerization of Gag, which in turn facilitates virus assembly [11] .

Viral assembly involves a coordinated and highly regulated process by which Gag is able to recruit all essential viral components into spherical virus particles of approximately 100 nm in diameter, which are ultimately released from infected cells with the help of cellular machinery. This process includes incorporation of the viral envelope glycoprotein (Env), encapsidation of viral genomic RNA (gRNA), and incorporation of other viral and cellular proteins [12]. During assembly, Gag has been observed to interact with plasma membrane microdomains such as tetraspanin-enriched microdomains (TEMs) and certain uropod-directed microdomains (UDMs) which are present in polarized T cells [13-17]. Gag has also been observed to actively reorganize these domains in ways which do not occur in uninfected cells [18-20].

T cells, which are a natural host of HIV-1 infection in-vivo, are highly motile and exhibit polarized morphology in secondary lymphoid tissues, where HIV-1 dissemination is thought to occur [21]. Previous studies conducted in our lab have demonstrated that Gag interacts with certain microdomains, termed class I UDMs in this thesis, composed of PSGL-1, CD43, and CD44 [16]. While this association is probably not required for

polarization of Gag to uropods, these interactions have been observed prior to cell polarization. Also, polarization of both Gag and UDMs is dependent upon the actin-myosin system [16].

Surprisingly, Gag has also been shown to exclude a second class of UDMs, termed class II UDMs, from virus assembly sites. CD59, ICAM-1, and ICAM-3 have all been observed to polarize to uropods, but not to associate with Gag in unpolarized T cells. Furthermore, ICAM-3, which is normally associated with the class I UDM protein CD44 in uninfected cells, is actively removed from these domains in the presence of Gag through an unknown mechanism [20].

Transmission of virus from infected cells to uninfected cells likely occurs at a virus-induced structure termed the virological synapse (VS). Formation of the VS is primarily mediated by interactions between Env on donor cells and CD4 on target cells [22]; however, synapses have also been observed in the absence of Env [23]. The VS is thought to be somewhat analogous to the well characterized immunological synapse (IS), which forms between antigen presenting cells and T cells [24]; however, it lacks the high degree of spatial organization seen in the IS [25]. Both are thought to be composed of critical receptor-ligand interactions, as well as additional adhesion molecules which promote sustained cell-to-cell contact [26].

Understanding the interactions which facilitate cell-to-cell virus transfer is of great importance in HIV research because this method of infection is much more efficient than infection by cell-free virus [27]. In addition, cell-to-cell transfer has been shown to be resistant to anti-viral drugs and neutralizing antibodies [28-31]. In order to treat and

prevent HIV infection, we must find ways to target cell-to-cell virus transmission, as it is likely the primary route of HIV dissemination in vivo.

While the precise role of UDMs in viral replication and dissemination remains to be elucidated, it is likely that HIV-1 has evolved to preferentially incorporate certain uropod-directed proteins at virus assembly sites for some purpose. Given that these transmembrane proteins all possess large extracellular domains, we speculate that their incorporation into viral envelopes may influence intercellular transfer of virus from infected to uninfected cells. In this study, we employ quantitative super-resolution localization microscopy methods to elucidate the mechanism of HIV-UDM interactions. We also use more conventional virological methods to determine the consequences of Gag-UDM interactions in viral replication.

Materials and Methods

Plasmids and siRNA

pNL4-3/Gag-mEos3.2 was generated by replacing the YFP coding sequence of pNL4-3 Gag-Venus with that of mEos3.2, with the initiator methionine residue removed, as in the constructs described in Chapter 2 of this thesis. pNL4-3/Fyn(10)/Gag-mEos3.2, pNL4-3/Fyn(10)/6A2T/Gag-mEos3.2, and pNL4-3/Fyn(10)/HBR_{switch}/Gag-mEos3.2 were constructed similarly from pNL4-3/Gag-Venus versions of these constructs, which were described previously [19, 20].

A plasmid encoding a full-length cDNA clone of human PSGL-1 (transcript variant 2), pCMV6-AC/PSGL-1, was obtained from Origene (NM_003006.3, Rockville, MD). pCMV6/empty was created by digesting pCMV6-AC/PSGL-1 with AgeI to remove

the entire MCS, followed by re-ligation of the vector. pCMV6-AC/PSGL-1 C310A and ΔCT (with a stop codon in place of L331) constructs were generated by standard PCR mutagenesis techniques. pCMV6-AC/PSGL-1 3A and 6A constructs were generated by the following substitutions (mutations in bold): 334-338 **R**LS**RK** → **A**LS**AA** (3A) and 385-394 **E**PR**ED**R**E**G**DD** → **A**PR**AA**R**A**G**AA** (6A), using standard PCR mutagenesis techniques.

Plasmids encoding full length cDNA clones of human CD43 (NM_003123), pCMV6-XL5/CD43, CD44 (NM_000610), pCMV6-XL5/CD44, ICAM-1 (NM_000201), pCMV6-XL5/ICAM-1, and ICAM-3 (NM_002162.2), pCMV6-AC/ICAM-3 were obtained from Origene (Rockville, MD). The chimeric constructs pCMV6-AC /ICAM-1-PCT and pCMV6-AC/ICAM-3-PCT were constructed by inserting the sequences encoding the extracellular and transmembrane portions of ICAM-1 and ICAM-3 respectively into pCMV6-AC/PSGL-1, in place of the PSGL-1 extracellular and transmembrane portions by standard molecular cloning techniques. The sequence of ICAM-1-PCT is as follows (ICAM-1 residues in bold): **MAPSSP…LSTYLY**AVRLSR… The sequence of ICAM-3-PCT is as follows (ICAM-3 residues in bold): **MATMVP…ALMYVF**AVRLSR…

siRNA sequences directed against Ezrin (CAAGAAGGCACCUGACUUU), Radixin (GAACUGGCAUGAAGAACAU), and Moesin (AUAAGGAAGUGCAUAA GUC) were described previously [32]. A control siRNA, which does not target any known human mRNA sequences (UUCUCCGAACGUGUCACGU), was also used [33]. Double-stranded RNA oligonucleotides by Integrated DNA Technologies (Coralville, IA).

Antibodies

A monoclonal mouse antibody directed against human PSGL-1 (clone KPL-1), was obtained from BD Biosciences (San Jose, CA). This antibody was directly labeled with Alexa Fluor 647 using an antibody labeling kit obtained from Life Technologies (Carlsbad, CA). Rabbit antibodies directed against human Ezrin, Radixin, and Moesin proteins were obtained from Cell Signalling Technology (Beverly, MA). Anti-HIV-Ig was obtained from the NIH AIDS Research and Reference Reagent Program (ARRRP).

Cells

HeLa cells were maintained in DMEM supplemented with 5% FBS, Pen/Strep, and L-glutamine. For STORM analysis, cells were plated at a density of $4.2x10^4$ cells per well in #1.5, 4-chamber coverslips from Fisher Scientific (Pittsburgh, PA). After overnight incubation, cells were transfected with 1 μg pNL4-3/Gag-mEos3.2 plasmids and 50 ng pCMV6-AC/PSGL-1 plasmids per well, using Lipofectamine 2000 reagent, according to the manufacturer's instructions (Life Technologies, Carlsbad, CA). MA-replacement constructs were additionally supplemented with 0.5 μg of pNLA-1 [34], a plasmid which encodes all viral proteins except Gag and GagPol, because these constructs display a splicing defect and only express Gag (IBH and JRG, unpublished ovservations). Cells were then incubated for 16 hours prior to fixation with 1X PBS + 4% PFA + 0.1% glutaraldehyde for 10 minutes followed by immunostaining with anti-PSGL-1 antibody.

293T cells were maintained in DMEM supplemented with 10% FBS, Pen/Strep, and L-glutamine. SupT1 and CEM-GFP cells were maintained in RPMI supplemented

with 10% FBS, Pen/Strep, and L-glutamine. CEM-GFP cell media was additionally supplemented with 500 μg/ml G418 to maintain LTR-dependent GFP expression.

Super-Resolution Localization Microscopy and Image Processing

Sample preparation, imaging conditions, and data analysis methods are described in detail in chapter 2 of this thesis. To compare total clustering in cross-correlation analyses, area under cross-correlation curves was integrated from 0-200 nm.

siRNA Knockdowns

For siRNA-mediated depletion of Ezrin, Radixin, and Moesin, HeLa cells were plated at a density of 10^5 cells per well in 24-well culture plates (Corning, Fairport, NY). After overnight incubation, cells were transfected with 20 pM siRNA (40 pM for Ezrin-directed siRNA) using Lipofectamine 2000, according to the manufacturer's instructions (Life Technologies, Carlsbad, CA). After 24 hours, cells were typsinized, counted, and plated at a density of $4.2x10^4$ cells per well in #1.5, 4-well chambered coverslips (Fisher Scientific, Pittsburgh, PA). Cells were incubated for an additional 24 hours before transfection as described above, giving a total of 64 hours post-transfection by siRNA and 16 hours post-transfection by PSGL-1 and Gag-mEos3.2 plasmids before fixation.

Infectivity Assay

293T cells were plated at a density of $5.6x10^5$ cells/well in 6-well culture plates (Corning Inc., Corning, NY), incubated overnight and transfected with 2 μg pNL4-3 and a total of 300 ng of plasmids encoding indicated proteins using polyethylenimine (PEI,

Polysciences, Warrington, PA), followed by 48 hour incubation at 37°C. Culture supernatants were collected, cleared by low-speed centrifugation and filtered through 0.45 μm filters, followed by centrifugation at 35,000 rpm for 45 minutes at 4°C. Virus pellets were resuspended in 100 μl RPMI + 10% FBS. 10 μl of each virus stock was then added to $2x10^5$ CEM-GFP cells in 12-well culture plates (Corning Inc., Corning, NY) and incubated for 48 hours at 37°C. Cells were fixed and analyzed by FACS. Relative amounts of virus production were determined by Western blotting of virus lysates with anti-HIV Ig, and quantitation of virus-associated p24.

Cell-to-cell Transfer Assay

HeLa cells were plated at a density of $5.6x10^5$ cells/well in 6-well culture plates (Corning Inc., Corning, NY), incubated overnight and transfected with 2 μg pNL4-3/Gag-YFP and a total of 300 ng of plasmids encoding indicated proteins using Lipofectamine 2000 (Life Technologies, Carlsbad, CA), followed by 16 hour incubation at 37°C. Culture media was removed and cells were washed once with media. Next, $4x10^5$ SupT1 cells were added to each well in RPMI + 10% FBS. Cells were incubated for 3 hours at 37°C before being removed from wells, fixed, and analyzed by FACS. HeLa and SupT1 cells were separated by differences in forward and side scattering.

Results

We have previously shown that HIV-1 Gag interacts with class I UDM proteins PSGL-1, CD43, and CD44 in unpolarized T cells [16, 20]. This interaction was found to be dependent upon the charge, but not specific amino acid sequence of the MA HBR

[20]. These previous studies were performed using an antibody copatching assay [19], which clusters proteins into visible patches that can be observed by traditional, diffraction-limited microscopy. However, this technique may not reflect the native distribution of proteins in live cells because proteins of interest are clustered by primary and secondary antibodies prior to fixation. To analyze the interactions between HIV-1 Gag and UDM proteins in greater detail, without the use of antibody copatching, we employed two-color super-resolution localization microscopy techniques (described in chapter 2 of this thesis), which have been used previously by our group and others to study virus-host interactions [35-37].

HeLa cells constitute a suitable model system in which to conduct these experiments because they are highly adherent, support HIV-1 virus production, and do not express endogenous UDM proteins. Although T cells are a more natural host for HIV-1 replication in vivo, they cannot be imaged by TIRF illumination unless adhered to coverglasses by immobilized extracellular matrix proteins or poly-L-lysine. This has the potential to alter the distribution and inhibit normal diffusion of UDM proteins, many of which possess adhesive properties. HeLa cells are also very amenable to transfection by plasmid DNA and siRNA, and therefore allow for analysis of the contributions of individual UDM proteins to HIV-1 assembly and transmission.

We first sought to determine whether Gag-UDM interactions occur in HeLa cells in a similar manner to that observed in T cells. It is possible that these interactions are dependent on certain factors which are present in T cells but absent in adherent cell lines. To determine whether these interactions take place in HeLa cells, we expressed PSGL-1 along with three Gag constructs fused to the photo-switchable, monomeric fluorescent

protein mEos3.2 [38]. The first, Fyn(10)/Gag (when fused to YFP) has been shown to behave similarly to wild type Gag, with respect to UDM association [16]. The second, Fyn(10)/6A2T/Gag, is a construct in which the 8 basic residues of the HBR, which

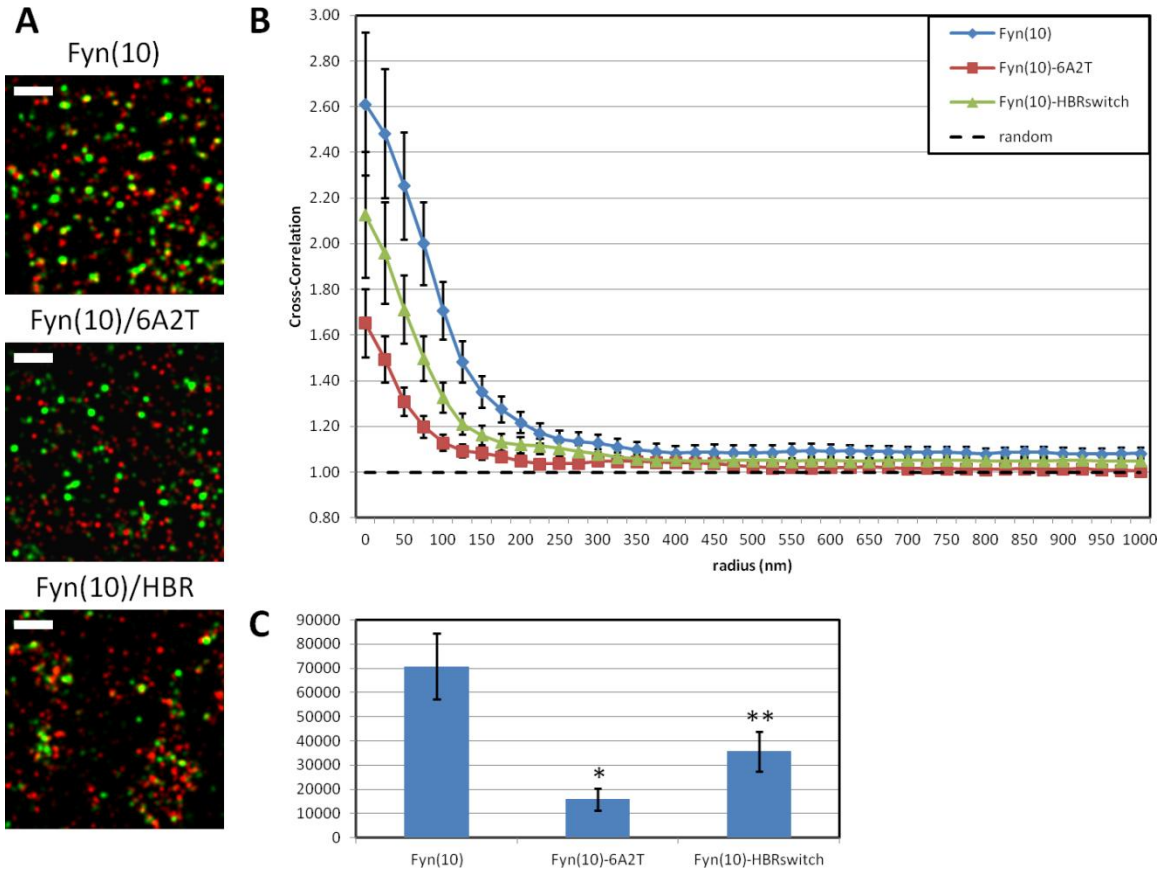

Figure 3.1. The basic charge of MA HBR promotes co-clustering of Gag and PSGL-1 in HeLa cells. HeLa cells were transfected with plasmids encoding Gag-mEos3.2 fusion constructs and wild type PSGL-1. Cells were fixed and stained for PSGL-1 with a monoclonal antibody against PSGL-1, which was directly labeled with AlexaFluor 647, and imaged by TIRF microscopy in reducing buffer (7,500 image frames per cell). (A) Reconstructed images were produced as described in Materials and Methods in chapter 2 of this thesis. Images show Gag-mEos3.2 in green and PSGL-1 in red. Scale bar = 500 nm. (B) Cross-correlation curves express co-clustering of molecules as a function of radius. (C) Total co-clustering was calculated by integrating area under cross-correlation curves from 0-200 nm as described in Materials and Methods in chapter 2 of this thesis. (B-C) Results shown include a total of 10 cells per condition from 2 independent experiments. Values shown indicate mean values ± sem. *significantly less than Fyn(10), $p < 0.05$. **significantly greater than Fyn(10)-6A2T and significantly less than Fyn(10), $p < 0.05$.

facilitate interactions between Gag and PI(4,5)P_2 have been replaced with neutral amino acids [20]. The third, Fyn(10)/HBR_{switch}/Gag, is a construct in which the identity of the 8

basic residues in the HBR has been exchanged (R→K and K→R). This construct has been shown to restore Gag-UDM interactions to similar levels to those observed with wild type and Fyn(10) Gag constructs by antibody copatching assay [20].

When expressed in HeLa cells, we observed that all of these constructs localize to the plasma membrane, as did PSGL-1. We found that, consistent with our findings in T cells, Fyn(10)/Gag-mEos3.2 clustered highly with PSGL-1. We also observed that Fyn(10)/6A2T/Gag-mEos3.2 showed very low levels of clustering with PSGL-1, and co-clustering was partially restored by the HBR_{switch} mutation, although not to the same level as when the wild type HBR sequence was present (Figure 3.1). These results indicate that Gag is able to associate with PSGL-1, a class I UDM protein, when expressed in HeLa cells. They also show that viral determinants of this interaction are similar to those observed in T cells.

Although exchanging the identity of the basic residues within the HBR did partially restore PSGL-1 co-clustering, it was not completely restored to wild type levels. While this mutant retains the same overall charge of the HBR, unlike wild type Gag, it is unable to bind to liposomes containing $PI(4,5)P_2$ without prior RNAse treatment [20]. While wild type Gag is able to interact specifically with $PI(4,5)P_2$, the HBR_{switch} mutant is likely to only interact with $PI(4,5)P_2$ through non-specific, electrostatic interactions. The finding that this mutant also displays lower clustering with PSGL-1 may suggest that $PI(4,5)P_2$ plays a role in recruitment of this protein to HIV-1 assembly sites. This hypothesis is also consistent with the observation that $PI(4,5)P_2$ depletion exerts a much more potent effect in HeLa cells than in T cells [1, 39].

In order to better understand how Gag recruits class I UDM proteins to virus assembly sites, we sought to identify which components of PSGL-1 are necessary for this interaction. Because PSGL-1 is always present as a dimer in cells, we asked whether dimerization is necessary for Gag-PSGL-1 interaction. To do this, we utilized a previously characterized mutant (C310A) which abolished dimerization of PSGL-1 [40]. We found that this mutation did not significantly decrease Gag-PSGL-1 co-clustering,

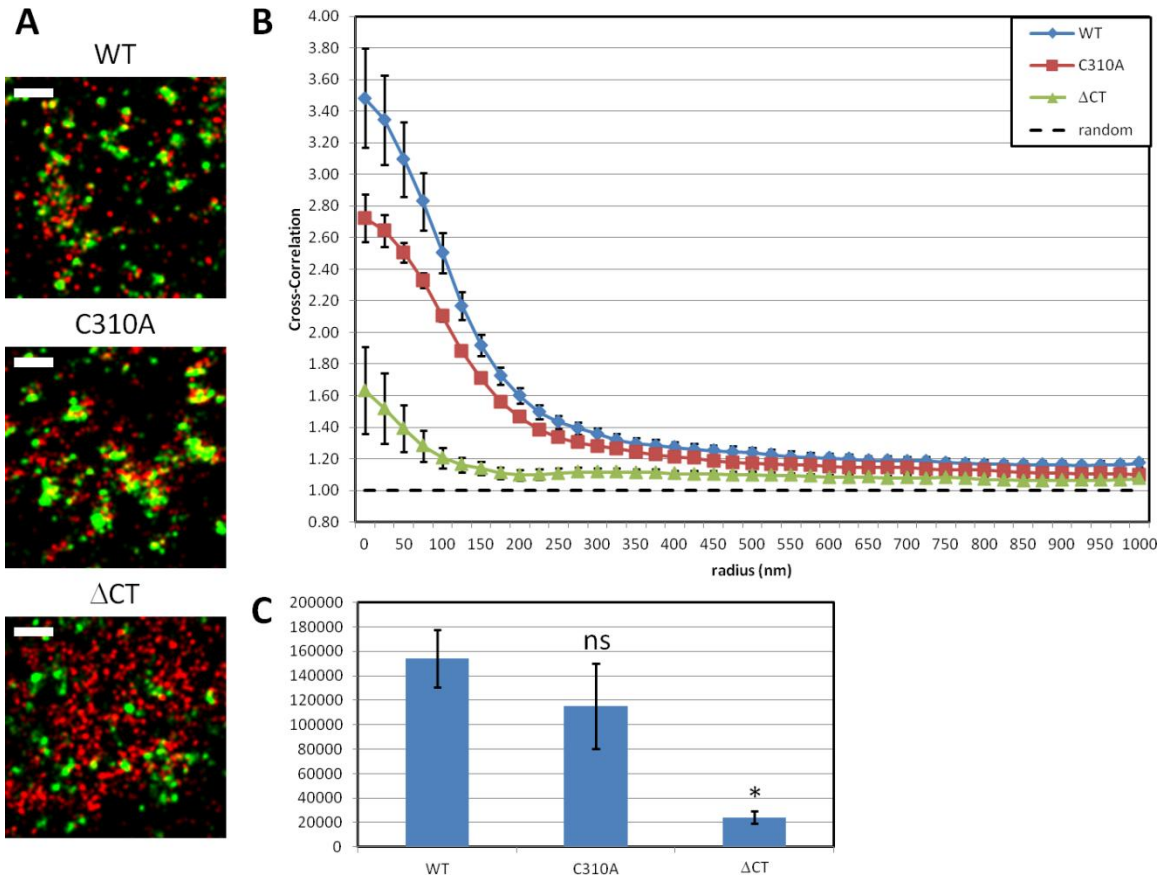

Figure 3.2. The cytoplasmic tail of PSGL-1, not dimerization, is required for co-clustering with Gag. HeLa cells were transfected with plasmids encoding wild type Gag-mEos3.2 and PSGL-1 mutants. Cells were prepared, imaged, and analyzed as in Figure 3.1. (A) Reconstructed images show Gag-mEos3.2 in green and PSGL-1 in red. Scale bar = 500 nm. (B) Cross-correlation curves express co-clustering of molecules as a function of radius. (C) Total co-clustering was calculated by integrating area under cross-correlation curves from 0-200 nm. (B-C) Results shown include a total of 10 cells per condition from 2 independent experiments. Values shown indicate mean values ± sem. *significantly less than WT, $p < 0.05$. ns, not significant.

ruling out a role for dimerization (Figure 3.2). Next, we sought to determine whether the cytoplasmic tail of PSGL-1, which may interact directly or indirectly with Gag or other viral components, is required for Gag-PSGL-1 interaction. We found that deletion of the cytoplasmic tail of PSGL-1 (truncated after residue 331) substantially reduced Gag-PSGL-1 interaction, although this mutant is expressed highly on the plasma membrane (Figure 3.2). This experiment identifies the cytoplasmic tail of PSGL-1 as the major determinant of Gag-PSGL-1 co-clustering. Given that co-clustering was not completely abolished by this truncation, the extracellular and transmembrane domains of this protein may also contribute to co-clustering with Gag.

Next, we sought to determine which features of the cytoplasmic tail of PSGL-1 are necessary for its recruitment to HIV-1 assembly sites. We generated two hypotheses which could be tested by mutagenesis of the cytoplasmic tail of PSGL-1. Given that basic residues within the HBR are critical for this interaction, we speculated that an acidic stretch near the C-terminus of the cytoplasmic tail of PSGL-1 may be interacting directly with the HBR of the MA domain. To test this hypothesis, we generated a mutant, PSGL-1/6A, in which these 6 residues have been replaced with an uncharged amino acid, alanine (**E**PR**ED**R**E**G**DD** $\rightarrow$ **A**PR**AA**R**A**G**AA**).

Our second hypothesis was based on the observation that PSGL-1, CD43, and CD44 all possess basic amino acids immediately C-terminal to their transmembrane domains, near the cytoplasmic leaflet of the lipid bilayer. Given that Gag can bind to acidic lipids such as $PI(4,5)P_2$ and PS through the HBR [3, 6], we speculated that clustering of acidic lipids at assembly sites by multimerizing Gag molecules may attract PSGL-1 and possibly also CD43 and CD44. To test this hypothesis, we generated a

mutant, PSGL-1/3A, in which three juxta-membrane basic residues have been replaced with alanine (**R**LS**RK** → **A**LS**AA**).

When expressed in HeLa cells, we found that PSGL-1/6A co-clusters with Gag-mEos3.2 to a similar extent as wild type PSGL-1, while co-clustering was significantly reduced by the 3A mutation (Figure 3.3). These results indicate that a basic motif near the plasma membrane is significantly enhances co-clustering of PSGL-1 with HIV-1

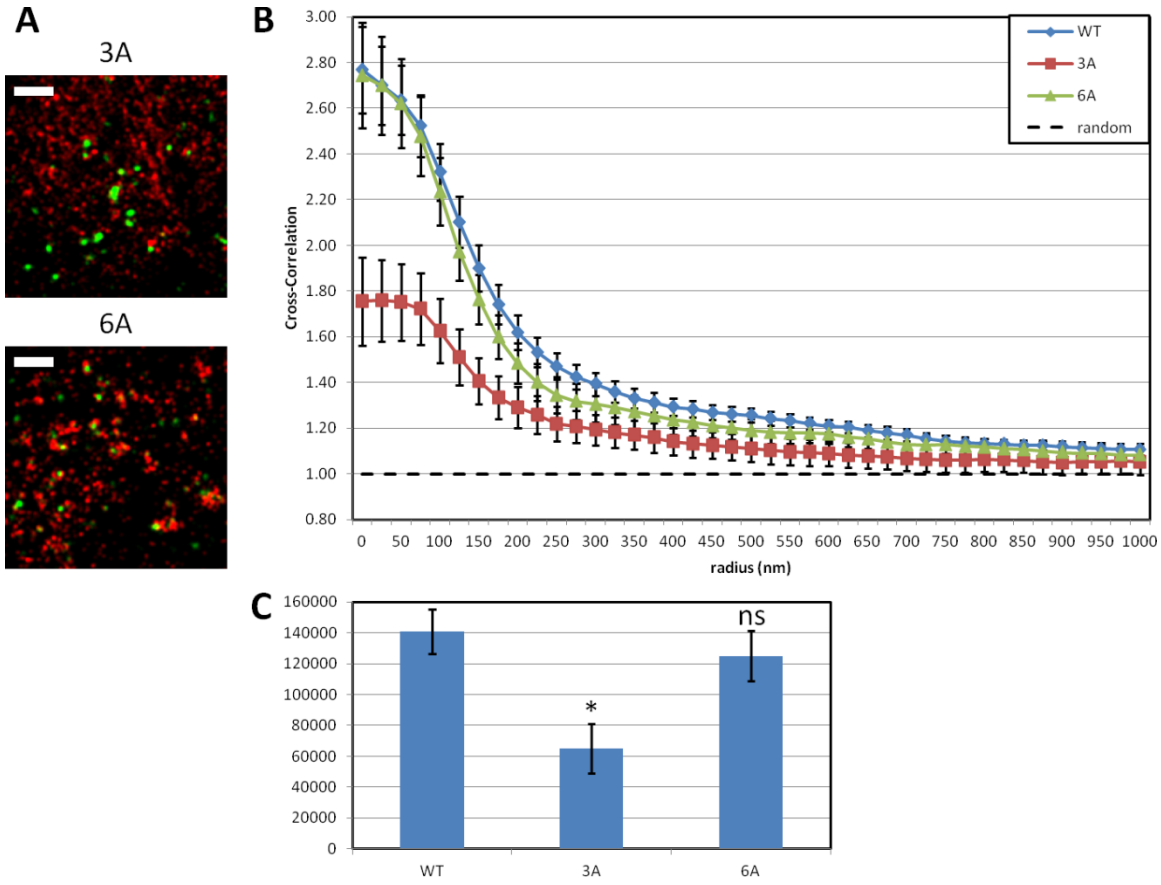

Figure 3.3. Basic residues in the cytoplasmic tail of PSGL-1 enhance co-clustering with Gag.
HeLa cells were transfected with plasmids encoding wild type Gag-mEos3.2 and PSGL-1 mutants. Cells were prepared, imaged, and analyzed as in Figure 3.1. (A) Reconstructed images show Gag-mEos3.2 in green and PSGL-1 in red. Scale bar = 500 nm. (B) Cross-correlation curves express co-clustering of molecules as a function of radius. (C) Total co-clustering was calculated by integrating area under cross-correlation curves from 0-200 nm. (B-C) Results shown include a total of 10 cells per condition from 2 independent experiments. Values shown indicate mean values ± sem. *significantly less than WT, $p < 0.05$. ns, not significant.

assembly sites. They also rule out a direct interaction between the highly-acidic C-terminus of PSGL-1 and the basic residues of the MA HBR. Although co-clustering of Gag and PSGL-1 was not completely abolished by the 3A mutation, it was substantially reduced compared to wild type PSGL-1. This may indicate the presence of additional determinants within the cytoplasmic tail of PSGL-1, which promote co-clustering with Gag, however the "**R**LS**RK"** motif is likely the major determinant of this interaction.

Interestingly, we found that PSGL-1/6A and ΔCT mutants are very highly expressed at the plasma membrane, as seen by microscopy (Figures 3.2 and 3.3) and FACS analysis (data not shown). This may indicate that the acidic motif "**E**PR**ED**R**E**G**DD**" may constitute a sorting or endocytic signal which regulates cell-surface levels of this protein. This observation also demonstrates the insensitivity of cross- correlation methods used in this thesis to relative protein expression levels. Both the 6A and ΔCT mutants were more highly expressed at the cell surface than wild type PSGL-1, while one of them (ΔCT) did not co-cluster highly with Gag-mEos3.2.

The ERM family of proteins, composed of Ezrin, Radixin, and Moesin (also related to Merlin and Band 4.1) interact with the actin cytoskeleton as well as plasma membrane by binding to plasma membrane proteins and phospholipids, including $PI(4,5)P_2$ [41]. These proteins have been seen to assume both a folded, inactive confirmation in the cytosol, as well as an active, phosphorylated form capable of linking the plasma membrane and actin cytoskeleton. These proteins play important roles in cell morphology, polarity, and motility [42].

Of interest to this study, several uropod-directed proteins contain binding sites for ERM proteins, including PSGL-1 [43, 44], CD43 [45], CD44 [46], ICAM-1 [47], and

ICAM-3 [43]. In particular, binding of PSGL-1 to Ezrin is mediated by an "RK" motif located near the plasma membrane. Given that these residues have been mutated in the PSGL-1/3A mutant, and that this mutation abolished PSGL-1-Ezrin interaction [44], we sought to determine whether ERM proteins play a role in Gag-PSGL-1 interaction. To accomplish this, we performed siRNA-mediated depletion of Ezrin, Radixin, and Moesin proteins individually and in combination. Following this, we expressed wild type PSGL-1 and Gag-mEos3.2 and performed STORM imaging and cross-correlation analyses.

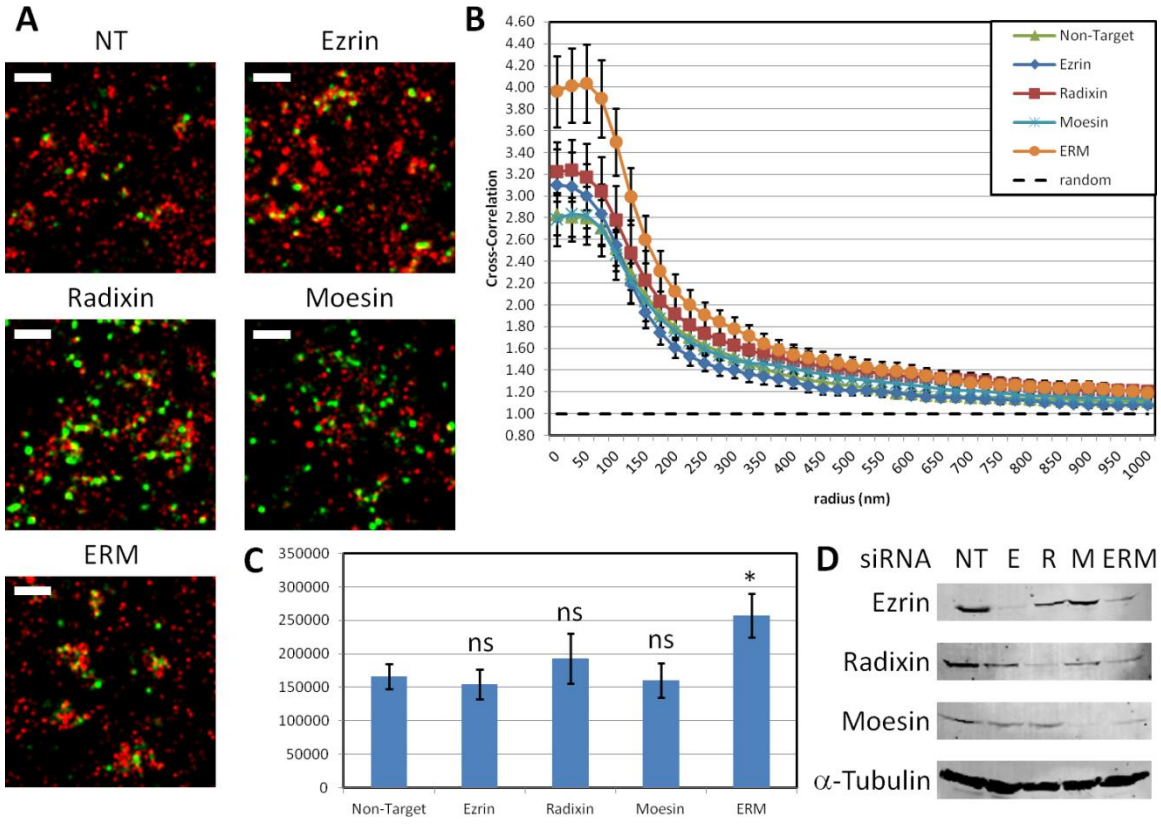

Figure 3.4. ERM proteins decrease co-clustering of Gag and PSGL-1.
HeLa cells were transfected with indicated siRNA oligonucleotides, followed by transfection with plasmids encoding wild type Gag-mEos3.2 and PSGL-1. Cells were prepared, imaged, and analyzed as in Figure 3.1. (A) Reconstructed images show Gag-mEos3.2 in green and PSGL-1 in red. Scale bar = 500 nm. (B) Cross-correlation curves express co-clustering of molecules as a function of radius. (C) Total co-clustering was calculated by integrating area under cross-correlation curves from 0-200 nm. (D) Western blots of Ezrin, Radixin, and Moesin from cells prepared under identical conditions to those used for microscopy. α-tubulin is shown as a loading control. (B-C) Results shown include a total of 9 cells per condition from 2 independent experiments. Values shown indicate mean values ± sem. *significantly greater than Non-Target, $p < 0.05$. ns, not significant.

We were able to achieve approximately 90% reduction in the levels of all 3 proteins when depleted individually, and approximately 80% reduction when all 3 were depleted simultaneously as compared to non-target siRNA-treated cells and assessed by Western blotting (Figure 3.4D). Under these conditions, we observed that depletion of Ezrin, Radixin, or Moesin individually did not significantly affect Gag-PSGL-1 co-clustering. In contrast, we observed that depletion of all three proteins led to a significant increase in Gag-PSGL-1 co-clustering (Figure 3.4A-C). Given the high degree of homology between these three proteins, it is not surprising that they may act redundantly, or compensate for the lack of one protein. These results indicate that not only are ERM proteins not required for Gag-PSGL-1 interaction, rather, they are slightly inhibitory when present in HeLa cells.

If ERM proteins are indeed inhibitory to PSGL-1 recruitment to virus assembly sites, it would be interesting to determine the effect of ERM over-expression on this process. If this effect is due to a competitive inhibition by ERM proteins, over-expression of these proteins would be expected to reduce co-clustering of Gag and PSGL-1.

There are several possible hypotheses which may explain this observation. First, the presence of ERM proteins and their interaction with basic residues in PSGL-1 cytoplasmic tail may prevent interaction with Gag or some other component present at assembly sites. Second, binding of ERM proteins to $PI(4,5)P_2$ at virus assembly sites may prevent efficient PSGL-1 recruitment. Third, uncoupling of the actin cytoskeleton and plasma membrane may allow for greater clustering of plasma membrane proteins and lipids, as has been predicted by biophysical simulations [48]. Fourth, linking of PSGL-1

to the cytoskeleton may inhibit its incorporation into virus assembly sites. This is consistent with the observation that the HIV-1 Nef protein appears to antagonize Ezrin [49], which is inhibitory to HIV-1 virus production [50].

While it is likely that ERM interactions are necessary for polarization of both class I and class II UDM proteins in polarized T cells, it is unlikely that ERM proteins participate directly in polarization of HIV-1 Gag to uropods. This hypothesis is based on the observation that replacement of MA domain by the Fyn(10) sequence abolishes Gag-UDM interactions (which depend on ERM proteins for polarization), but does not inhibit polarization of Gag [20]. Instead, it is more likely that Gag polarization is instead dependent upon bulk membrane flow, mediated by the actin-myosin system and ERM-linked membrane proteins. This is supported by the finding that treatment of T cells with a myosin light chain kinase inhibitor, ML7, results in depolarization of Gag. Thus, while ERM proteins may be critical for maintaining rearward flow of membrane components toward the uropod, they may not be directly involved in HIV-1 polarization.

Given that HIV-1 associates selectively with class I UDM proteins in polarized T cells, which are a natural host of HIV-1 infection in vivo, we sought to understand what role, if any, these interactions play in HIV-1 infection and dissemination. We hypothesized that because Gag-UDM interactions take place during viral assembly, these proteins may be involved in virus production, cell-to-cell transmission, or infectivity of virus particles.

To test these hypotheses, we first examined whether virus production is affected by expression of individual UDM proteins in HeLa and 293T cells. With the exception of CD44, which caused a modest reduction in virus production in 293T cells, all UDM

proteins examined in this study had no significant affect on virus production (data not shown). The defect in virus production observed in CD44-expressing 293T cells may possibly be accounted for by a specific cellular stress caused by over-expression of this protein. Another possibility is that because CD44 is a receptor for extracellular matrix components [51], its incorporation into virus particles may cause them to be retained within the extracellular matrix of producer cells.

We next tested whether UDM proteins have any effect on viral infectivity. This was done by deriving wild-type pNL4-3 virus stocks from 293T cells transfected with plasmids encoding UDM proteins of interest. These viruses were added to CEM-GFP cells, which express GFP under the control of the HIV-1 LTR. In the case of ICAM-1 and ICAM-3, we developed additional chimeric constructs (ICAM-1-PCT and ICAM-3-PCT) in which the cytoplasmic tails of these proteins was substituted with the cytoplasmic tail of PSGL-1. We reasoned that because the cytoplasmic tail of PSGL-1 contains the major determinants for co-clustering with Gag (Figure 3.2), it should allow for efficient incorporation of ICAM-1 and ICAM-3 into assembly sites and virus particles, which are not normally enriched at virus assembly sites in T cells [16, 20].

Unexpectedly, expression of PSGL-1, CD43, and CD44, either individually or in combination, reduced viral infectivity to approximately 40% of control virus (Figure 3.5A). We also observed a similar level of inhibition with ICAM-3, regardless of whether it contained its native cytoplasmic tail, or the cytoplasmic tail of PSGL-1 (Figure 3.5A). In contrast, we observed that ICAM-1 only reduced viral infectivity when it contained the cytoplasmic tail of PSGL-1 (Figure 3.5A).

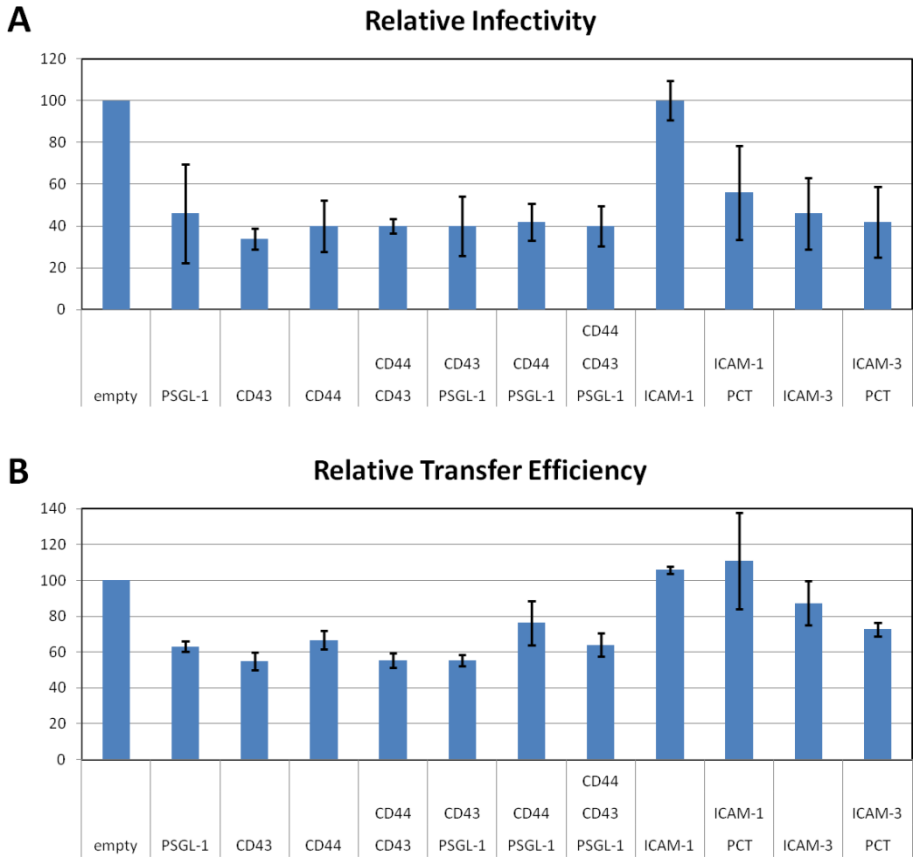

Figure 3.5. PSGL-1, CD43, CD44, and ICAM-3 decrease infectivity and cell-to-cell transfer of HIV-1. (A) Virus was purified by ultracentrifugation from supernatants of 293T cells transfected with pNL4-3 and plasmids encoding the proteins indicated or an empty vector control. Virus was then added to CEM-GFP cells, which express GFP under the control of the HIV-1 LTR. Cells were incubated for 48 hours, followed by fixation and FACS analysis. Values shown are the mean percent GFP-positive cells, normalized to p24 abundance in virus preparations (assessed by Western blotting). Values were further normalized to the empty vector control condition. Infection rate for the empty vector control was 5%. (B) HeLa cells were transfected with pNL4-3/Gag-YFP and plasmids encoding indicated proteins. After 16 hour incubation at 37°C, cells were washed and $4x10^5$ SupT1 cells were added to each well. Cells were co-cultured for 3 hours at 37°C before being removed from wells, fixed, and analyzed by FACS. Values shown are the percent YFP-positive SupT1 cells normalized to the percent YFP-positive HeLa cells in each condition. Values were further normalized to the empty vector control condition. YFP positive rate of CEM-GFP cells for empty vector control was 58%. Error bars represent the variation in two independent experiments performed for each assay.

As many UDM proteins are known to function as adhesive proteins, and participate in cellular contacts such as the immunological synapse [24], we examined whether they also modulate cell-to-cell transfer of virus particles. To test this hypothesis, we transfected HeLa cells with pNL4-3/Gag-YFP and plasmids encoding UDM proteins

of interest. Next, we added SupT1 T cells and co-cultured these cells for 3 hours. We have previously demonstrated efficient cell-to-cell transfer of Gag-YFP VLPs by this method [16]. Finally, cells were removed from culture plates, fixed and analyzed by FACS.

By this assay, we observed that all UDM proteins tested, with the exception of ICAM-1, modestly inhibited virus transfer from HeLa to SupT1 T cells (Figure 3.5B). ICAM-1 appeared to have little effect on transfer efficiency whether it contained its native cytoplasmic tail or that of PSGL-1 (Figure 3.5B). Western blotting of these proteins in cell and virus lysates would be the best method to separate these possibilities, and would allow for direct measurement of rates of incorporation of these proteins into virus particles. Thus far, detection of these proteins under denaturing conditions has been not been achieved.

Discussion

We have previously observed that HIV-1 Gag associates with uropod-directed microdomains composed of CD43, CD44, and PSGL-1 [16, 20]. This association occurs in both unpolarized and polarized T cells. Of note, these previous studies were conducted using an antibody copatching assay which may be prone to artifactual clustering of proteins. In the present study, we employ super-resolution microscopy methods which are able to resolve single virus assembly sites as well as single UDM proteins. These studies are carried out in cells which have been fixed prior to immunostaining, reducing the possibility of artifactual clustering of proteins.

Consistent with previous findings, we found that association of Gag with PSGL-1 is dependent upon the HBR of the MA domain. Replacing the 8 basic amino acids within the HBR substantially reduced Gag-PSGL-1 co-clustering. Exchanging the basic residues of the HBR from lysine to arginine and vice versa did still allow some recruitment of PSGL-1, but this was significantly less than that observed with wild type PSGL-1 (Figure 3.1). Like wild type Gag, this construct is capable of binding to liposomes containing PS, after RNAse treatment [20]. This result suggests that the overall structure of the MA domain is not grossly perturbed by these substitutions. However, it is currently unknown whether this mutant is able to interact with $PI(4,5)P_2$ after RNAse treatment [20]. It would be interesting to determine whether this mutant is unable to interact with $PI(4,5)P_2$, while still retaining the same overall charge of the HBR. A lack of this specificity may support a role for $PI(4,5)P_2$ in Gag-UDM interactions.

The observation that the HBR_{switch} construct is still able to recruit PSGL-1 to some level suggests that electrostatic interactions, rather than specific $PI(4,5)P_2$ interaction may be sufficient for recruitment of UDM proteins such as PSGL-1 to virus assembly sites. It will be interesting to determine whether this mutant is able to recruit CD43 and CD44 as well. It would also be interesting to determine whether these proteins are recruited independently, or whether CD43 and CD44 require PSGL-1 for efficient recruitment.

We next observed that the cytoplasmic tail of PSGL-1 contains the major determinants for co-clustering with Gag (Figure 3.2). Based on this finding, we speculate that the cytoplasmic tail of PSGL-1 may interact, either directly or indirectly, with Gag or some other component of HIV-1 assembly sites. While it is formally possible that the

extracellular domains of PSGL-1 and Env may interact and facilitate recruitment of PSGL-1 this is unlikely given the observation that Gag-PSGL-1 copatching still occurs in the absence of Env (GNL, unpublished observations). Furthermore, we found that basic residues within the cytoplasmic tail are responsible for the majority of Gag-PSGL-1 co-clustering (Figure 3.3). While these residues also constitute a binding site for ERM proteins, we found that depletion of ERM proteins did not inhibit Gag-PSGL-1 co-clustering. Rather, we found that depletion of Ezrin, Raxidin, and Moesin simultaneously enhanced this interaction slightly, but significantly (Figure 3.4).

Given the observations that basic residues are required on both sides of the interaction between Gag and PSGL-1, we hypothesize that there must be some acidic factor which links Gag and PSGL-1. Since these basic residues are likely positioned very close to the cytoplasmic leaflet of the plasma membrane, we further hypothesized that this unknown factor is likely an acidic lipid present in the inner leaflet of the plasma membrane. In a pilot experiment, we failed to observe any detectable co-clustering between PSGL-1 and the PH domain of PLCδ1, which specifically binds to $PI(4,5)P_2$, or the C2 domain of Lactadherin, which specifically binds to PS (data not shown).This result suggests that PSGL-1 does not associate strongly with these lipids in Gag-negative cells, or does so at undetectable levels. Additionally it may suggest that either of these lipids, which are abundant in the plasma membrane, are not necessary for recruitment of PSGL-1 to virus assembly sites. Alternatively, it is possible that local clustering of acidic lipids such as PS and $PI(4,5)P_2$ could occur at virus assembly sites during the process of Gag multimerization.

We are currently in the process of separating these possibilities through the use of MA-replacement constructs. These chimeric Gag proteins contain peptides or protein domains known to interact with different subsets of plasma membrane lipids in place of the MA domain of Gag. This strategy has previously been employed successfully with the PH domain of PLCδ1[19]. If PSGL-1 is drawn to virus assembly sites by high local concentrations of acidic lipids rather than some specific sequence present in the MA domain, it should be detectable with these constructs, which entirely lack the globular head of the MA domain and all known natural determinants of Gag-membrane binding.

While it is known that several UDM proteins participate in adherence, motility, cell-to-cell contact, and cell signaling events in lymphocytes [24, 52-55], it is unknown what role, if any these proteins play in HIV-1 replication. CD43, CD44, and PSGL-1 co-localize strongly with Gag and are likely incorporated efficiently into virus particles [16, 20] (unpublished observations). In contrast, ICAM-1 and ICAM-3 have been shown to be excluded from virus assembly sites, and are unlikely to be efficiently incorporated into virus particles [16, 20].

We speculated that as proteins with adhesive properties, class I UDM proteins may enhance infectivity or cell-to-cell transfer of virus between lymphocytes. However, we observed that both infectivity and cell-to-cell transfer of virus are modestly inhibited by CD43, CD44, and PSGL-1, whether expressed individually or in combination. We also observed that ICAM-3 modestly decreases infectivity and cell-to-cell transfer (Figure 3.6). Interestingly, we found that when containing the cytoplasmic tail of PSGL-1, ICAM-1 also exerted a negative effect (Figure 3.6). This may indicate that ICAM-1 is

not normally incorporated to virus assembly sites and thus has no effect, but the chimera used in this study is efficiently incorporated and is slightly inhibitory.

It is likely that HIV-1 has evolved to incorporate UDM proteins into virus particles for some purpose which is beneficial for viral replication and dissemination. Currently, however, this purpose remains unknown. Alternatively, it is possible that Gag-UDM interactions are simply a consequences of the unique way in which Gag binds to and recognizes membranes. It may also be possible that Gag interaction with class I UDMs is necessary for polarization of Gag in T cells. While replacement of the MA domain with a triple-acylation signal derived from Fyn kinase results in association of Gag with a different set of UDMs, it does not inhibit polarization of Gag [20]. This result was initially interpreted as indicating that association between Gag and class I UDMs is dispensable for Gag polarization to uropods.

However, an alternative model is also possible. We have previously found that constructs containing this Fyn modification are severely deficient in infection of T cells (GNL, JRG unpublished observations). This may indicate that the inability of MA to detach from the membrane may have detrimental effects during viral entry, uncoating, or nuclear import. Therefore, it is possible that although association of Gag bearing the Fyn membrane binding sequence with different UDMs can support polarization of Gag to uropods in T cells, association of Gag with class I UDMs is required for polarization of Gag bearing a WT Matrix sequence. It is also formally possible that association of Fyn(10)-Gag with a different subset of UDMs is detrimental to viral infectivity.

We favor the possibility that UDM proteins may serve some purpose during viral infection. We are currently developing a trans-infection model, which will be described

in chapter 4 of this thesis. Using this assay, we aim to determine whether UDM proteins modulate trans-infection of T cells by virus particles which have been previously captured by dendritic cells. Development of additional models will likely be necessary to understand the role UDM proteins play in HIV infection in vivo. It is possible that simplified cell-based assays do not adequately reflect the complexity of HIV biology which occurs within the human body, especially within the complicated cellular milieu of secondary lymphoid tissues.

Acknowledgements

We thank members of the Ono and Veatch labs for helpful discussions. We thank Jingga Inlora for characterization of MA replacement constructs by liposome binding assay and Matt Stone for help with image processing. The following reagents were obtained from the AIDS Research and Reference Reagent Program, Division of AIDS, NIAID, NIH: HIV-Ig from NABI and NHLBI and the CEM-GFP cell line. This work was supported by R21 AI095022 and R56 AI089282 (to AO). JRG is supported by the Dr. Clayton Willison and Emma Elizabeth Willison Endowed Graduate Fellowship.

References

1. Ono, A., et al., *Phosphatidylinositol (4,5) bisphosphate regulates HIV-1 Gag targeting to the plasma membrane.* Proc Natl Acad Sci U S A, 2004. **101**(41): p. 14889-94.

2. Saad, J.S., et al., *Structural basis for targeting HIV-1 Gag proteins to the plasma membrane for virus assembly.* Proc Natl Acad Sci U S A, 2006. **103**(30): p. 11364-9.

3. Chukkapalli, V., et al., *Interaction between the human immunodeficiency virus type 1 Gag matrix domain and phosphatidylinositol-(4,5)-bisphosphate is essential for efficient gag membrane binding.* J Virol, 2008. **82**(5): p. 2405-17.

4. Saad, J.S., et al., *Structure of the myristylated human immunodeficiency virus type 2 matrix protein and the role of phosphatidylinositol-(4,5)-bisphosphate in membrane targeting.* J Mol Biol, 2008. **382**(2): p. 434-47.

5. Ono, A., *HIV-1 assembly at the plasma membrane.* Vaccine, 2010. **28 Suppl 2**: p. B55-9.

6. Chukkapalli, V., S.J. Oh, and A. Ono, *Opposing mechanisms involving RNA and lipids regulate HIV-1 Gag membrane binding through the highly basic region of the matrix domain.* Proc Natl Acad Sci U S A, 2010. **107**(4): p. 1600-5.

7. Chukkapalli, V., et al., *Evidence in support of RNA-mediated inhibition of phosphatidylserine-dependent HIV-1 Gag membrane binding in cells.* J Virol, 2013.

8. Dick, R.A., et al., *HIV-1 Gag protein can sense the cholesterol and acyl chain environment in model membranes.* Proc Natl Acad Sci U S A, 2012. **109**(46): p. 18761-6.

9. Vlach, J. and J.S. Saad, *Trio engagement via plasma membrane phospholipids and the myristoyl moiety governs HIV-1 matrix binding to bilayers.* Proc Natl Acad Sci U S A, 2013. **110**(9): p. 3525-30.

10. Ono, A. and E.O. Freed, *Plasma membrane rafts play a critical role in HIV-1 assembly and release.* Proc Natl Acad Sci U S A, 2001. **98**(24): p. 13925-30.

11. Ono, A., A.A. Waheed, and E.O. Freed, *Depletion of cellular cholesterol inhibits membrane binding and higher-order multimerization of human immunodeficiency virus type 1 Gag.* Virology, 2007. **360**(1): p. 27-35.

12. Sundquist, W.I. and H.G. Krausslich, *HIV-1 assembly, budding, and maturation.* Cold Spring Harb Perspect Med, 2012. **2**(7): p. a006924.

13. Nydegger, S., et al., *Mapping of tetraspanin-enriched microdomains that can function as gateways for HIV-1.* J Cell Biol, 2006. **173**(5): p. 795-807.

14. Booth, A.M., et al., *Exosomes and HIV Gag bud from endosome-like domains of the T cell plasma membrane.* J Cell Biol, 2006. **172**(6): p. 923-35.

15. Jolly, C. and Q.J. Sattentau, *Human immunodeficiency virus type 1 assembly, budding, and cell-cell spread in T cells take place in tetraspanin-enriched plasma membrane domains.* J Virol, 2007. **81**(15): p. 7873-84.

16. Llewellyn, G.N., et al., *Nucleocapsid promotes localization of HIV-1 gag to uropods that participate in virological synapses between T cells.* PLoS Pathog, 2010. **6**(10): p. e1001167.

17. Hogue, I.B., G.N. Llewellyn, and A. Ono, *Dynamic Association between HIV-1 Gag and Membrane Domains.* Mol Biol Int, 2012. **2012**: p. 979765.

18. Krementsov, D.N., et al., *HIV-1 assembly differentially alters dynamics and partitioning of tetraspanins and raft components.* Traffic, 2010. **11**(11): p. 1401-14.

19. Hogue, I.B., et al., *Gag induces the coalescence of clustered lipid rafts and tetraspanin-enriched microdomains at HIV-1 assembly sites on the plasma membrane.* J Virol, 2011. **85**(19): p. 9749-66.

20. Llewellyn, G.N., et al., *HIV-1 Gag Associates with Specific Uropod-Directed Microdomains in a Manner Dependent on its MA Highly Basic Region.* J Virol, 2013.

21. Miller, M.J., et al., *Two-photon imaging of lymphocyte motility and antigen response in intact lymph node.* Science, 2002. **296**(5574): p. 1869-73.

22. Jolly, C., et al., *HIV-1 cell to cell transfer across an Env-induced, actin-dependent synapse.* J Exp Med, 2004. **199**(2): p. 283-93.

23. Rodriguez-Plata, M.T., et al., *The infectious synapse formed between mature dendritic cells and CD4+ T cells is independent of the presence of the HIV-1 envelope glycoprotein.* Retrovirology, 2013. **10**: p. 42.

24. Dustin, M.L., A.K. Chakraborty, and A.S. Shaw, *Understanding the structure and function of the immunological synapse.* Cold Spring Harb Perspect Biol, 2010. **2**(10): p. a002311.

25. Vasiliver-Shamis, G., M.L. Dustin, and C.E. Hioe, *HIV-1 Virological Synapse is not Simply a Copycat of the Immunological Synapse.* Viruses, 2010. **2**(5): p. 1239-60.

26. Sattentau, Q., *Avoiding the void: cell-to-cell spread of human viruses.* Nat Rev Microbiol, 2008. **6**(11): p. 815-26.

27. Dimitrov, D.S., et al., *Quantitation of human immunodeficiency virus type 1 infection kinetics.* J Virol, 1993. **67**(4): p. 2182-90.

28. Gupta, P., et al., *Cell-to-cell transmission of human immunodeficiency virus type 1 in the presence of azidothymidine and neutralizing antibody.* J Virol, 1989. **63**(5): p. 2361-5.

29. Chen, P., et al., *Predominant mode of human immunodeficiency virus transfer between T cells is mediated by sustained Env-dependent neutralization-resistant virological synapses.* J Virol, 2007. **81**(22): p. 12582-95.

30. Sigal, A., et al., *Cell-to-cell spread of HIV permits ongoing replication despite antiretroviral therapy.* Nature, 2011. **477**(7362): p. 95-8.

31. Durham, N.D., et al., *Neutralization resistance of virological synapse-mediated HIV-1 Infection is regulated by the gp41 cytoplasmic tail.* J Virol, 2012. **86**(14): p. 7484-95.

32. Aranda, J.F., et al., *MYADM controls endothelial barrier function through ERM-dependent regulation of ICAM-1 expression.* Mol Biol Cell, 2013. **24**(4): p. 483-94.

33. Morita, E., et al., *Human ESCRT-III and VPS4 proteins are required for centrosome and spindle maintenance.* Proc Natl Acad Sci U S A, 2010. **107**(29): p. 12889-94.

34. Strebel, K., et al., *The HIV 'A' (sor) gene product is essential for virus infectivity.* Nature, 1987. **328**(6132): p. 728-30.

35. Lehmann, M., et al., *Quantitative multicolor super-resolution microscopy reveals tetherin HIV-1 interaction.* PLoS Pathog, 2011. **7**(12): p. e1002456.

36. Grover, J.R., et al., *Roles Played by Capsid-Dependent Induction of Membrane Curvature and Gag-ESCRT Interactions in Tetherin Recruitment to HIV-1 Assembly Sites.* J Virol, 2013. **87**(8): p. 4650-64.

37. Muranyi, W., et al., *Super-resolution microscopy reveals specific recruitment of HIV-1 envelope proteins to viral assembly sites dependent on the envelope C-terminal tail.* PLoS Pathog, 2013. **9**(2): p. e1003198.

38. Zhang, M., et al., *Rational design of true monomeric and bright photoactivatable fluorescent proteins.* Nat Methods, 2012. **9**(7): p. 727-9.

39. Monde, K., V. Chukkapalli, and A. Ono, *Assembly and replication of HIV-1 in T cells with low levels of phosphatidylinositol-(4,5)-bisphosphate.* J Virol, 2011. **85**(7): p. 3584-95.

40. Epperson, T.K., et al., *Noncovalent association of P-selectin glycoprotein ligand-1 and minimal determinants for binding to P-selectin.* J Biol Chem, 2000. **275**(11): p. 7839-53.

41. Maniti, O., et al., *Binding of moesin and ezrin to membranes containing phosphatidylinositol (4,5) bisphosphate: a comparative study of the affinity constants and conformational changes.* Biochim Biophys Acta, 2012. **1818**(11): p. 2839-49.

42. Neisch, A.L. and R.G. Fehon, *Ezrin, Radixin and Moesin: key regulators of membrane-cortex interactions and signaling.* Curr Opin Cell Biol, 2011. **23**(4): p. 377-82.

43. Alonso-Lebrero, J.L., et al., *Polarization and interaction of adhesion molecules P-selectin glycoprotein ligand 1 and intercellular adhesion molecule 3 with moesin and ezrin in myeloid cells.* Blood, 2000. **95**(7): p. 2413-9.

44. Spertini, C., B. Baisse, and O. Spertini, *Ezrin-radixin-moesin-binding sequence of PSGL-1 glycoprotein regulates leukocyte rolling on selectins and activation of extracellular signal-regulated kinases.* J Biol Chem, 2012. **287**(13): p. 10693-702.

45. Cannon, J.L., et al., *CD43 interaction with ezrin-radixin-moesin (ERM) proteins regulates T-cell trafficking and CD43 phosphorylation.* Mol Biol Cell, 2011. **22**(7): p. 954-63.

46. Mori, T., et al., *Structural basis for CD44 recognition by ERM proteins.* J Biol Chem, 2008. **283**(43): p. 29602-12.

47. Heiska, L., et al., *Association of ezrin with intercellular adhesion molecule-1 and -2 (ICAM-1 and ICAM-2). Regulation by phosphatidylinositol 4, 5-bisphosphate.* J Biol Chem, 1998. **273**(34): p. 21893-900.

48. Machta, B.B., et al., *Minimal model of plasma membrane heterogeneity requires coupling cortical actin to criticality.* Biophys J, 2011. **100**(7): p. 1668-77.

49. Bregnard, C., et al., *Comparative proteomic analysis of HIV-1 particles reveals a role for Ezrin and EHD4 in the Nef-dependent increase of virus infectivity.* J Virol, 2013. **87**(7): p. 3729-40.

50. Capalbo, G., et al., *Knockdown of ERM family member moesin in host cells increases HIV type 1 replication.* AIDS Res Hum Retroviruses, 2011. **27**(12): p. 1317-22.

51. Williams, K., et al., *CD44 integrates signaling in normal stem cell, cancer stem cell and (pre)metastatic niches.* Exp Biol Med (Maywood), 2013. **238**(3): p. 324-38.

52. Clark, M.C. and L.G. Baum, *T cells modulate glycans on CD43 and CD45 during development and activation, signal regulation, and survival.* Ann N Y Acad Sci, 2012. **1253**: p. 58-67.

53. Kawashima, H. and M. Fukuda, *Sulfated glycans control lymphocyte homing.* Ann N Y Acad Sci, 2012. **1253**: p. 112-21.

54. Zarbock, A., et al., *Leukocyte ligands for endothelial selectins: specialized glycoconjugates that mediate rolling and signaling under flow.* Blood, 2011. **118**(26): p. 6743-51.

55. Jacobelli, J., et al., *Myosin-IIA and ICAM-1 regulate the interchange between two distinct modes of T cell migration.* J Immunol, 2009. **182**(4): p. 2041-50.

CHAPTER IV

Discussion

Summary of Results

Interactions between assembling HIV-1 virions and plasma membrane proteins present in host cells likely constitute an important mechanism of selective incorporation of beneficial cellular components into virus particles. Furthermore, exclusion of certain proteins by HIV-1 is also likely to enhance viral replication and dissemination in vivo. In chapter 2 of this thesis I have defined the mechanism by which an antiviral protein, BST-2/tetherin is incorporated into HIV-1 assembly sites in the absence of viral antagonism. In chapter 3 of this thesis, I have addressed the mechanism by which HIV-1 selectively incorporates certain uropod-directed microdomain (UDM) proteins into virus assembly sites.

While many have speculated that tetherin is incorporated into HIV-1 virus assembly sites through a lipid raft-dependent mechanism, I have shown evidence that this is not the case (Figure 2.2). I have also shown that tetherin does not appear to associate with lipid raft markers that can be found in association with HIV-1 assembly sites (Figure 2.1) [1]. This model of lipid-raft dependent recruitment of tetherin was based on the observations that cholesterol-depletion drastically decreases HIV-1 virus particle

production [2], and that tetherin can be recovered from detergent-resistant membrane fractions [3].

Findings presented in chapter 2 of this thesis are consistent with the observation of another group, that tetherin does not associate with GM-1, a lipid raft marker [4]. They are also consistent with the finding that association of Vpu with detergent-resistant membrane fractions is not correlated with its ability to antagonize tetherin [5]. Furthermore, another group has shown that antagonism of tetherin function by Vpu does not involve removal of tetherin from detergent-resistant membrane fractions [6]. Together these results support a model where tetherin localization to HIV-1 assembly sites is a lipid raft-independent process, and that lipid raft association of tetherin and Vpu is dispensable for the association and function of these proteins.

Through the use of confocal and super-resolution localization microscopy techniques, I was able to demonstrate that both membrane curvature, specifically determined by residues in the N-terminal region of the capsid (CA) domain of Gag, as well as interactions between Gag and components of the endosomal sorting complex required for transport (ESCRT) mediate and enhance tetherin recruitment to HIV-1 assembly sites respectively (Figures 2.3, 2.5 and 2.7). I was also able to demonstrate that Gag-ESCRT interactions enhance tetherin recruitment in a T cell line, as late domain mutations significantly reduced tetherin-Gag colocalization in these cells (Figure 2.4).

Finally, I found that while disruption of Gag-ESCRT interactions significantly reduces tetherin recruitment, to levels undetectable by confocal microscopy (Figures 2.3 and 2.5), tetherin is still recruited at low levels under these conditions (Figure 2.7). I also found that these low levels of tetherin recruitment are sufficient for full restriction of

HIV-1 virus particle release in HeLa and T cells (Figure 2.6).

Previous studies in our laboratory have shown that Gag co-polarizes to uropods along with a subset of uropod directed microdomain proteins. We have also shown that polarization of both Gag and UDMs is dependent on an intact actin myosin system. Additionally, we have demonstrated that polarization of Gag is dependent upon Gag multimerization, specifically that mediated by the NC domain [7]. Recently, we have identified the MA HBR as the critical determinant which mediates Gag-UDM interactions [8].

In ongoing studies, which are presented in chapter 3 of this thesis, I address the mechanism by which HIV-1 is able to associate with certain uropod-directed proteins present in T cells. While previous studies have characterized which proteins are brought to HIV-1 assembly sites, and which appear to be excluded by Gag, they have not addressed either the underlying mechanism of Gag-UDM association or the relevance of these interactions to HIV-1 biology [7, 8].

To extend on these previous studies in T cells, which were carried out using an antibody co-patching assay, I have employed super-resolution microscopy techniques developed in chapter 2 of this thesis to determine the nature of Gag-UDM interactions in greater detail. I first tested whether Gag-UDM association occurs in HeLa cells, which are more tractable to TIRF microscopy, transgene introduction, and siRNA-mediated protein depletion. Consistent with previous findings, I observed high levels of co-clustering between Gag and PSGL-1 when both were expressed exogenously (Figure 3.1). This result indicates that HeLa cells constitute an acceptable model in which to

study Gag-UDM interactions, because the necessary determinants of these interactions are also present in these cells.

Using PSGL-1 as a model UDM protein, I next sought to identify the determinants of Gag-PSGL-1 interaction. I found that consistent with our findings in T cells, the MA HBR is required for efficient recruitment of PSGL-1 to virus assembly sites (Figure 3.1). In contrast to previous observations, however, I found that exchanging the identity of basic residues in the HBR did not completely restore PSGL-1 recruitment. While this observation may reflect cell-type-specific differences between HeLa and T cells, the use of different methods may also contribute to the quantitative differences observed between the current and previous studies. Of note, it is likely that super-resolution localization microscopy more accurately captures the native distribution of proteins, as it does not require antibody copatching prior to fixation.

I next sought to identify the determinants present in PSGL-1 which mediate its recruitment to virus assembly sites. I found that deletion of the cytoplasmic tail of PSGL-1 resulted in a drastic reduction in PSGL-1 recruitment, while mutation of a cysteine residue critical for dimerization of PSGL-1 had no effect (Figure 3.2). Given that the cytoplasmic tail of PSGL-1 contains the major determinants of its recruitment to HIV-1 assembly sites, I examined the sequence of the cytoplasmic tail of this protein and formed two hypotheses. First, that acidic residues within the cytoplasmic tail of PSGL-1 may interact directly with the MA HBR. Second, that basic residues near the transmembrane domain of PSGL-1 may mediate its recruitment to assembly sites presumably through interaction with some acidic, intermediate factor.

By making mutations in these two regions of PSGL-1, and observing these proteins by super-resolution microscopy, I found that three membrane-proximal basic residues constitute the major determinant of PSGL-1 recruitment to virus assembly sites (Figure 3.3). While mutation of acidic residues near the C-terminus of the protein appeared to increase surface levels of PSGL-1, it did not affect co-clustering with Gag (Figure 3.3).

It is well known that two of the residues substituted in the basic residue mutant, PSGL-1 3A, constitute an Ezrin binding site in PSGL-1 [9]. This interaction is thought to be required for polarization of this protein to T cell uropods. It is possible that this interaction may also mediate association of PSGL-1 with HIV-1 assembly sites. Unexpectedly, I found that depletion of Ezrin, Radixin, and Moesin individually had no significant effect on Gag-PSGL-1 co-clustering. However, I found that depletion of all three proteins simultaneously resulted in increased co-clustering (Figure 3.4). This result indicates that rather than being necessary for Gag-PSGL-1 interaction, these proteins are slightly inhibitory to this interaction, in a redundant manner.

Taken together, the results presented in chapter 3 of this thesis (Figures 3.1 – 3.4) indicate that basic residues are necessary on both sides of the interaction between Gag and PSGL-1. Given these findings, I hypothesized the existence of some acidic factor which mediates recruitment of PSGL-1, as well as other UDM proteins to HIV-1 assembly sites. Given the proximity to the membrane, this factor is likely an acidic lipid, of which many different types can be found in the inner leaflet of the plasma membrane. Future experiments, using chimeric Gag constructs with different lipid specificities, should be able to determine the identity of this unknown factor, if it is indeed an acidic

lipid. Alternatively, it is also possible that this factor could be a protein, small molecule, or nucleic acid, which is membrane-proximal and links Gag and PSGL-1.

Finally, I sought to determine the functional significance of recruitment of UDM proteins to virus assembly sites in the context of HIV-1 replication and spread. To address this, I tested the effects of expression of class I and II UDM proteins in 293T cells also expressing a full-length molecular clone of HIV (pNL4-3). By this method, I observed a modest inhibition of viral infectivity by all proteins tested, with the exception of ICAM-1 (Figure 3.5). However, this protein was also somewhat inhibitory when bearing the cytoplasmic tail of PSGL-1 (Figure 3.5). This finding likely reflects the absence of wild type ICAM-1 in association with viral assembly sites [8].

Next, I tested the effect of expression of UDM proteins on cell-to-cell transfer. This was done by expressing a molecular clone which encodes Gag-YFP, along with plasmids encoding UDM proteins, in HeLa cells. These cells were then washed and co-cultured with SupT1 T cells. After a 3 hour co-incubation, cells were fixed and analyzed by FACS to quantify the relative amounts of VLPs which had been transferred to target T cells. We have previously shown robust acquisition of Gag-YFP virus-like particles (VLPs) by T cells using a similar assay [7]. Consistent with the results of the infectivity experiment, I found that expression of UDM proteins modestly inhibited cell-to-cell transfer of Gag-YFP VLPs (Figure 3.5). Further experiments will be necessary to directly assess to what extent these proteins are incorporated into virus particles under these conditions. Development of additional assays will also likely be needed to clarify the role UDM proteins play in HIV-1 replication and dissemination.

Future Directions

In chapter two of this study, I have presented data consistent with a model in which membrane curvature, induced by HIV-1 virus assembly, mediates recruitment of tetherin to virus assembly sites. This observation has many potential implications. Structural studies of tetherin have shown that it possesses some structural similarities with other proteins which can sense and manipulate membrane curvature [10].

Structural analyses have also revealed the presence of positively-charged residues near the ends of the ectodomain of tetherin, which may allow it to interact with the negatively-charged extracellular face of the plasma membrane, while negatively-charged residues in the central portion may repel the membrane [10, 11]. In addition to this observation, tetherin has been found to display considerable flexibility, determined by the presence of two possible hinge regions in this protein [10, 11]. It has been suggested that while tetherin is primarily a dimeric protein, it possess the ability to form tetrameric complexes under reducing conditions [10, 12], however mutation of a residue critical for this tetramerization (L70D) only modestly decreased the potency of virus release inhibition by tetherin [12]. Therefore, while tetramerization of tetherin may enhance its capacity to sense membrane curvature, it is not required for inhibition of HIV-1 release.

While results presented in chapter 2 of this thesis are consistent with a model where tetherin is able to sense membrane curvature induced by viral assembly, it would be interesting to determine whether residues which confer flexibility to the ectodomain of tetherin (A88 and G109) are required for this curvature-sensing ability [11].

I have also shown that ESCRT proteins, specifically Tsg101 and Alix, both enhance tetherin recruitment to virus assembly sites; however this enhancement is not

necessary for inhibition of HIV-1 release. Currently, it is not known whether these proteins directly recruit tetherin to HIV-1 assembly sites, or if downstream ESCRT components are required for this activity. It is also unclear how ESCRT engagement enhances tetherin recruitment. If the latter possibility is correct, that Tsg and Alix enhance tetherin recruitment through downstream ESCRT components such as ESCRT-III [13], it is possible that polymerization of ESCRT-III proteins may form a barrier which prevents diffusion of tetherin away from assembly sites .

Another possibility is that ESCRT-induced membrane deformation, which ultimately progresses to membrane scission, may create a unique environment in which extreme membrane curvature is present [13-15]. Though difficult to address experimentally, if this hypothesis were correct, it would further strengthen the model in which tetherin is inherently a sensor of membrane curvature.

Furthermore, while ESCRT-dependent enhancement of tetherin recruitment is not necessary for restriction of HIV-1 release, it is possible that other larger enveloped viruses, which like HIV-1 rely on ESCRT machinery for fission, may be susceptible to these higher levels of tetherin recruitment. It is likely that as larger viruses like filoviruses and filamentous orthomyxoviruses may experience greater shearing forces, they may also require more tetherin molecules to retain them at the cell surface.

Additionally, it is currently not known whether tetherin inhibits budding of other particles from the cell surface, such as exosomes or other vesicles. If tetherin recruitment is indeed dependent upon membrane curvature, these other budding events may also be sensitive to tetherin. It would be interesting to examine whether other ESCRT-dependent

membrane budding events, such as MVB formation, cytokinesis, and autophagy are also inhibited by tetherin [14].

Recently, it has been reported that tetherin may serve as an innate sensor for viral infection. This hypothesis is supported by the observation that tetherin expression enhances NF-κB activity in a virus-dependent manner [16, 17]. Furthermore, another study found that while expression of an MLV clone resulted in tetherin-dependent induction of NF-κB, mutation of the late domain of MLV Gag abolished this induction [18]. If tetherin is indeed a true pathogen recognition receptor, it would be interesting to determine whether ESCRT-mediated enhancement of tetherin recruitment to HIV-1 assembly sites also enhances NF-κB activation upon HIV-1 infection. While membrane curvature can induce sufficient recruitment of tetherin to inhibit virus release, it is possible that additional recruitment may be necessary to initiate or strengthen NF-κB signaling by tetherin in response to HIV-1 infection.

In chapter 3 of this thesis, I have presented data which are consistent with a model where UDM proteins are recruited to HIV-1 assembly sites through the presence of an acidic intermediate. It is currently unknown whether this intermediate factor is a lipid, protein, or nucleic acid. Experiments are currently underway to separate these possibilities. As these studies have only examined the mechanism of PSGL-1 recruitment, it will be interesting to determine whether CD43 and CD44 are recruited to HIV-1 assembly sites through a similar mechanism. Also, the mechanism by which Gag is able to exclude other UDM proteins, such as ICAM-1 and ICAM-3, from virus assembly sites remains unknown.

It would also be interesting to determine at which stage of viral assembly UDM interactions take place. This could be done by examining both early assembly mutants I developed in collaboration with Nick Llewellyn in our laboratory [8], and late stage mutants described in chapter 2 of this thesis and elsewhere [8, 19] by super-resolution microscopy. Interestingly, we found that while a Gag molecule bearing a trimeric leucine zipper sequence did not polarize to uropods in T cells, a similar construct bearing a tetrameric leucine zipper sequence polarized to a similar extent to wild type Gag [8].

Furthermore, the functional consequences of HIV-UDM interactions remain to be fully elucidated. Thus far, I have examined the effects of these proteins on infectivity and cell-to-cell transfer of HIV-1. Unexpectedly, all UDM proteins tested modestly decrease both infectivity and virus transfer, with the exception of ICAM-1. Development of additional assays will be necessary to examine what role, if any, UDM proteins play in HIV-1 replication and dissemination, and whether these proteins indeed confer some advantage to HIV-1 as I have hypothesized.

Currently, I am working to develop a trans-infection assay using a human monocytic cell line, THP-1. Through the addition of cytokines, these cells can be induced to differentiate into cells exhibiting characteristics of both immature and mature dendritic cells (iDC and mDC) [20]. Given that the class II UDM protein ICAM-3 is a natural ligand for DC-SIGN, which mediates trans-infection of T cells by dendritic cell-associated HIV-1 [21-23], I hypothesized that this protein may interfere with the process of trans-infection if incorporated into HIV-1 virions. Thus far, I have successfully derived cells with iDC and mDC characteristics, including DC-SIGN expression, adherence, and cell morphology (Figure 4.1 A-B). I have also observed robust trans-infection of CEM-

GFP cells when THP-1-derived iDC and mDC were pre-incubated with virus. In this assay, CEM-GFP cells were observed making extensive contacts with iDC and mDC, and appear to exhibit contact-induced polarization, although this has not yet been assessed quantitatively (Figure 4.1 C). I am currently in the process of determining whether UDM proteins modulate trans-infection in this system.

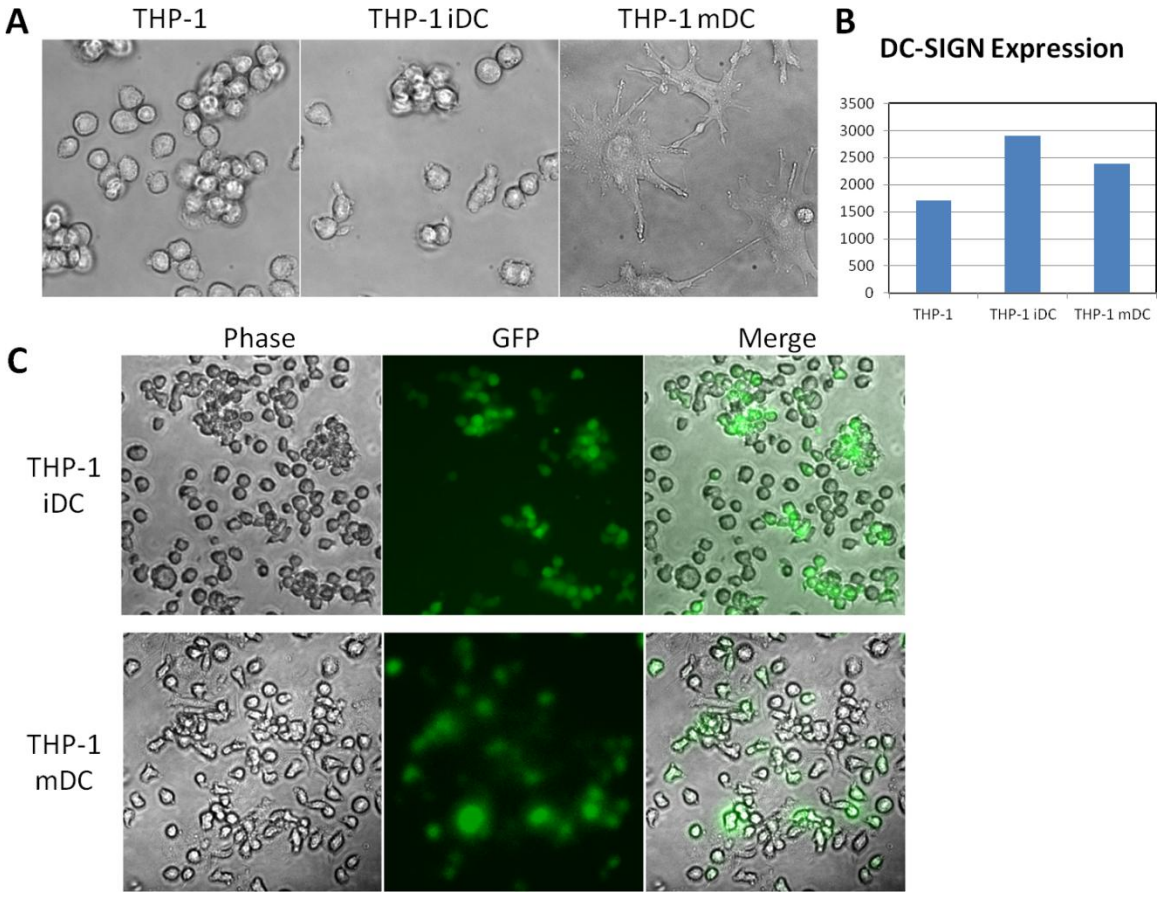

Figure 4.1. Development of a trans-infection assay using THP-1-derived, human dendritic cells.
A) THP-1 cells (a human monocytic cell line) were incubated in RPMI containing 10% FBS, or media containing 10% FBS, rhGM-CSF, and rhIL-4 for 5 days (iDC), or media lacking FBS containing rhGM-CSF, rhIL-4, rhTNF-α, and ionomycin for 3 days (mDC). While THP-1 cells are primarily round and not adherent, iDC display a lobate morphology and are weakly adherent, while mDC display a stellate morphology and are strongly adherent, similar to iDC and mDC derived from primary human monocytes. B) Cells were then fixed and analyzed for surface DC-SIGN expression by FACS analysis. C) Cells cultured under the conditions described above were inoculated with single-round HIV-1 virus particles (pNL4-3 Env- + pEBB NL-Env) obtained from 293T cells. After 2 hour incubation, cells were washed and CEM-GFP cells were added and co-cultured for 2 days, prior to microscopic observations.

In chapters 2 and 3 of this thesis, I have developed quantitative super-resolution localization microscopy techniques well suited to the study of virus-host interactions. These techniques are able to resolve single virus particles as well as single host proteins, and are likely not prone to significant antibody-mediated artifacts. Prior to immunostaining, cells are fixed with paraformaldehyde and glutaraldehyde to prevent diffusion of transmembrane proteins observed in these experiments [24]. Although these techniques are quantitative and able to resolve proteins distributions with extremely high precision (10-30 nm), they have been limited to two colors in the experiments presented in this thesis.

It is formally possible that 3 color imaging could be performed under similar conditions. In particular, YFP is able to fluoresce strongly under reducing conditions, and is spectrally distinct from both Alexa Fluor 532 and Alexa Fluor 647. In a pilot experiment, I was able to observe YFP by TIRF, along with Alexa Fluors 532 and 647 by dSTORM (Figure 4.2). While super-resolution information was not extrapolated from YFP signals, it could also be possible to use Alexa Fluor 488 with Alexa 647 and either Alexa Fluor 532 or mEos3.2. YFP has also been used successfully for PALM imaging previously [25], although it may not be compatible with reducing buffers commonly used for dSTORM. Another combination of Alexa Fluors 488, 561, and 647 has been reported previously [26]. I am currently in the process of exploring these possibilities to further understand Gag-UDM interactions.

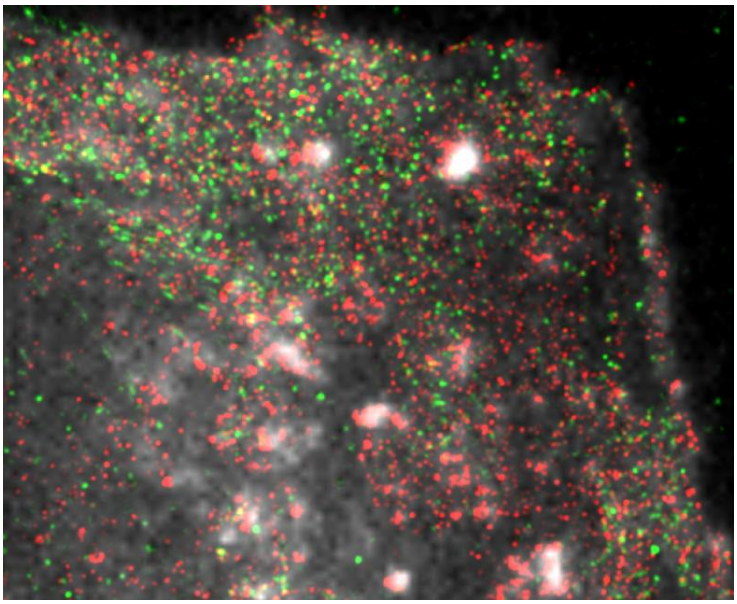

Figure 4.2. Demonstrating the feasibility of triple-color super-resolution localization microscopy. HeLa cells were transfected with plasmids encoding Gag-YFP, ICAM-3, and PSGL-1. Cells were fixed and stained with an Alexa Fluor 532-labeled antibody against ICAM-3, and an Alexa Fluor 647-labeled antibody against PSGL-1. Cells were first imaged by TIRF to obtain YFP images, followed by dSTORM imaging to determine the location of molecules of ICAM-3 and PSGL-1 with high precision (~15 nm). YFP is shown in gray, ICAM-3 is shown in green, PSGL-1 is shown in red. Notably, PSGL-1 is seen in association with Gag-YFP, while ICAM-3 is not.

Conclusions

HIV-1 is an extremely successful viral pathogen. Although infection progresses slowly, especially when HAART therapy is employed, it is nearly always fatal due to the emergence of drug-resistant viruses. There is only one known case where an HIV-1 positive individual has been cured completely of infection, by bone marrow transplantation from a CCR5 Δ32 homozygous donor [27]. While pathogen elimination is always the goal of therapeutic intervention, this has proved difficult in the case of HIV. This is primarily due to three factors. First, as a retrovirus, HIV-1 becomes integrated into the chromosomal DNA of host cells [28]. Second, HIV-1 is able to establish extremely long lived latent reservoirs [29]. Third, HIV-1 is able to inhibit many immune mechanisms that would otherwise result in its elimination from the body [30-32].

Once infection has been established, HIV-1 is extremely efficient at avoiding or circumventing host immune responses. Many viruses, including HIV-1, frequently escape control by the adaptive immune system through mutation of immunogenic epitopes of viral proteins. As discussed in chapter 1 of this thesis, immune evasion can also be accomplished through the activities of the HIV-1 accessory proteins Vif, Vpr, Vpu, and Nef. In some cases, immune evasion can also result from mutation of the viral targets of cellular restriction factors. While most HAART drugs have been developed to target the viral enzymes, the viral envelope, and viral receptors [33] it may also be possible to target the activities of accessory proteins as well. It is likely that the extremely high levels of selective pressure exerted on HIV-1 by these conventional therapies frequently results in the emergence of drug resistance. As the accessory proteins of HIV-1 have been shown to be dispensable for viral replication in cell culture, they are thought to enhance virulence and pathogenicity in vivo primarily through the antagonism of various immune pathways.

It is conceivable that targeting viral accessory proteins through pharmacologic intervention may significantly reduce pathogenesis of HIV-1, while still allowing viral replication to occur. This may relieve some of the selective pressure imposed by conventional HAART therapy and result in less frequent development of drug resistance, which is an ongoing problem in the application of HAART therapy. Alternatively, regimens could be developed which target both viral enzymes and accessory proteins. In order to be able to develop inhibitors of the accessory proteins, we must first understand their functions in greater detail. As most accessory proteins target antiviral restriction

factors, also discussed in chapter 1 of this thesis, we must also work to understand the functions of restriction factors.

Another strategy which may prove useful would be to devise ways to enhance the functions of restriction factors. Toward this end, I have examined and defined the mechanism by which tetherin is recruited to HIV-1 assembly sites in chapter 2 of this thesis. Along with many other studies into the function of this protein, this information may prove useful in the development of strategies to inhibit Vpu function, or alternatively enhance tetherin antiviral function.

Other approaches are likely to prove useful in combating HIV-1 infection and disease progression. These include identification and characterization of latent viral reservoirs. Once well understood, it may be possible to either eliminate these reservoirs, or induce their reactivation which may promote clearance of infected reservoirs by the immune system [34-36].

Gene therapy is another promising tool for the eradication of HIV-1. While current studies are focused on replacement of wild type CCR5 genes with the Δ32 allele [37], it may also be possible to introduce genes encoding more potent versions of known restriction factors by gene therapy techniques. For example, the TRIM5α protein found in Rhesus macaques potently inhibits HIV-1, unlike the human homologue of this protein [38]. Alternatively, introduction of a tetherin variant which is insensitive to Vpu antagonism may also be useful [39].

While the conventional view of viral replication is that viruses simply utilize cellular components to promote their replication, recent findings point to viruses like HIV hijacking or repurposing cellular pathways to their advantage. In many cases, this is

manifest as the creation of a specific cellular niche in which viruses replicate. For example, many enveloped viruses utilize the ESCRT machinery to accomplish scission of host and viral membranes. This involves redirection of a complex normally associated with intracellular membranes to the plasma membrane of the cell [40].

Work from our laboratory, as well as many others, has shown that HIV-1, primarily through the Gag protein, specifically reorganizes both lipid and protein components of the host cell plasma membrane [19]. In particular, it selectively associates with certain domains in T cells [7, 8]. As discussed in chapter 3 of this thesis, HIV has likely evolved to interact specifically with these proteins for some purpose. Although this purpose is not yet clear, it may be related to cell-to-cell transfer of virus from infected to uninfected cells.

We have observed that HIV-1 preferentially associates with PSGL-1, CD43, and CD44 [7, 8]. CD43 and PSGL-1 bind specifically to a class of adhesive proteins present on endothelial cells termed selectins. This interaction promotes leukocyte rolling along endothelial surfaces [41]. In the context of HIV-1, it is possible that these proteins are specifically incorporated into virus particles to facilitate their attachment to endothelial surfaces. By doing this, HIV-1 may be more efficiently acquired by rolling leukocytes in the vasculature and lymphatic systems. CD44 is a receptor for extracellular matrix components, particularly hyaluronic acid, and is involved in migration, homing, and activation of T cells [42]. It is possible that HIV-1 incorporates this protein to allow it to attach to the extracellular matrix (ECM) of uninfected cells prior to viral entry. Alternatively, retention of progeny virions at the surface of infected cells by CD44-ECM interactions may potentially enhance cell-to-cell transfer of virus.

We have observed that two other UDM proteins, ICAM-1 and ICAM-3, are actively excluded from HIV-1 assembly sites [7, 8]. Both of these proteins bind to integrins such as LFA-1 (α-L/β-2). LFA-1 is primarily localized at the leading edge of polarized T cells [7]. It is possible that incorporation of ICAM-1 and ICAM-3 into virus particles would increase their adhesion to LFA-1 on the surface of producer T cells. As LFA-1 polarizes away from the uropod in infected cells, where virolgical synapses (VSs) form and cell-to-cell transmission likely occurs [7], HIV-1 may have evolved to avoid incorporation of these proteins in order to prevent its relocation away from sites of cell-cell contact.

Interestingly, we have recently reported that ICAM-3 is present in association with CD44 in uninfected T cells. However, when HIV-1 Gag is expressed, this protein is actively excluded from Gag-associated UDMs [8]. It is tempting to speculate that this specific exclusion of ICAM-3 from virus assembly sites must serve some function in viral replication. In addition to LFA-1, ICAM-3 is also known to bind to DC-SIGN, a lectin present on dendritic cells, which facilitates HIV-1 trans-infection [21]. It is possible that acquisition of virus by dendritic cells, while able to enhance trans-infection of T cells, may also result in increased presentation of virus-derived antigens to the adaptive immune system. Therefore, if ICAM-3 were efficiently incorporated into virus particles it may be detrimental to viral immune evasion strategies. Consistent with this hypothesis, enhanced replication of HIV-1 has been observed in cells lacking ICAM-3 [43].

HIV-1 lacks the Vpx accessory protein, found in related viruses SIV and HIV-2. As this protein is known to enhance infection of macrophages and dendritic cells by antagonism of SAMHD1 [44], it may be that HIV-1 has evolved to be primarily a

pathogen of T cells, and therefore lacks this accessory protein. In the case of HIV-1, evolution may have favored robust infection of T cells rather than infection of macrophages and dendritic cells, which possess many antiviral properties and the ability to efficiently present viral antigens. This may, in turn, explain the less severe pathology associated with HIV-2 and SIV infection in their natural primate hosts compared to that observed with HIV-1 in humans. Regardless of the specific roles played by these proteins in HIV-1 replication, many further studies will be necessary to fully understand how HIV-1 has become such a successful pathogen in humans, how it manipulates immune cells to create a niche in which to replicate, and why despite our best efforts, a cure remains elusive.

References

1. Hogue, I.B., et al., *Gag induces the coalescence of clustered lipid rafts and tetraspanin-enriched microdomains at HIV-1 assembly sites on the plasma membrane.* J Virol, 2011. **85**(19): p. 9749-66.

2. Ono, A. and E.O. Freed, *Plasma membrane rafts play a critical role in HIV-1 assembly and release.* Proc Natl Acad Sci U S A, 2001. **98**(24): p. 13925-30.

3. Kupzig, S., et al., *Bst-2/HM1.24 is a raft-associated apical membrane protein with an unusual topology.* Traffic, 2003. **4**(10): p. 694-709.

4. Lehmann, M., et al., *Quantitative multicolor super-resolution microscopy reveals tetherin HIV-1 interaction.* PLoS Pathog, 2011. **7**(12): p. e1002456.

5. Fritz, J.V., et al., *HIV-1 Vpu's lipid raft association is dispensable for counteraction of the particle release restriction imposed by CD317/Tetherin.* Virology, 2012. **424**(1): p. 33-44.

6. Lopez, L.A., et al., *Anti-tetherin activities of HIV-1 Vpu and Ebola virus glycoprotein do not involve tetherin removal from lipid rafts.* J Virol, 2012.

7. Llewellyn, G.N., et al., *Nucleocapsid promotes localization of HIV-1 gag to uropods that participate in virological synapses between T cells.* PLoS Pathog, 2010. **6**(10): p. e1001167.

8. Llewellyn, G.N., et al., *HIV-1 Gag Associates with Specific Uropod-Directed Microdomains in a Manner Dependent on its MA Highly Basic Region.* J Virol, 2013.

9. Spertini, C., B. Baisse, and O. Spertini, *Ezrin-radixin-moesin-binding sequence of PSGL-1 glycoprotein regulates leukocyte rolling on selectins and activation of extracellular signal-regulated kinases.* J Biol Chem, 2012. **287**(13): p. 10693-702.

10. Swiecki, M., et al., *Structural and biophysical analysis of BST-2/tetherin ectodomains reveals an evolutionary conserved design to inhibit virus release.* J Biol Chem, 2011. **286**(4): p. 2987-97.

11. Yang, H., et al., *Structural insight into the mechanisms of enveloped virus tethering by tetherin.* Proc Natl Acad Sci U S A, 2010. **107**(43): p. 18428-32.

12. Schubert, H.L., et al., *Structural and functional studies on the extracellular domain of BST2/tetherin in reduced and oxidized conformations.* Proc Natl Acad Sci U S A, 2010. **107**(42): p. 17951-6.

13. Hanson, P.I., et al., *Plasma membrane deformation by circular arrays of ESCRT-III protein filaments.* J Cell Biol, 2008. **180**(2): p. 389-402.

14. Hurley, J.H. and P.I. Hanson, *Membrane budding and scission by the ESCRT machinery: it's all in the neck.* Nat Rev Mol Cell Biol, 2010. **11**(8): p. 556-66.

15. Effantin, G., et al., *ESCRT-III CHMP2A and CHMP3 form variable helical polymers in vitro and act synergistically during HIV-1 budding.* Cell Microbiol, 2013. **15**(2): p. 213-26.

16. Cocka, L.J. and P. Bates, *Identification of alternatively translated Tetherin isoforms with differing antiviral and signaling activities.* PLoS Pathog, 2012. **8**(9): p. e1002931.

17. Tokarev, A., et al., *Stimulation of NF-kappaB activity by the HIV restriction factor BST2.* J Virol, 2013. **87**(4): p. 2046-57.

18. Galao, R.P., et al., *Innate sensing of HIV-1 assembly by Tetherin induces NFkappaB-dependent proinflammatory responses.* Cell Host Microbe, 2012. **12**(5): p. 633-44.

19. Hogue, I.B., G.N. Llewellyn, and A. Ono, *Dynamic Association between HIV-1 Gag and Membrane Domains.* Mol Biol Int, 2012. **2012**: p. 979765.

20. Berges, C., et al., *A cell line model for the differentiation of human dendritic cells.* Biochem Biophys Res Commun, 2005. **333**(3): p. 896-907.

21. Geijtenbeek, T.B., et al., *DC-SIGN, a dendritic cell-specific HIV-1-binding protein that enhances trans-infection of T cells.* Cell, 2000. **100**(5): p. 587-97.

22. Masso, M., *DC-SIGN points the way to a novel mechanism for HIV-1 transmission.* MedGenMed, 2003. **5**(2): p. 2.

23. McDonald, D., *Dendritic Cells and HIV-1 Trans-Infection.* Viruses, 2010. **2**(8): p. 1704-17.

24. Tanaka, K.A., et al., *Membrane molecules mobile even after chemical fixation.* Nat Methods, 2010. **7**(11): p. 865-6.

25. Biteen, J.S., et al., *Super-resolution imaging in live Caulobacter crescentus cells using photoswitchable EYFP.* Nat Methods, 2008. **5**(11): p. 947-9.

26. Burnette, D.T., et al., *Bleaching/blinking assisted localization microscopy for superresolution imaging using standard fluorescent molecules.* Proc Natl Acad Sci U S A, 2011. **108**(52): p. 21081-6.

27. Hutter, G., et al., *Long-term control of HIV by CCR5 Delta32/Delta32 stem-cell transplantation.* N Engl J Med, 2009. **360**(7): p. 692-8.

28. Emerman, M., A.T. Panganiban, and H.M. Temin, *Insertion of Genes into Retrovirus Genomes and of Retrovirus DNA into Cell Genomes.* Progress in Medical Virology, 1985. **32**: p. 174-188.

29. Siliciano, R.F. and W.C. Greene, *HIV latency.* Cold Spring Harb Perspect Med, 2011. **1**(1): p. a007096.

30. Wonderlich, E.R., J.A. Leonard, and K.L. Collins, *HIV immune evasion disruption of antigen presentation by the HIV Nef protein.* Adv Virus Res, 2011. **80**: p. 103-27.

31. Harris, R.S., J.F. Hultquist, and D.T. Evans, *The restriction factors of human immunodeficiency virus.* J Biol Chem, 2012. **287**(49): p. 40875-83.

32. Mashiba, M. and K.L. Collins, *Molecular mechanisms of HIV immune evasion of the innate immune response in myeloid cells.* Viruses, 2013. **5**(1): p. 1-14.

33. Montagnier, L., *25 years after HIV discovery: prospects for cure and vaccine.* Virology, 2010. **397**(2): p. 248-54.

34. Lassen, K., et al., *The multifactorial nature of HIV-1 latency.* Trends Mol Med, 2004. **10**(11): p. 525-31.

35. Xing, S. and R.F. Siliciano, *Targeting HIV latency: pharmacologic strategies toward eradication.* Drug Discov Today, 2012.

36. Shan, L. and R.F. Siliciano, *From reactivation of latent HIV-1 to elimination of the latent reservoir: The presence of multiple barriers to viral eradication.* Bioessays, 2013.

37. Li, L., et al., *Genomic Editing of the HIV-1 Coreceptor CCR5 in Adult Hematopoietic Stem and Progenitor Cells Using Zinc Finger Nucleases.* Mol Ther, 2013.

38. Zhang, J., et al., *Retroviral restriction factors TRIM5alpha: therapeutic strategy to inhibit HIV-1 replication.* Curr Med Chem, 2011. **18**(17): p. 2649-54.

39. Vigan, R. and S.J. Neil, *Determinants of tetherin antagonism in the transmembrane domain of the human immunodeficiency virus type 1 Vpu protein.* J Virol, 2010. **84**(24): p. 12958-70.

40. McCullough, J., L.A. Colf, and W.I. Sundquist, *Membrane Fission Reactions of the Mammalian ESCRT Pathway.* Annu Rev Biochem, 2013.

41. Carlow, D.A., et al., *PSGL-1 function in immunity and steady state homeostasis.* Immunol Rev, 2009. **230**(1): p. 75-96.

42. Milstone, L.M., et al., *Epican, a heparan/chondroitin sulfate proteoglycan form of CD44, mediates cell-cell adhesion.* J Cell Sci, 1994. **107 (Pt 11)**: p. 3183-90.

43. Biggins, J.E., et al., *ICAM-3 influences human immunodeficiency virus type 1 replication in CD4(+) T cells independent of DC-SIGN-mediated transmission.* Virology, 2007. **364**(2): p. 383-94.

44. Laguette, N., et al., *SAMHD1 is the dendritic- and myeloid-cell-specific HIV-1 restriction factor counteracted by Vpx.* Nature, 2011. **474**(7353): p. 654-7.